Density slicing (Pseudocolors)

It is an enhancement technique that emphasizes differences between ***DN***'s by means of colors.
It is used also for non-imaging data.

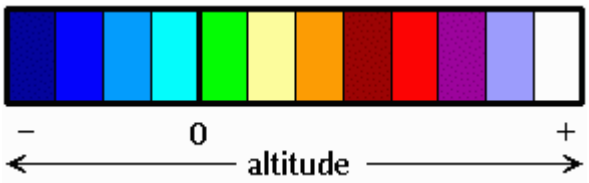

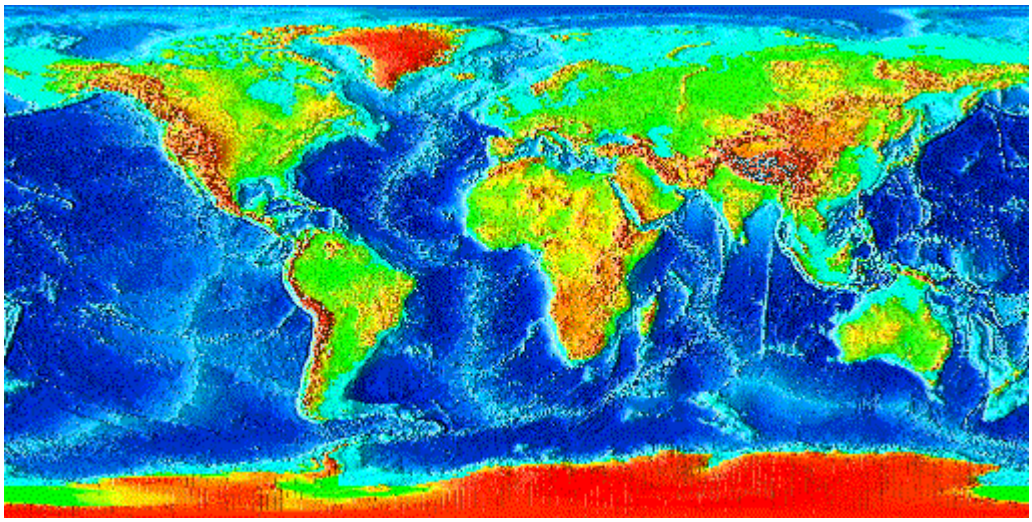

DN's are sliced in a series of intervals, and a color is assigned at each interval.

Blue, Green and Red are the so-called
additive primary colors:
When equal amounts of each are added
(and in the maximum available quantity)
white light is formed.

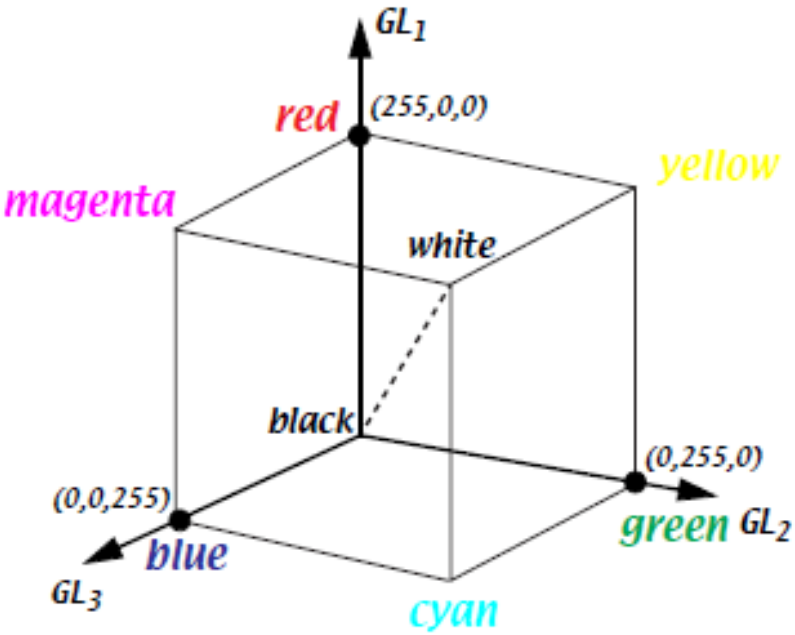

Adding primary colors in different proportions,
it is possible to get all color shades.

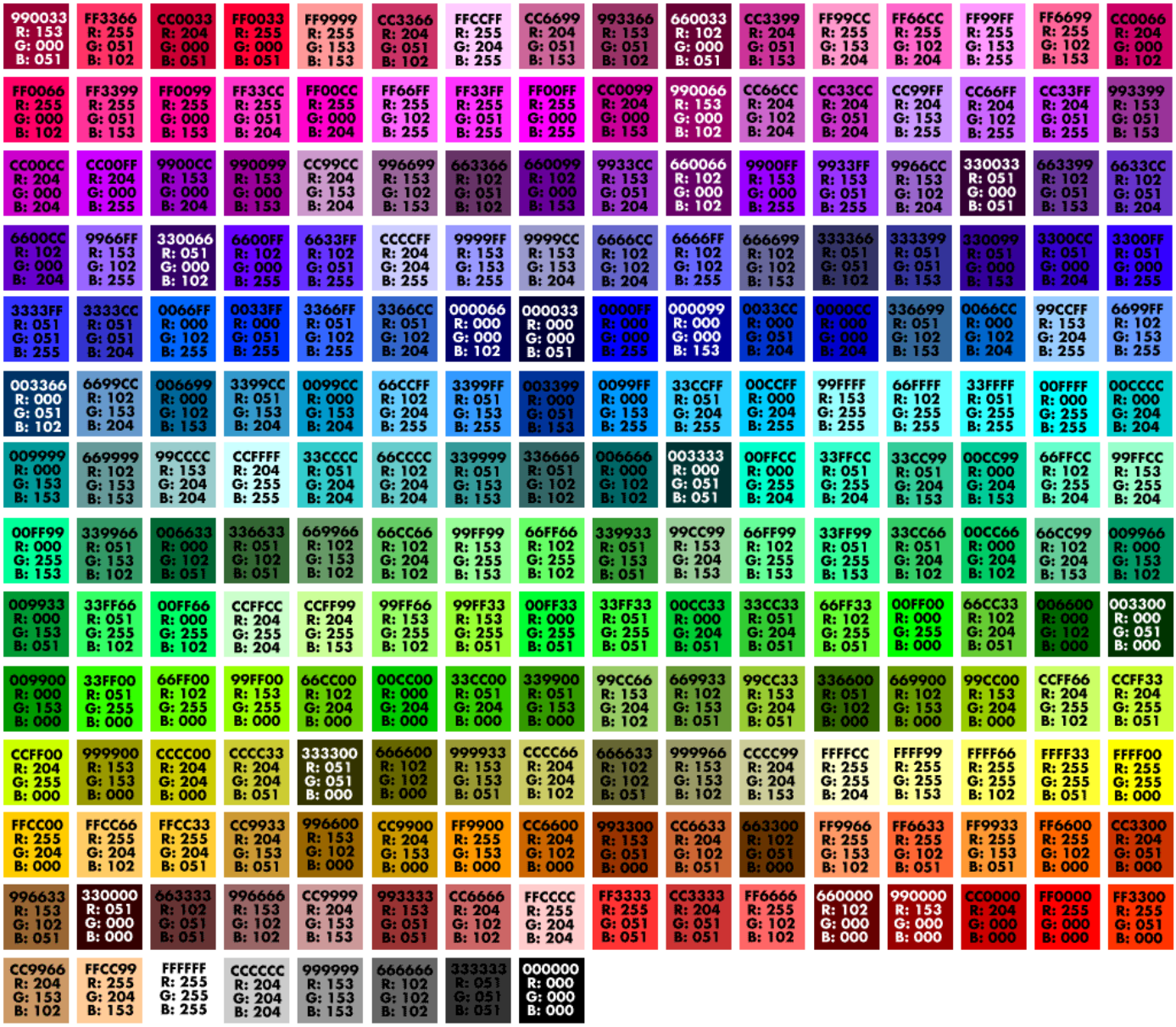
990033 R: 153 G: 000 B: 051
FF3366 R: 255 G: 051 B: 102
CC0033 R: 204 G: 000 B: 051
FF0033 R: 255 G: 000 B: 051
FF9999 R: 255 G: 153 B: 153
CC3366 R: 204 G: 051 B: 102
FFCCFF R: 255 G: 204 B: 255
CC6699 R: 204 G: 051 B: 153
993366 R: 153 G: 051 B: 102
660033 R: 102 G: 000 B: 051
CC3399 R: 204 G: 051 B: 153
FF99CC R: 255 G: 153 B: 204
FF66CC R: 255 G: 102 B: 204
FF99FF R: 255 G: 153 B: 255
FF6699 R: 255 G: 102 B: 153
CC0066 R: 204 G: 000 B: 102
FF0066 R: 255 G: 000 B: 102
FF3399 R: 255 G: 051 B: 153
FF0099 R: 255 G: 000 B: 153
FF33CC R: 255 G: 051 B: 204
FF00CC R: 255 G: 000 B: 204
FF66FF R: 255 G: 102 B: 255
FF33FF R: 255 G: 051 B: 255
FF00FF R: 255 G: 000 B: 255
CC0099 R: 204 G: 000 B: 153
990066 R: 153 G: 000 B: 102
CC66CC R: 204 G: 102 B: 204
CC33CC R: 204 G: 051 B: 204
CC99FF R: 204 G: 153 B: 255
CC66FF R: 204 G: 102 B: 255
CC33FF R: 204 G: 051 B: 255
993399 R: 153 G: 051 B: 153
CC00CC R: 204 G: 000 B: 204
CC00FF R: 204 G: 000 B: 255
9900CC R: 153 G: 000 B: 204
990099 R: 153 G: 000 B: 153
CC99CC R: 204 G: 153 B: 204
996699 R: 153 G: 102 B: 153
663366 R: 102 G: 051 B: 102
660099 R: 102 G: 000 B: 153
9933CC R: 153 G: 051 B: 204
660066 R: 102 G: 000 B: 102
9900FF R: 153 G: 000 B: 255
9933FF R: 153 G: 051 B: 255
9966CC R: 153 G: 102 B: 204
330033 R: 051 G: 000 B: 051
663399 R: 102 G: 051 B: 153
6633CC R: 102 G: 051 B: 204
6600CC R: 102 G: 000 B: 204
9966FF R: 153 G: 102 B: 255
330066 R: 051 G: 000 B: 102
6600FF R: 102 G: 000 B: 255
6633FF R: 102 G: 051 B: 255
CCCCFF R: 204 G: 204 B: 255
9999FF R: 153 G: 153 B: 255
9999CC R: 153 G: 153 B: 204
6666CC R: 102 G: 102 B: 204
6666FF R: 102 G: 102 B: 255
666699 R: 102 G: 102 B: 153
333366 R: 051 G: 051 B: 102
333399 R: 051 G: 051 B: 153
330099 R: 051 G: 000 B: 153
3300CC R: 051 G: 000 B: 204
3300FF R: 051 G: 000 B: 255
3333FF R: 051 G: 051 B: 255
3333CC R: 051 G: 051 B: 204
0066FF R: 000 G: 102 B: 255
0033FF R: 000 G: 051 B: 255
3366FF R: 051 G: 102 B: 255
3366CC R: 051 G: 102 B: 204
000066 R: 000 G: 000 B: 102
000033 R: 000 G: 000 B: 051
0000FF R: 000 G: 000 B: 255
000099 R: 000 G: 000 B: 153
0033CC R: 000 G: 051 B: 204
0000CC R: 000 G: 000 B: 204
336699 R: 051 G: 102 B: 153
0066CC R: 000 G: 102 B: 204
99CCFF R: 153 G: 204 B: 255
6699FF R: 102 G: 153 B: 255
003366 R: 000 G: 051 B: 102
6699CC R: 102 G: 153 B: 204
006699 R: 000 G: 102 B: 153
3399CC R: 051 G: 153 B: 204
0099CC R: 000 G: 153 B: 204
66CCFF R: 102 G: 204 B: 255
3399FF R: 051 G: 153 B: 255
003399 R: 000 G: 051 B: 153
0099FF R: 000 G: 153 B: 255
33CCFF R: 051 G: 204 B: 255
00CCFF R: 000 G: 204 B: 255
99FFFF R: 153 G: 255 B: 255
66FFFF R: 102 G: 255 B: 255
33FFFF R: 051 G: 255 B: 255
00FFFF R: 000 G: 255 B: 255
00CCCC R: 000 G: 204 B: 204
009999 R: 000 G: 153 B: 153
669999 R: 102 G: 153 B: 153
99CCCC R: 153 G: 204 B: 204
CCFFFF R: 204 G: 255 B: 255
33CCCC R: 051 G: 204 B: 204
66CCCC R: 102 G: 204 B: 204
339999 R: 051 G: 153 B: 153
336666 R: 051 G: 102 B: 102
006666 R: 000 G: 102 B: 102
003333 R: 000 G: 051 B: 051
00FFCC R: 000 G: 255 B: 204
33FFCC R: 051 G: 255 B: 204
33CC99 R: 051 G: 204 B: 153
00CC99 R: 000 G: 204 B: 153
66FFCC R: 102 G: 255 B: 204
99FFCC R: 153 G: 255 B: 204
00FF99 R: 000 G: 255 B: 153
339966 R: 051 G: 153 B: 102
006633 R: 000 G: 102 B: 051
336633 R: 051 G: 102 B: 051
669966 R: 102 G: 153 B: 102
66CC66 R: 102 G: 204 B: 102
99FF99 R: 153 G: 255 B: 153
66FF66 R: 102 G: 255 B: 102
339933 R: 051 G: 153 B: 051
99CC99 R: 153 G: 204 B: 153
66FF99 R: 102 G: 255 B: 153
33FF99 R: 051 G: 255 B: 153
33CC66 R: 051 G: 204 B: 102
00CC66 R: 000 G: 204 B: 102
66CC99 R: 102 G: 204 B: 153
009966 R: 000 G: 153 B: 102
009933 R: 000 G: 153 B: 051
33FF66 R: 051 G: 255 B: 102
00FF66 R: 000 G: 255 B: 102
CCFFCC R: 204 G: 255 B: 204
CCFF99 R: 204 G: 255 B: 153
99FF66 R: 153 G: 255 B: 102
99FF33 R: 153 G: 255 B: 051
00FF33 R: 000 G: 255 B: 051
33FF33 R: 051 G: 255 B: 051
00CC33 R: 000 G: 204 B: 051
33CC33 R: 051 G: 204 B: 051
66FF33 R: 102 G: 255 B: 051
00FF00 R: 000 G: 255 B: 000
66CC33 R: 102 G: 204 B: 051
006600 R: 000 G: 102 B: 000
003300 R: 000 G: 051 B: 000
009900 R: 000 G: 153 B: 000
33FF00 R: 051 G: 255 B: 000
66FF00 R: 102 G: 255 B: 000
99FF00 R: 153 G: 255 B: 000
66CC00 R: 102 G: 204 B: 000
00CC00 R: 000 G: 204 B: 000
33CC00 R: 051 G: 204 B: 000
339900 R: 051 G: 153 B: 000
99CC66 R: 153 G: 204 B: 102
669933 R: 102 G: 153 B: 051
99CC33 R: 153 G: 204 B: 051
336600 R: 051 G: 102 B: 000
669900 R: 102 G: 153 B: 000
99CC00 R: 153 G: 204 B: 000
CCFF66 R: 204 G: 255 B: 102
CCFF33 R: 204 G: 255 B: 051
CCFF00 R: 204 G: 255 B: 000
999900 R: 153 G: 153 B: 000
CCCC00 R: 204 G: 204 B: 000
CCCC33 R: 204 G: 204 B: 051
333300 R: 051 G: 051 B: 000
666600 R: 102 G: 102 B: 000
999933 R: 153 G: 153 B: 051
CCCC66 R: 204 G: 204 B: 102
666633 R: 102 G: 102 B: 051
999966 R: 153 G: 153 B: 102
CCCC99 R: 204 G: 204 B: 153
FFFFCC R: 255 G: 255 B: 204
FFFF99 R: 255 G: 255 B: 153
FFFF66 R: 255 G: 255 B: 102
FFFF33 R: 255 G: 255 B: 051
FFFF00 R: 255 G: 255 B: 000
FFCC00 R: 255 G: 204 B: 000
FFCC66 R: 255 G: 204 B: 102
FFCC33 R: 255 G: 204 B: 051
CC9933 R: 204 G: 153 B: 051
996600 R: 153 G: 102 B: 000
CC9900 R: 204 G: 153 B: 000
FF9900 R: 255 G: 153 B: 000
CC6600 R: 204 G: 102 B: 000
993300 R: 153 G: 051 B: 000
CC6633 R: 204 G: 102 B: 051
663300 R: 102 G: 051 B: 000
FF9966 R: 255 G: 153 B: 102
FF6633 R: 255 G: 102 B: 051
FF9933 R: 255 G: 153 B: 051
FF6600 R: 255 G: 102 B: 000
CC3300 R: 204 G: 051 B: 000
996633 R: 153 G: 102 B: 051
330000 R: 051 G: 000 B: 000
663333 R: 102 G: 051 B: 051
996666 R: 153 G: 102 B: 102
CC9999 R: 204 G: 153 B: 153
993333 R: 153 G: 051 B: 051
CC6666 R: 204 G: 102 B: 102
FFCCCC R: 255 G: 204 B: 204
FF3333 R: 255 G: 051 B: 051
CC3333 R: 204 G: 051 B: 051
FF6666 R: 255 G: 102 B: 102
660000 R: 102 G: 000 B: 000
990000 R: 153 G: 000 B: 000
CC0000 R: 204 G: 000 B: 000
FF0000 R: 255 G: 000 B: 000
FF3300 R: 255 G: 051 B: 000
CC9966 R: 204 G: 153 B: 102
FFCC99 R: 255 G: 204 B: 153
FFFFFF R: 255 G: 255 B: 255
CCCCCC R: 204 G: 204 B: 204
999999 R: 153 G: 153 B: 153
666666 R: 102 G: 102 B: 102
333333 R: 051 G: 051 B: 051
000000 R: 000 G: 000 B: 000

Color remote sensing images can be realized exploiting the additive properties of the primary colors.

The images collected by the sensor in three spectral bands are selected, and a primary color is assigned to each band.

A Color Composite image is obtained projecting simultaneously the three bands through the primary color that has been assigned to them.

In this way, the visual impact is improved and the spectral information is also displayed

Pixel Space

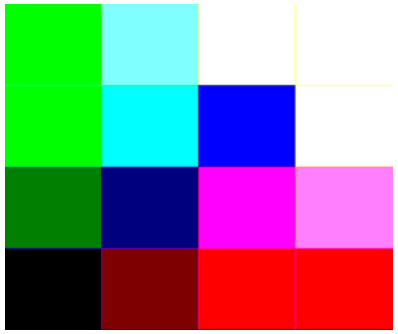

Band k1

0	127	255	255
0	0	0	255
0	0	255	255
0	127	255	255

Band k2

255	255	255	255
255	255	0	255
127	0	0	127
0	0	0	0

Band k3

0	255	255	255
0	255	255	255
0	127	255	255
0	0	0	0

R

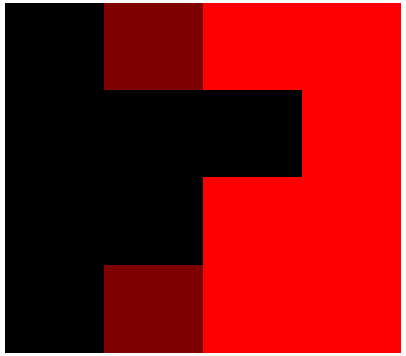

G

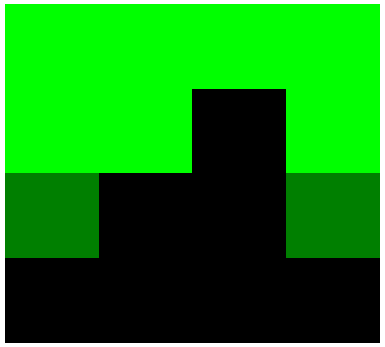

B

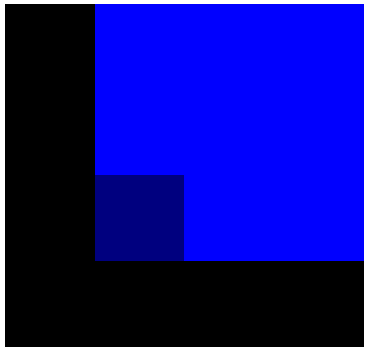

TM1 (0.45-0.52μ)

TM2 (0.52-0.6μ)

TM3 (0.63-0.69 μ)

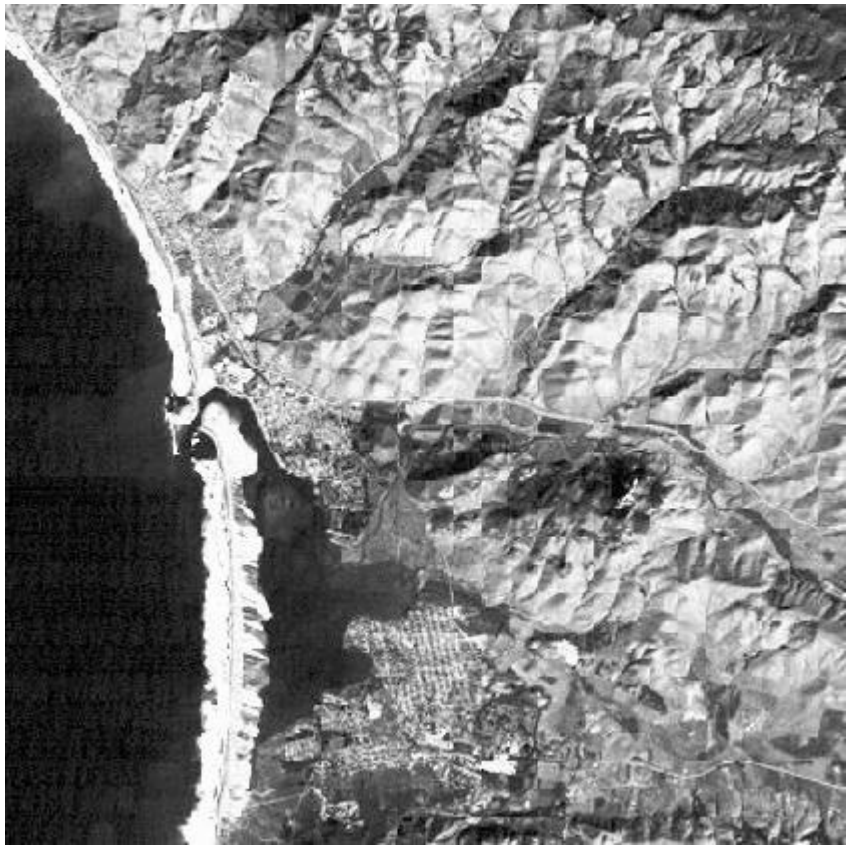

True color composite
TM1 – Blue
TM2 – Green
TM3 – Red

Spectral Signatures

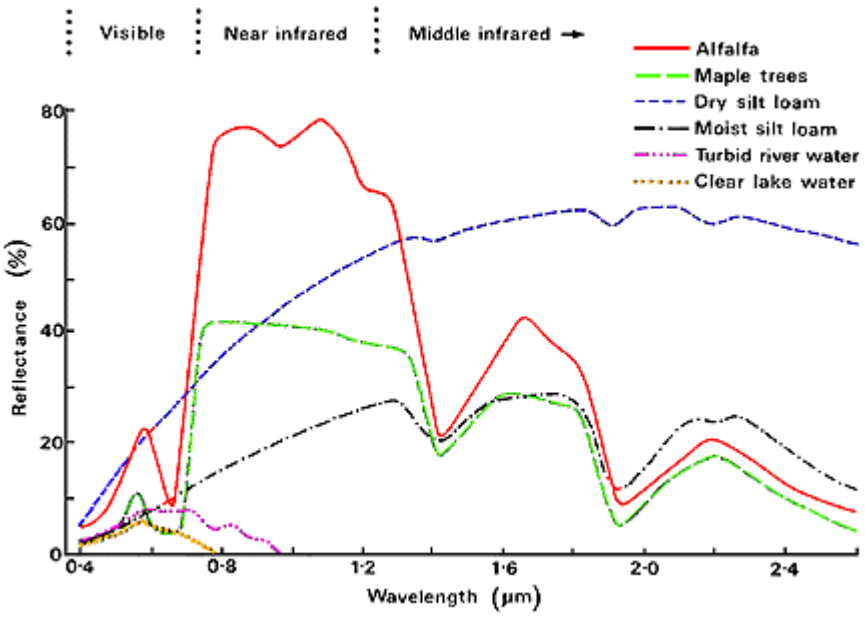

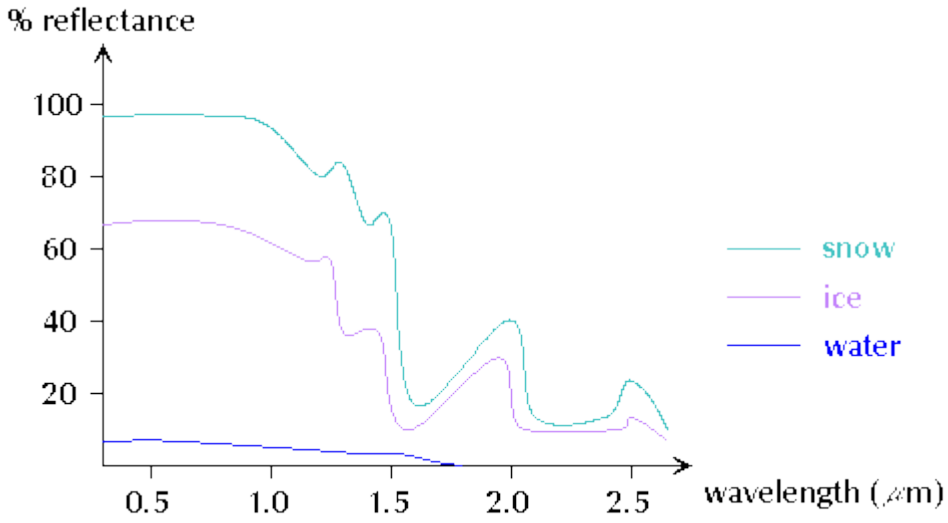

False color composite
TM2 (0.52-0.6μ) – Blue
TM3 (0.63-0.69μ) – Green
TM4 (0.76-0.9μ) - Red

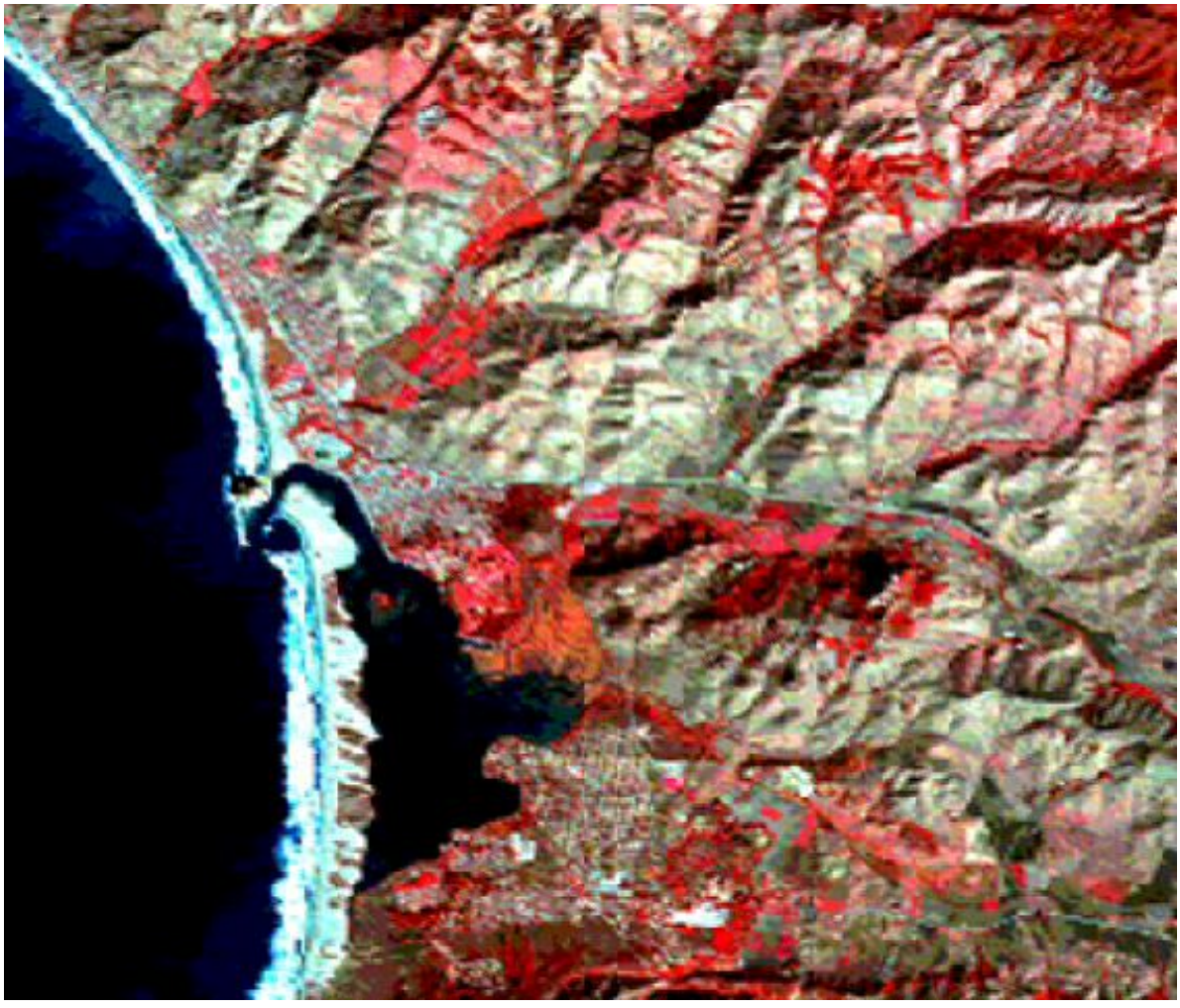

False color composite
TM5 (1.55-1.75μ) – Blue
TM7 (2.08-2.35μ) – Green
TM6 (10.4-12.5μ) - Red

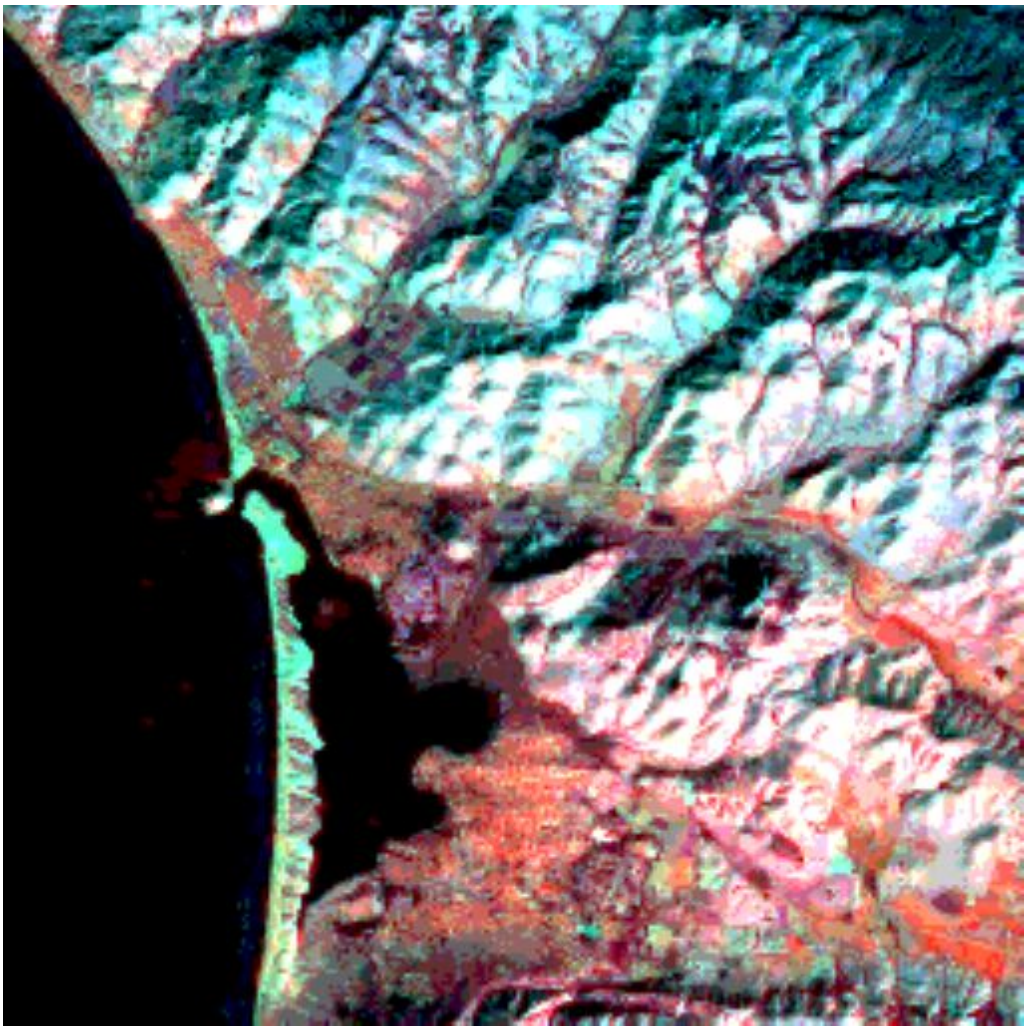

Ratio Images

Are built dividing the DN_{ij} of band k by the corresponding DN_{ij} of band l.

$$DN'_{ij} = \frac{DN_{ijk}}{DN_{ijl}} \qquad \begin{matrix} i=1 \div N_{rows} \\ j=1 \div N_{columns} \end{matrix}$$

They are used to enhance differences between bands.

Dark pixels = pixels with l band reflectance larger than k band reflectance.

Light pixels = pixels with k band reflectance larger than l band reflectance.

In order to display:

$$DN'_{ij} = R \cdot \tan^{-1} \frac{DN_{ijk}}{DN_{ijl}} \qquad \text{with } R=162.3$$

Band ratio can be applied to reduce the effects of topography or illumination conditions (shadows).

In addition, band ratio helps discrimination between soils and vegetation

Ratio Image TM4/TM1

Change Detection Images

involves the use of multi-temporal datasets with the aim of discriminating areas of land cover change between dates of imaging.

Image differencing (algebraic change detection) consists in subtracting one image from an image of the same site but acquired on a different date.

The resulting **DN**s can be positive, or negative in areas of radiance change, and zero values in areas of no change.

$$DN_{ijk} = DN_{ijk}^{(1)} - DN_{ijk}^{(2)} + c$$

See previous slide for the meaning of ijk

When 8-bit data are analyzed in this manner, the potential range of difference values in the change image is **[–255, 255].** The results can be transformed into positive values by adding a constant, **c** (e.g., 127).

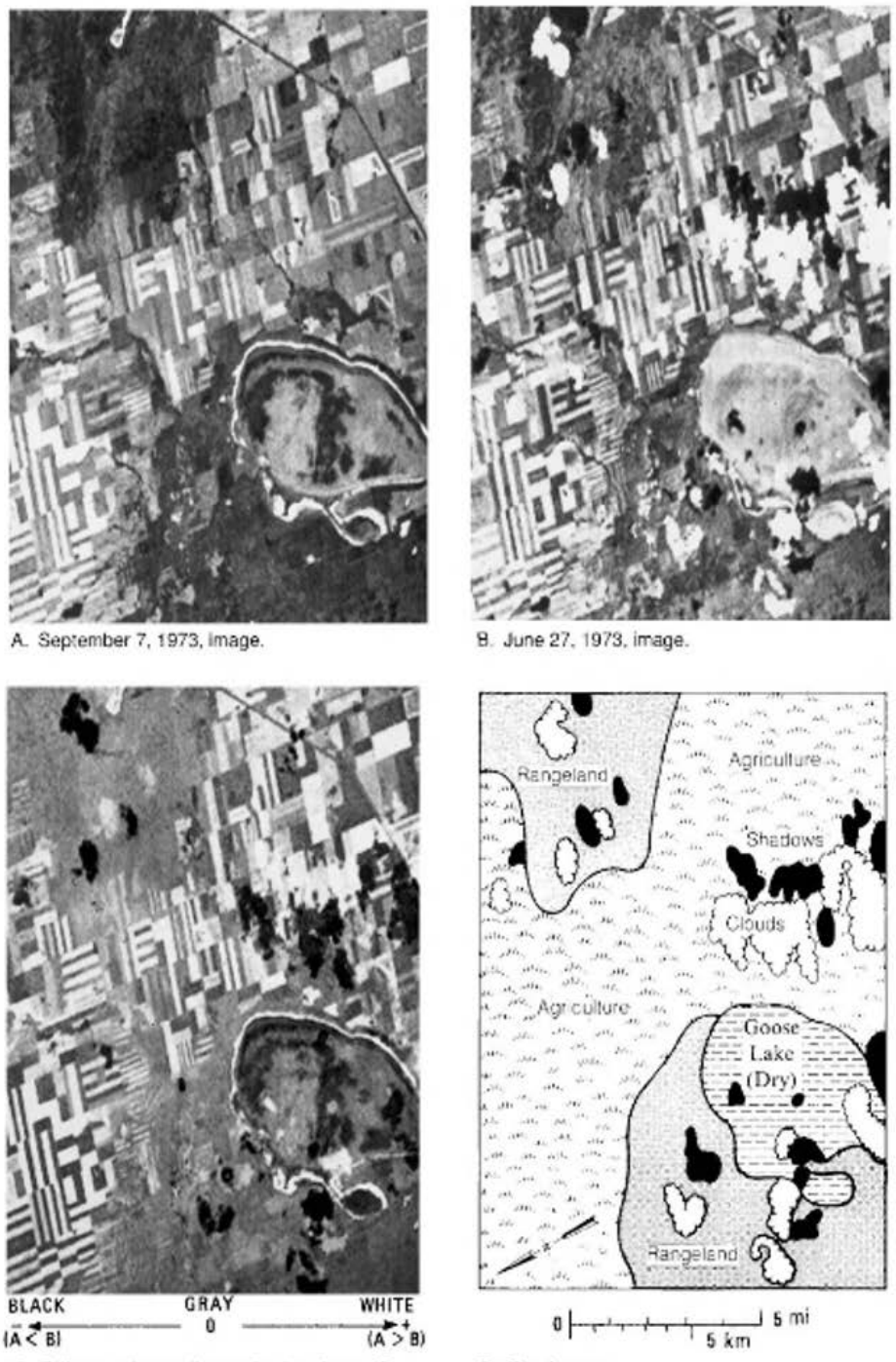

Figure 8-35 Change-detection image computed from seasonal Landsat MSS images, Saskatchewan, Canada. From Rifman and others (1975, Figures 2-14, 2-15, 2-17).

Black=pixels with negative change from date 1 to date 2
White = pixels with positive change

Change detection aims to:

- Detect all changes of interest that are **real**, e.g.
  - Deforestation
  - Flooding
  - Expansion of urban areas
  - Change in crop cover

- Avoid detecting changes that are **spurious** (false alarms), e.g.
  - Changes in viewing geometry and other sensor characteristics
  - Changes in atmosphere (e.g. cloud, cloud shadow, fog)
  - Changes in soil moisture
  - Normal vegetation growth

Change detection

To improve chances of detecting real change, use images …

- with accurate spatial registration (less than 0.5 pixel error)

- taken using the same sensor, i.e. with same:
  - Radiometric units (reflectance)
  - Spatial resolution
  - Radiometric resolution
  - Spectral resolution
  - View angle

- taken at same time of day

- taken at same time of year (anniversary images)
- with similar atmospheric conditions (cloud coverage <20%)

Radiance, band 4 (1975)

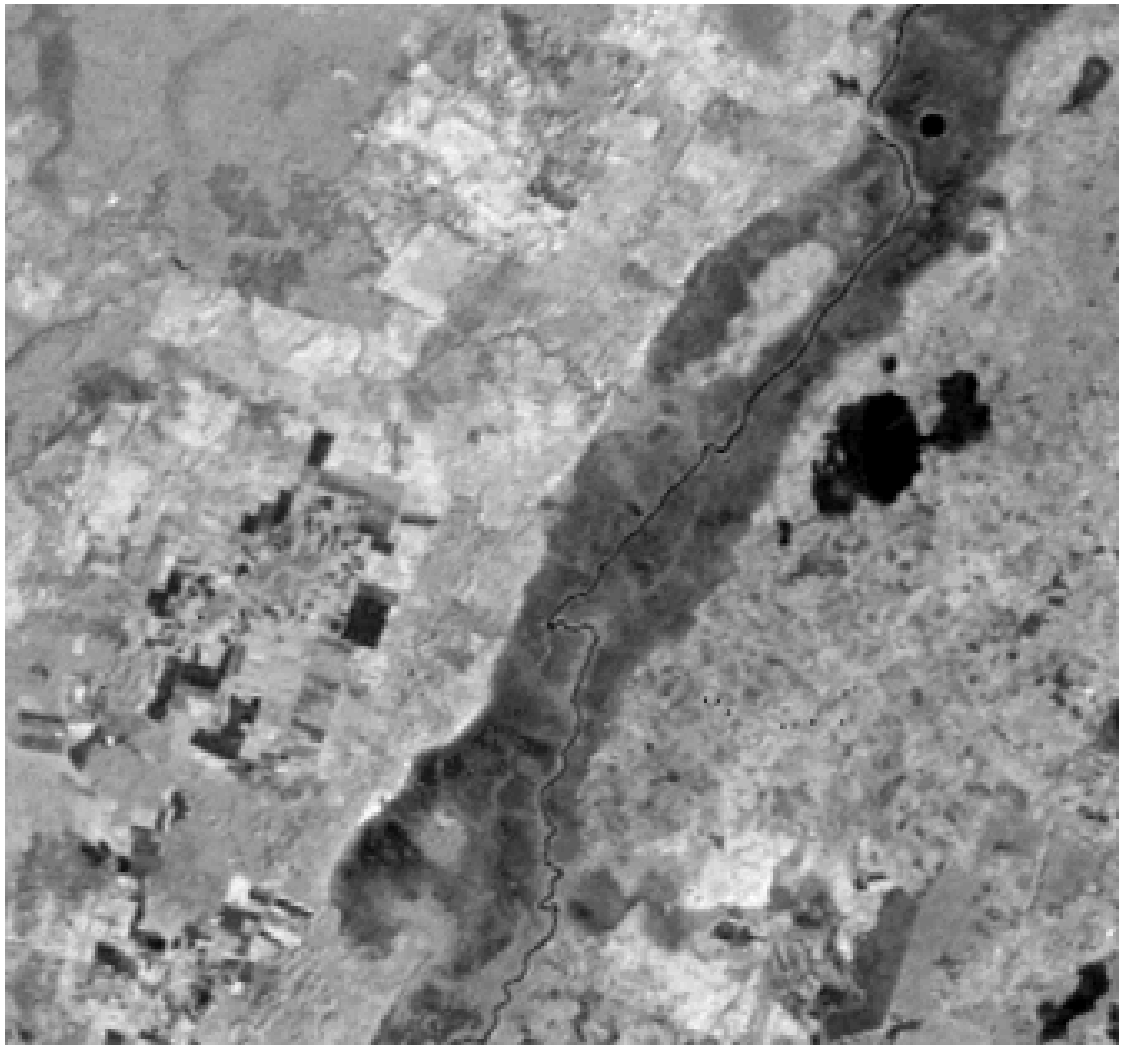

Radiance, band 4 (1984)

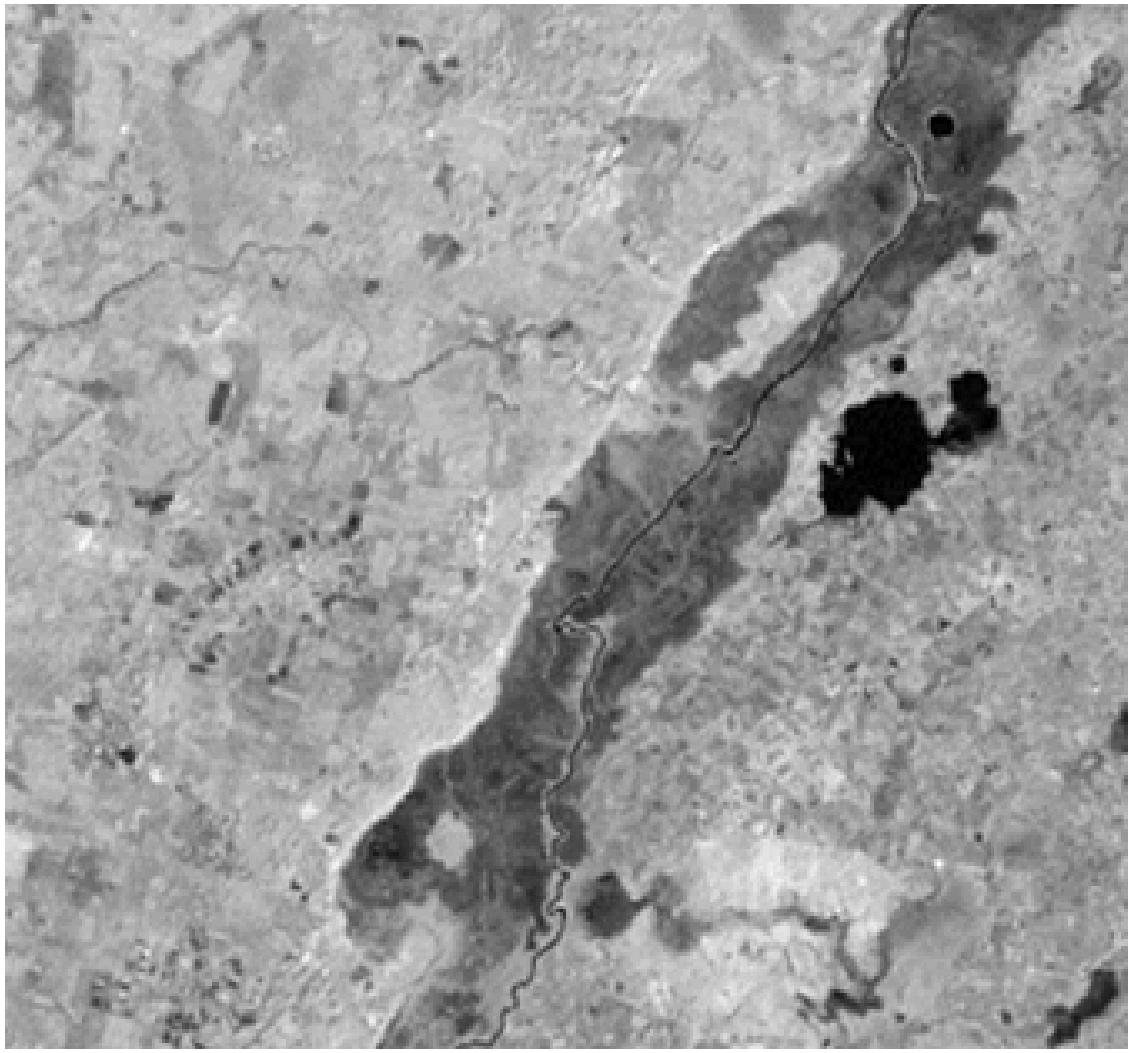

The change detection 75-84 between the non calibrated two images shows a histogram with mean value =-10.3

The change detection of the two calibrated images shows a histogram with mean value = 0.2

Multispectral Change Detection

LandSat TM 542

San Francisco Bay

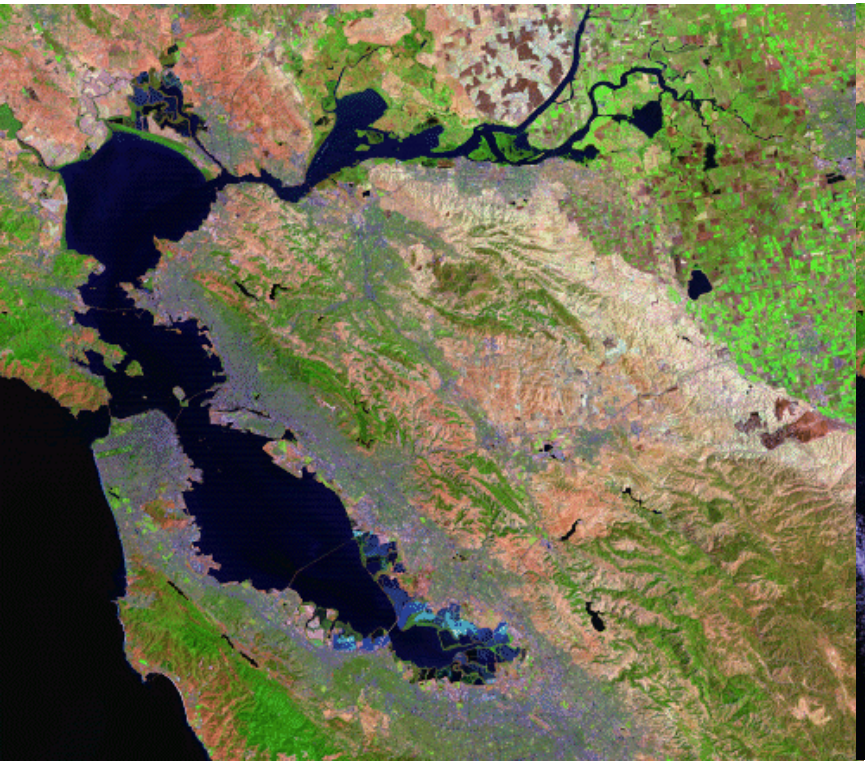

September 1984

September 1993

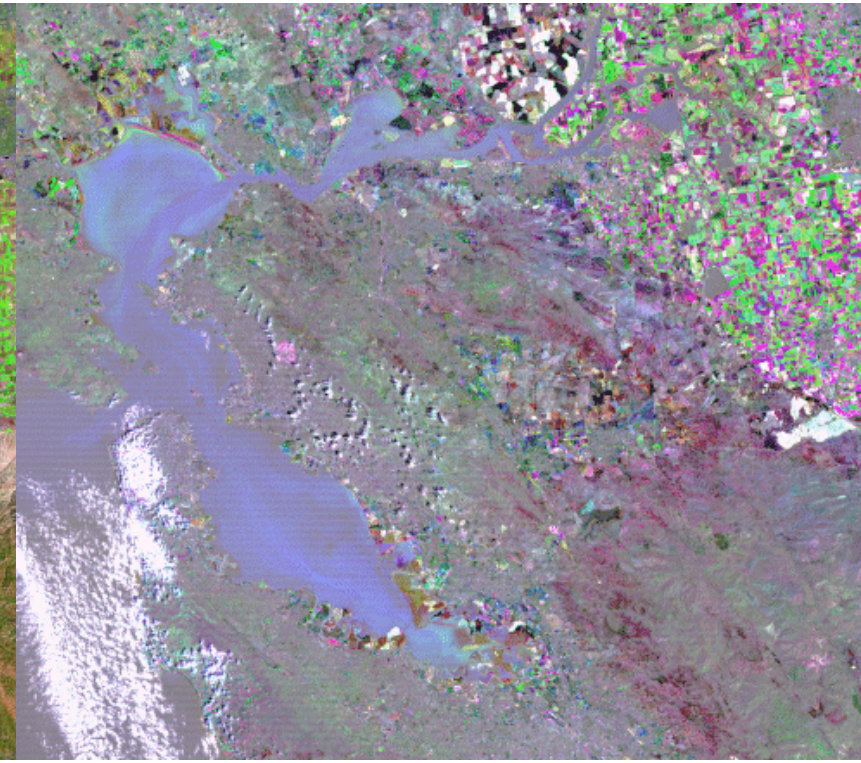

Change Detection
1993-1984

Multidate Visual Change detection

Can be realized displaying through RGB filters two or three radar images acquired on different dates.

Date 1 **Red**
Date 2 **Green**
Date 3 **Blue**

In order to compare only two dates, one filter remains unused, or the same date is projected through two different filters

ERS C-Band SAR
Prague
R & G August 16, 2002
B August 13, 1998

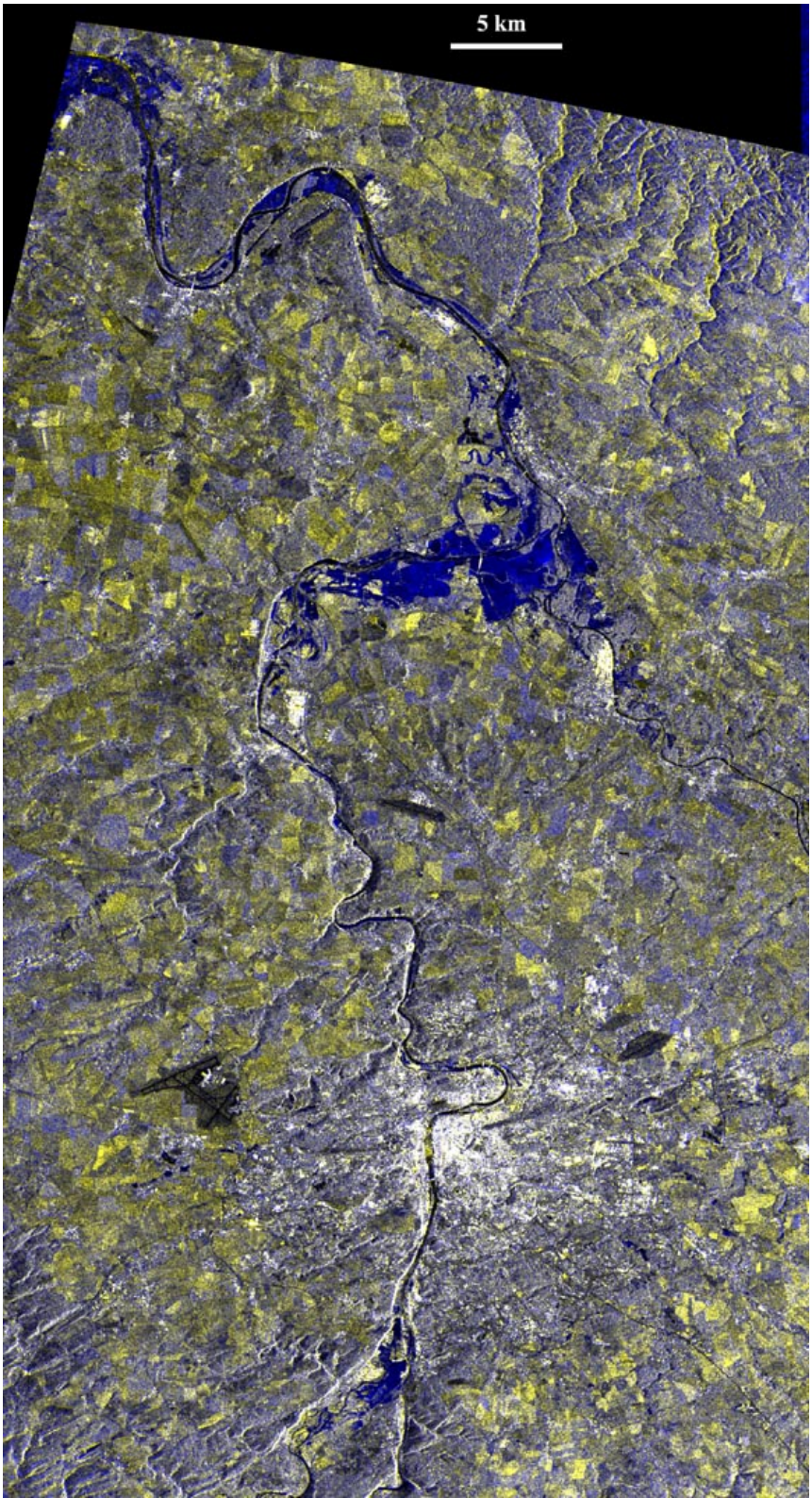

$\Gamma^{\parallel}$, - - $\Gamma^{\perp}$

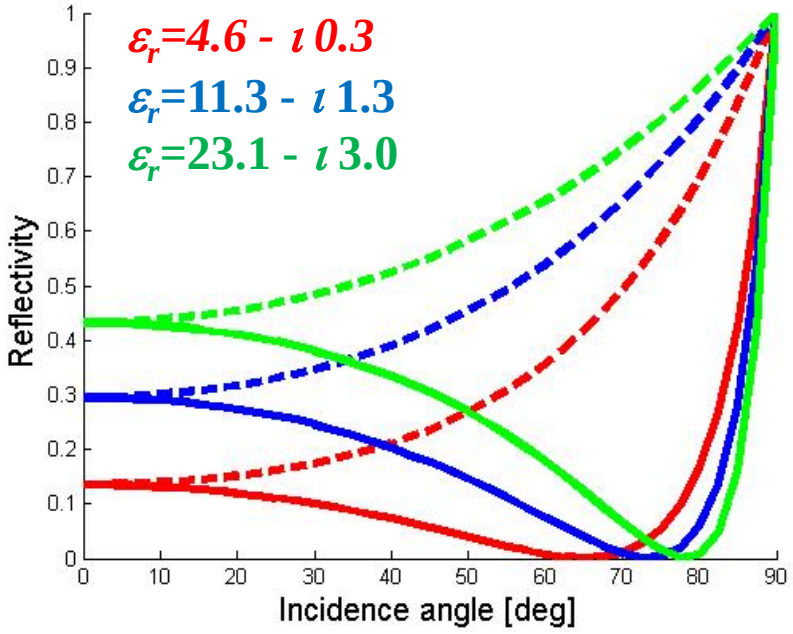

Increasing M_v

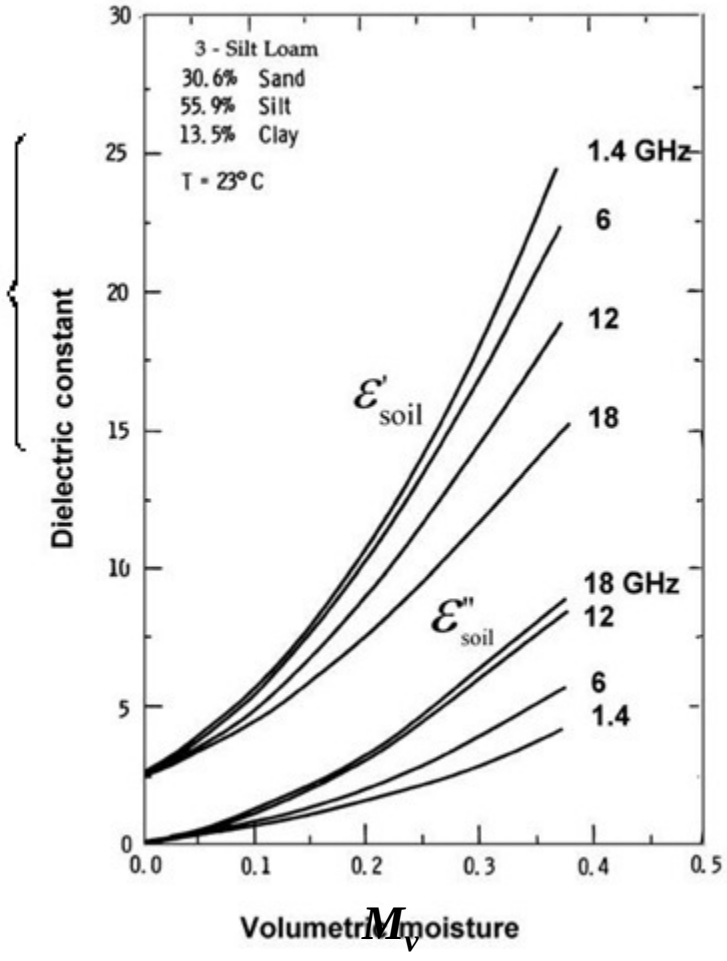

Flood Monitoring

Red River, Manitoba Spring 1996

March 23, 1996

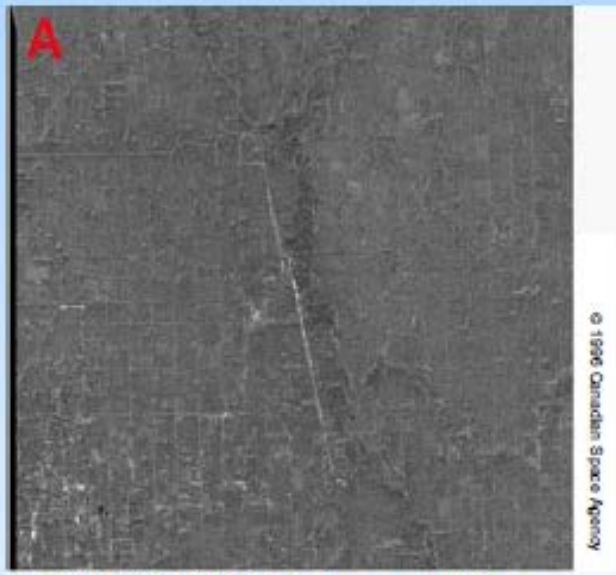

RADARSAT S1 ascending

April 25, 1996

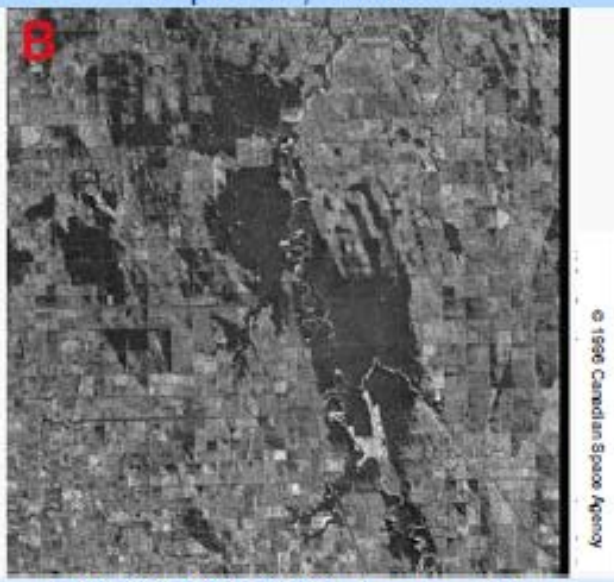

RADARSAT S1 descending

May 09, 1996

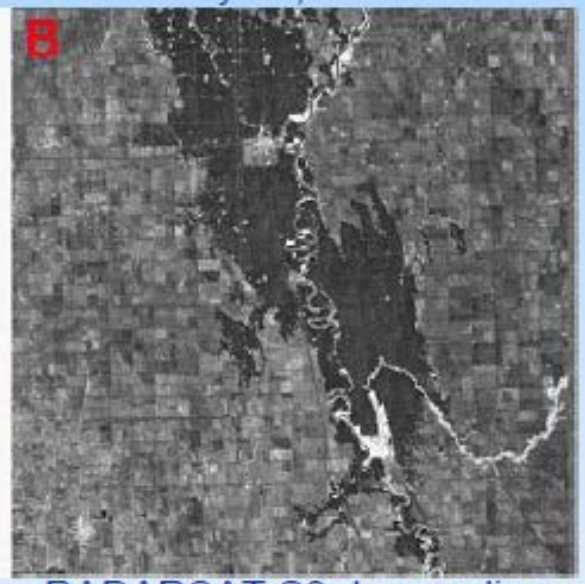

RADARSAT S3 descending

A During the acquisition on March 23, the site was covered by a thick layer of snow. The air tempterature was below the freezing point creating dry snow conditions transparent to the microwave. The ground was also frozen during the acquisition, which explains the lack of contrast between features on the image.

B The combination of above normal snow precipitation and late spring runoff created optimal conditions for the development of a flood event on the Red River. The flood extent on the April 25 and May 9 images is identified by the darker tones. The very bright features are classified as flooded standing vegetation.

Canada Centre for Remote Sensing, Natural Resources Canada

Source: Pultz, T.J., Yves Crevier, 1996.

GLOBE SAR

Flood Monitoring

Red River, Manitoba Spring 1996

C A color composite image was created using the May 9, April 25 and March 23 images. This RADARSAT color combination is showing the evolution of the flood during a 2 week period. The dark blue tones are classified as the common flood area on the two dates. The red features, located on the west side of the Red River, are identiifed as the flooded area on the early date. The blue/green surfaces, north of Morris, are flooded areas only on the later date. The yellow rectangle is the levee-protected town of Morris, located approximately 60 km south of Winnipeg. This example demonstrates the strong potential of RADARSAT for flood extent mapping, damage assessment and flood monitoring.

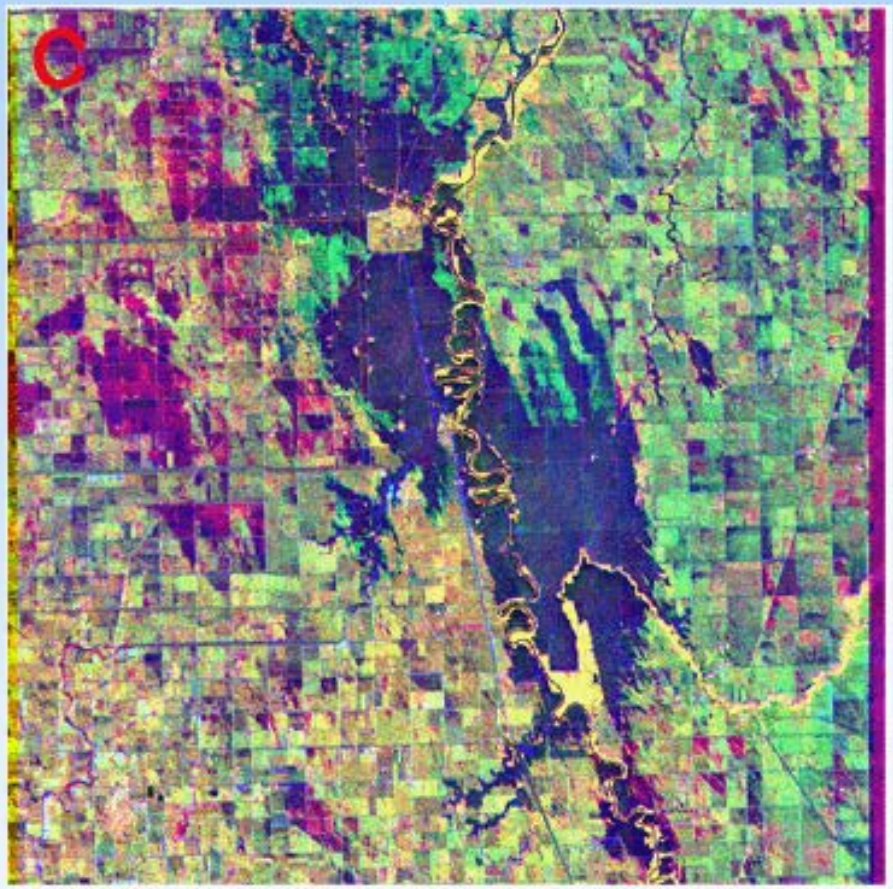

R=May 9 (F)
G=April 26 (F)
B=March 23 (NF)

Source: Pultz, T.J., Yves Crevier, 1996. "Early Demonstration of RADARSAT for Applications in Hydrology". Third International Workshop on Applications of Remote Sensing in Hydrology, Greenbelt, Maryland. October 16-18, pp.271-282.

Vegetation monitoring

It is important both for environmental reasons and for economical reasons.
Vegetation owns a spectral signature that is easily distinguished from that of bare soil.

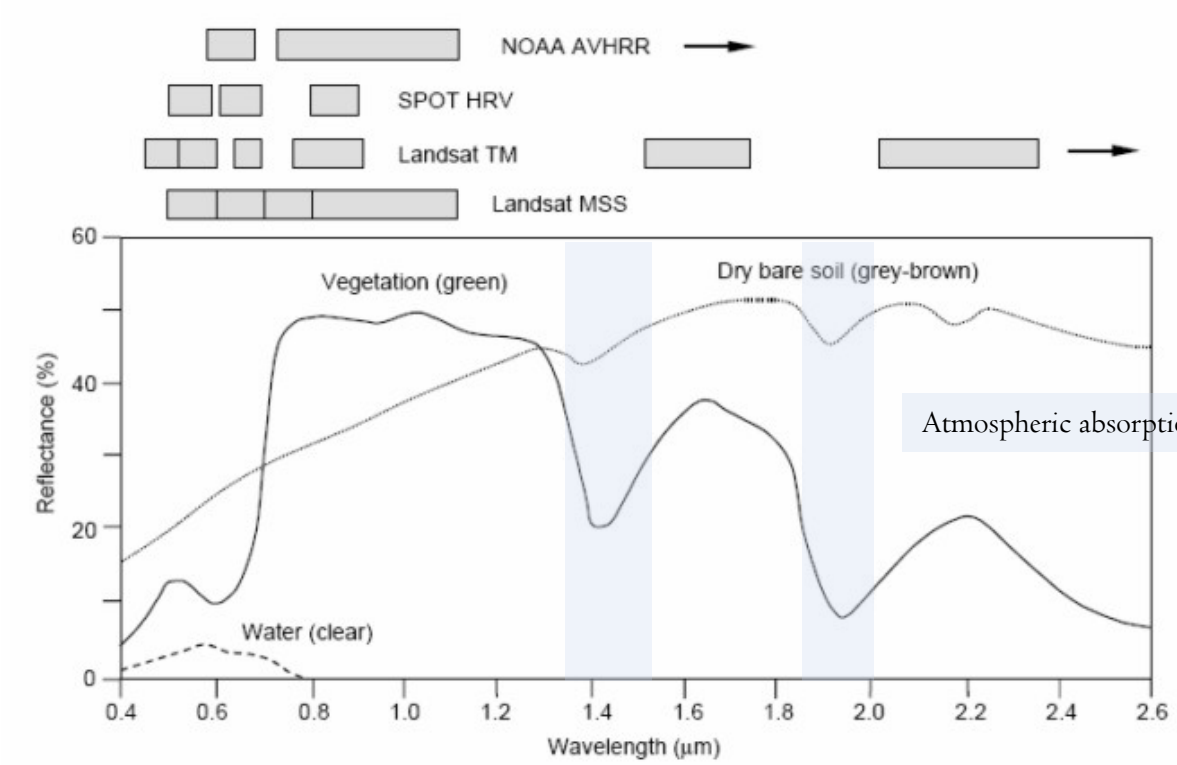

Spectral bands mostly used to discriminate vegetation are at green, red and Near IR wavelengths

diagrammatic cross section of a leaf ...high IR reflectance caused by cell structure

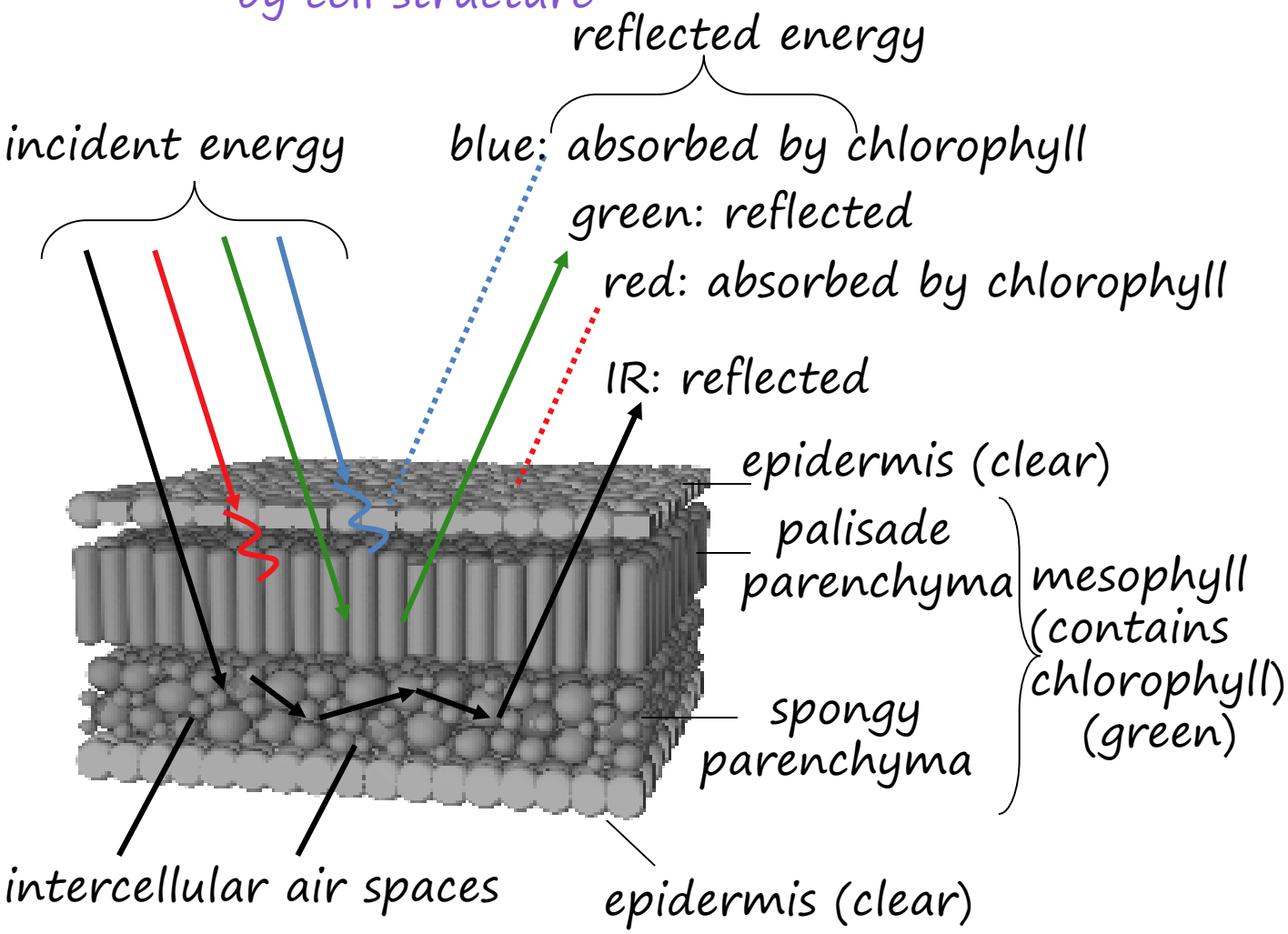

Chlorophyll in the epidermis and in the mesophyll absorbs blue and red light, whereas reflects green wavelength.
IR radiation is reflected by intercellular spaces in the innermost stratus.
Lack of water causes a collapse of the innermost stratus earlier than a modification of the chlorophyll concentration

Kansas: LandSat NIR FCC

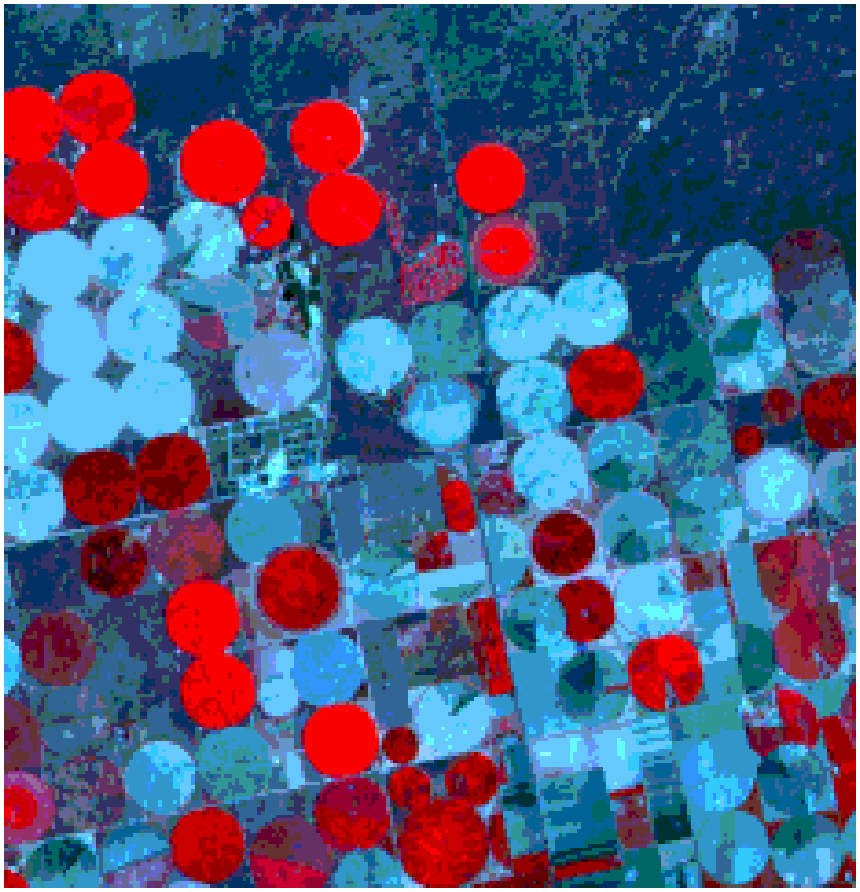

pivot irrigation

red circles: irrigated fields
of winter wheat
blue circles: fallow fields
Shades of red: lower wetness or
water lack

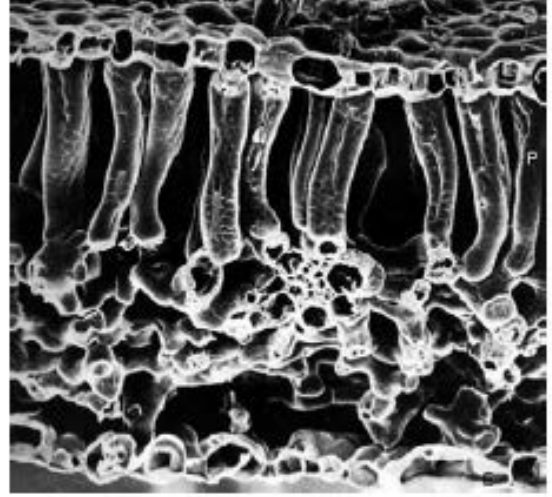

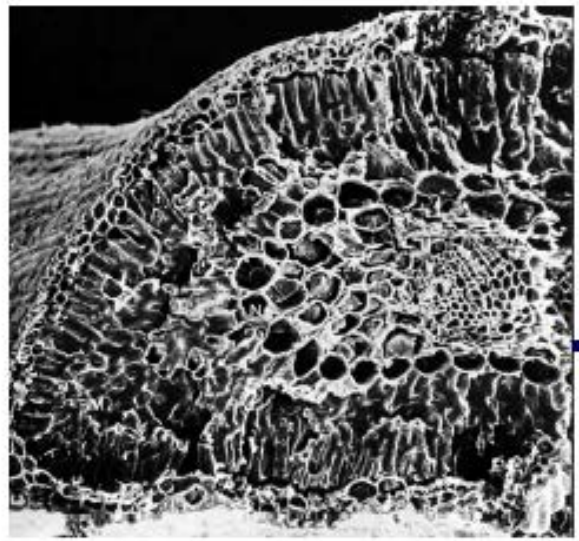

Maple & Pine reflectance$_\lambda$

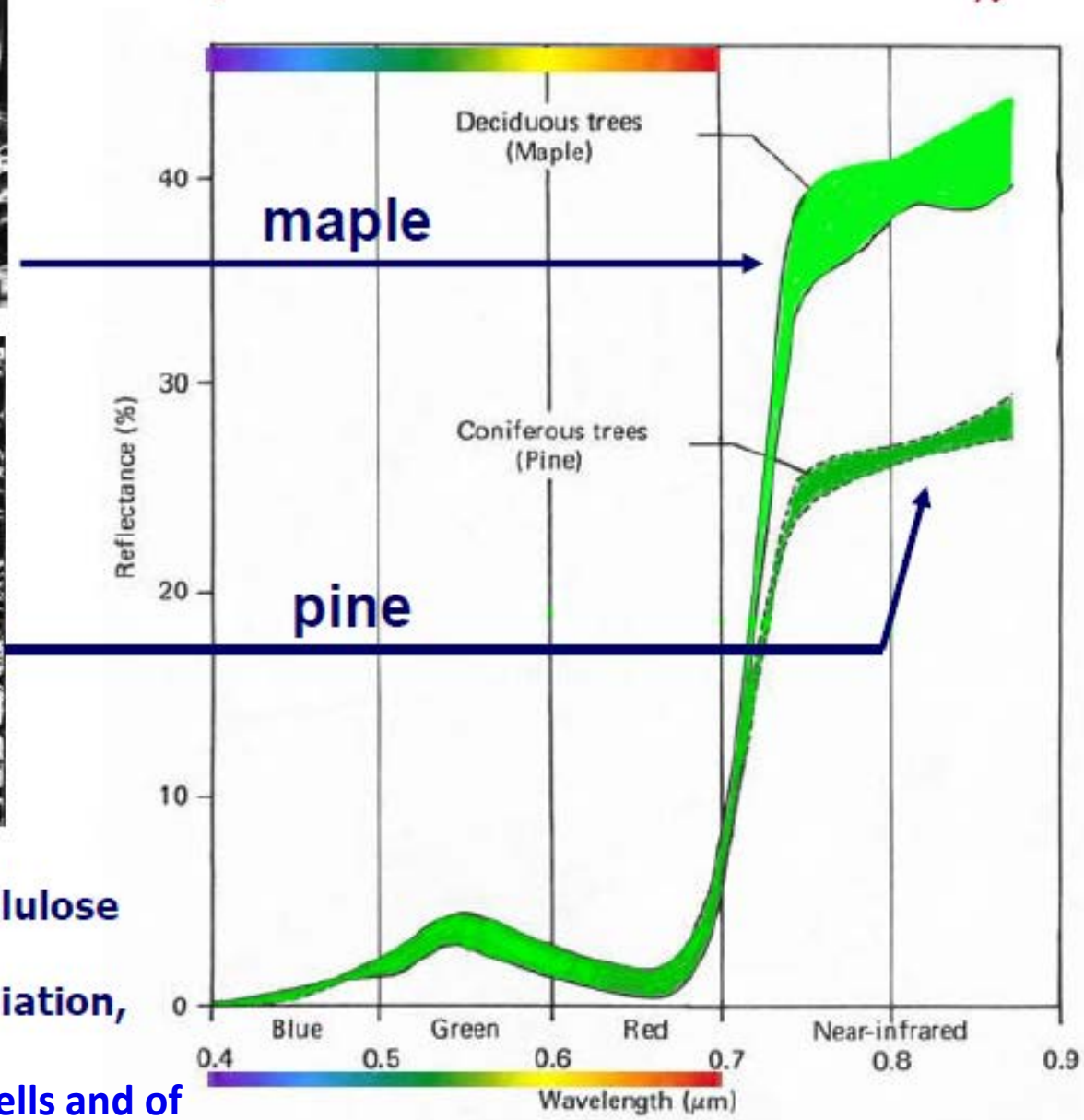

- Pine trees have higher cellulose content than maple trees
- Cellulose absorbs NIR radiation, and lowers reflectance

NIR reflection is influenced by the size of cells and of intercellular spaces in the mesophyll

The most famous parameter in vegetation monitoring is the

Normalized Difference of Vegetation Index

$$NDVI = \frac{NIR - R}{NIR + R}$$

$$-1 \le NDVI \le 1$$

NIR=DN or Radiance at NIR wavelength
R=DN or Radiance at Red wavelength

It is based on the contrast between the maximum absorption in the red due to chlorophyll pigments and the maximum reflection in the infrared caused by leaf cellular structure

High values indicate high concentration of green vegetation (***NDVI*>0.5**)
Low values indicate bare soils
Negative values indicate water, ice or snow

The NDVI allows meaningful comparisons of seasonal and inter-annual changes in vegetation growth.

AVHRR images are used to monitor vegetation on a global scale at periodic time scale.

NDVI bi-weekly maps

NOAA satellites provide two images per day with swath $W \sim 3000$ km.

- N_i cloudless images are selected
- Registration, radiometric calibration (and atmospheric correction) are performed
- $NDVI$ of each pixel is calculated
- Among the N_i values, the one with maximum $NDVI$ is selected for each pixel

European NDVI

NOAA AVHRR

March 1995

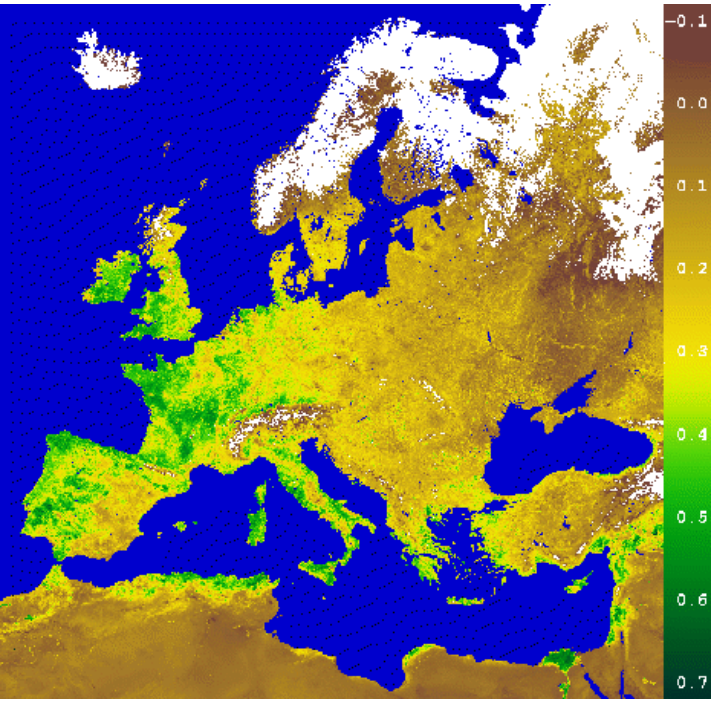

April 1995

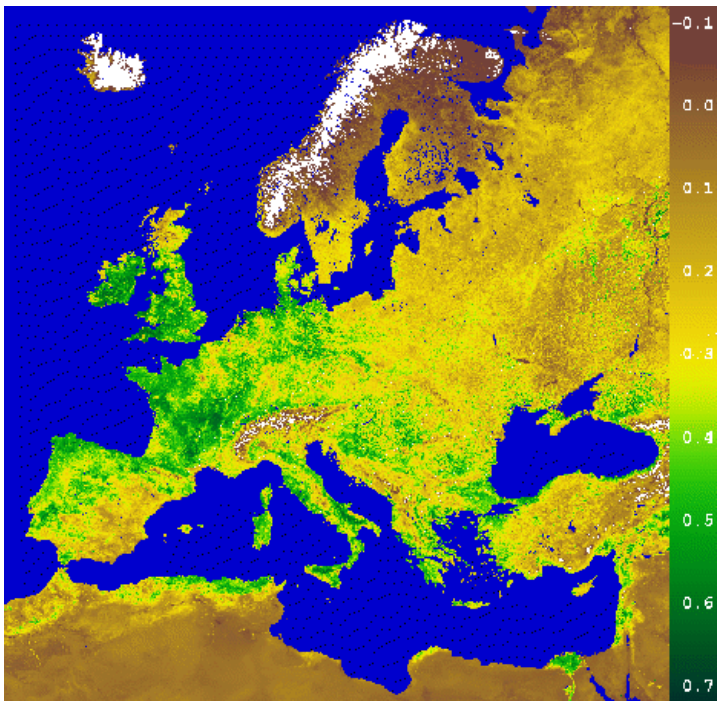

May 1995

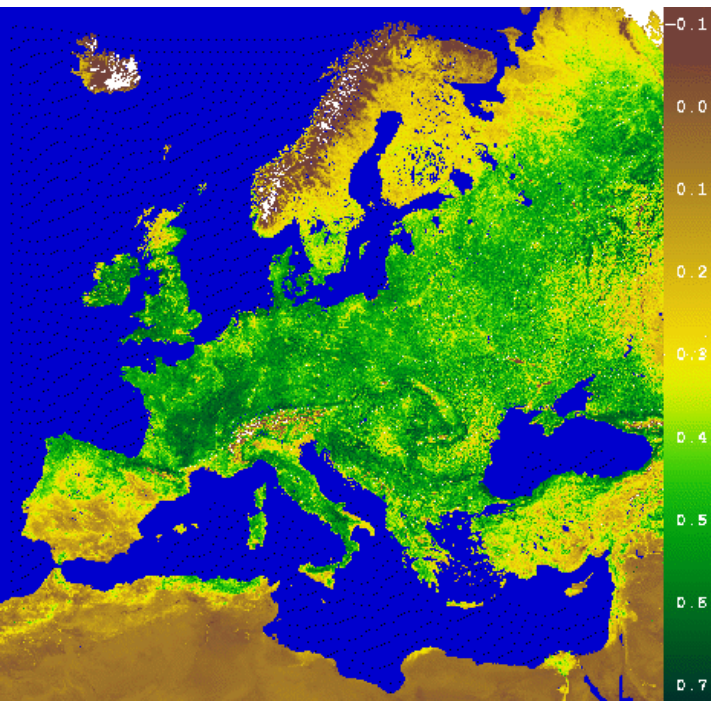

June 1995

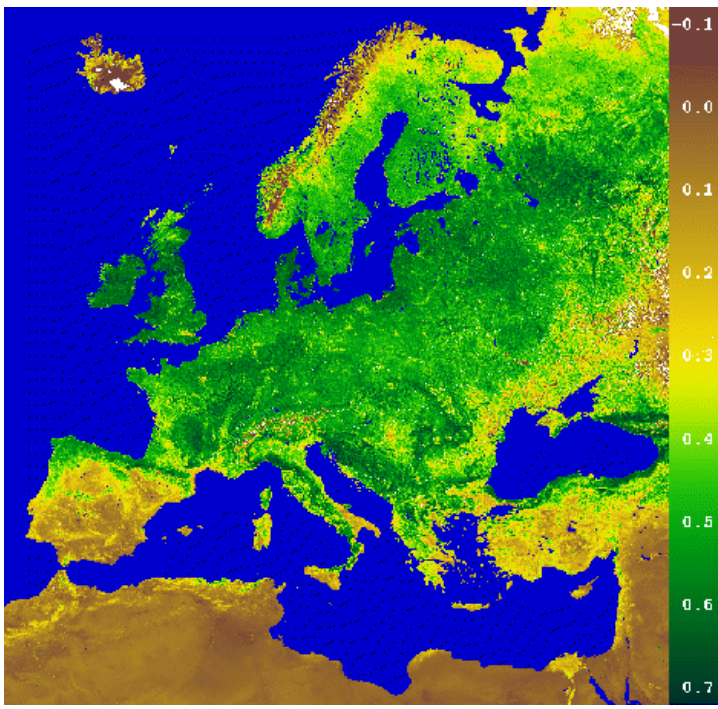

Surface Roughness

Surface roughness is the terrain property that most strongly influences the strength of the radar backscatter.

The surface roughness we are talking about is usually measured in centimeters,

i.e. *micro-relief surface roughness* characteristics,

rather than topographic relief.

Smooth ($\sigma^\circ \sim 0$)

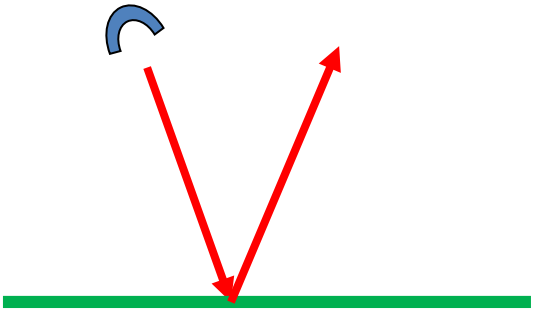

Moderately rough (σ° is low)

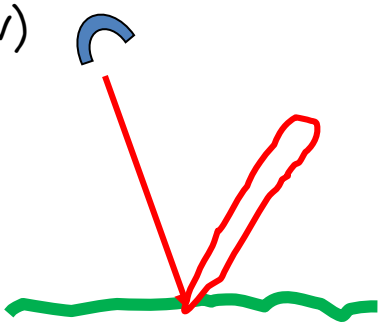

Very rough (σ° increases)

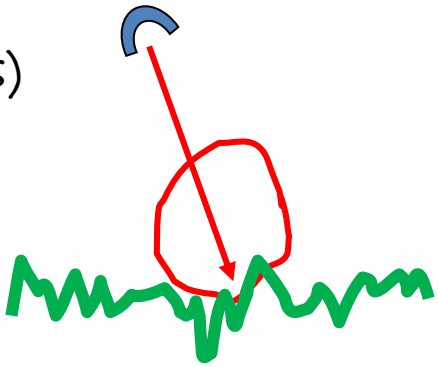

Bare soils

Effect of roughness on microwave (radar) scattering (by Ulaby, Moore, Fung, 82)

Ground based measurements (U.S.A.)
σ° vs. angle,
1.1 GHz (L band)

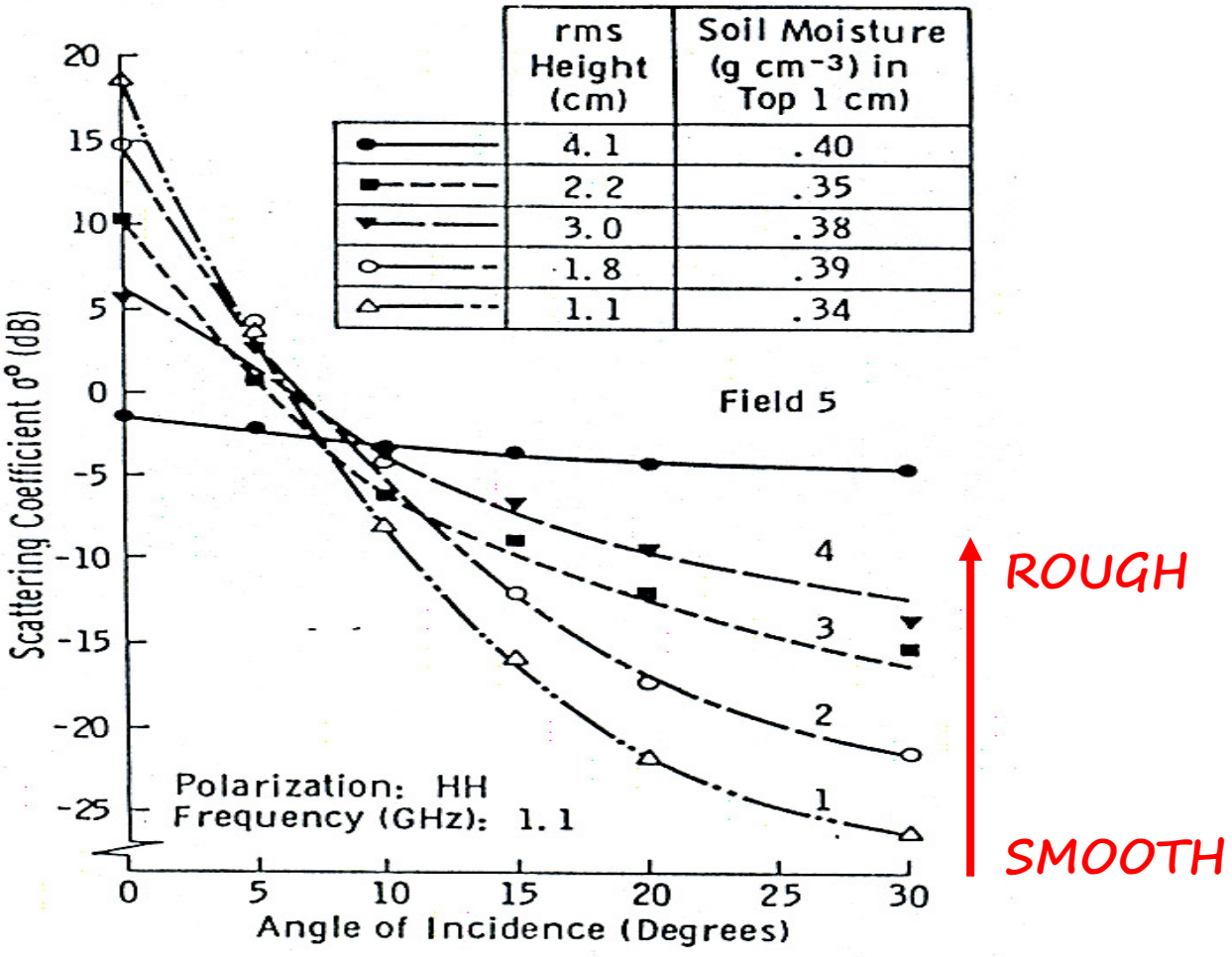

Target Parameters
~ Surface Roughness Parameters ~

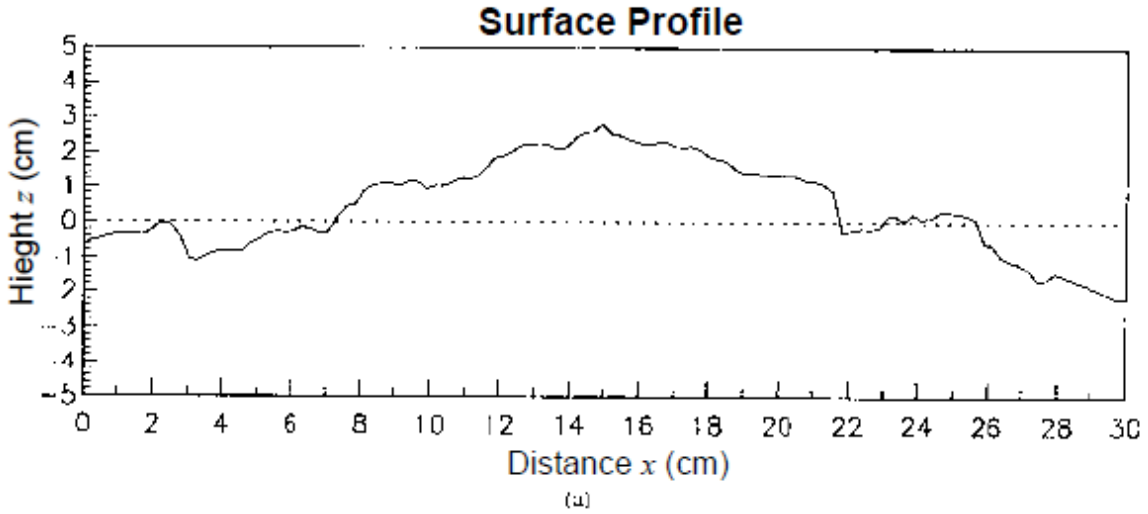

The standard deviation of surface height (σ) and the surface correlation length (l) are vertical and horizontal measures of surface roughness.

$$\sigma = \left[\frac{1}{N-1} \left(\sum_{i=1}^{N} (z_i)^2 - N(\overline{z})^2 \right) \right]^{1/2}$$

where $\overline{z} = \frac{1}{N} \sum_{i=1}^{N} z_i$

A surface may be considered electromagnetically "smooth" when

Rayleigh Criterion: $\sigma < \frac{\lambda}{8 \cos \theta}$

Fraunhofer Criterion: $\sigma < \frac{\lambda}{32 \cos \theta}$ (for targets where $\lambda \sim \sigma$)

σ=rms height, θ= incidence angle, λ=wavelength

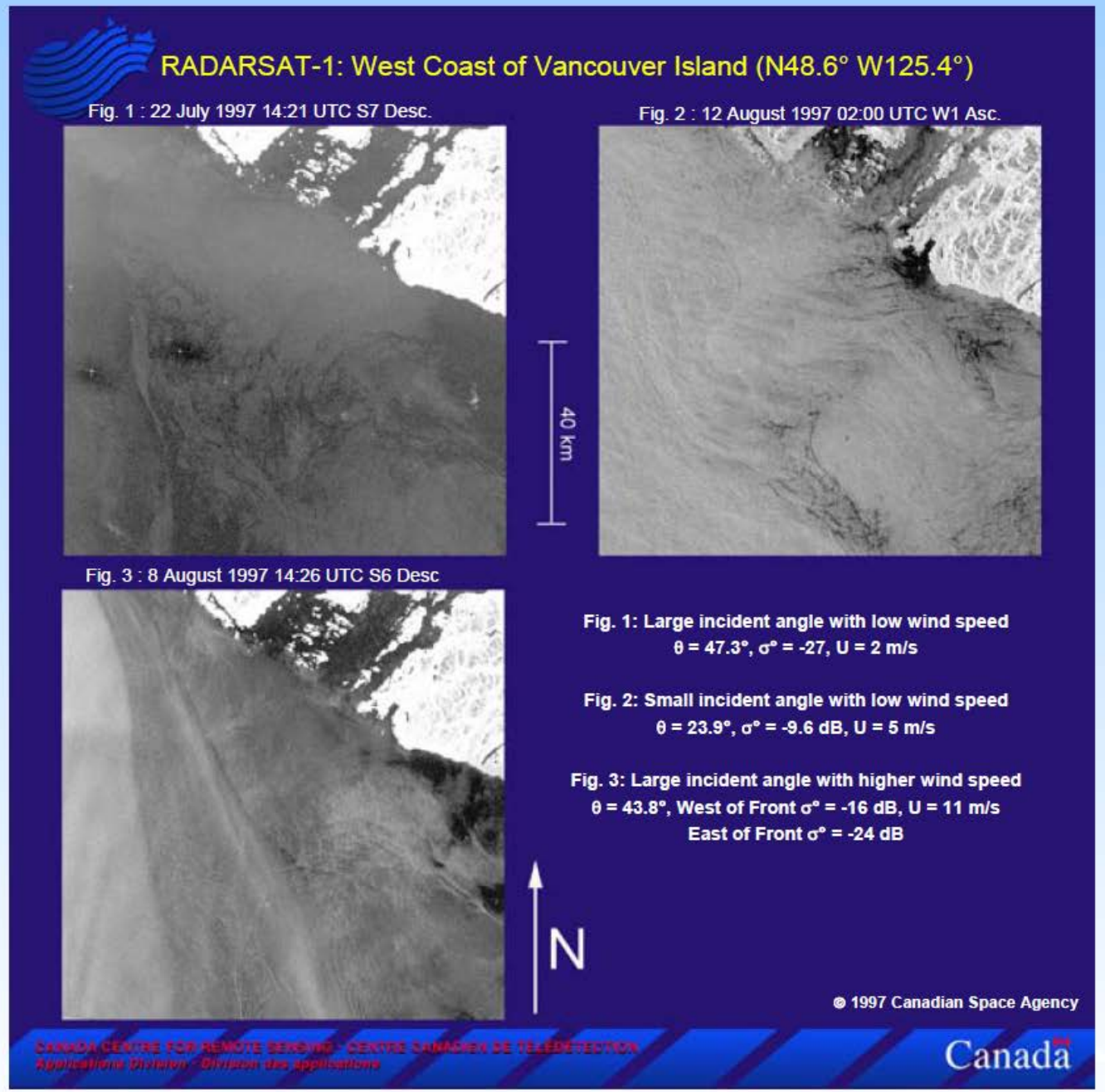

Vachon P. W. and R. Olsen, 1998

Wind Blowing over the Ocean Generates Waves

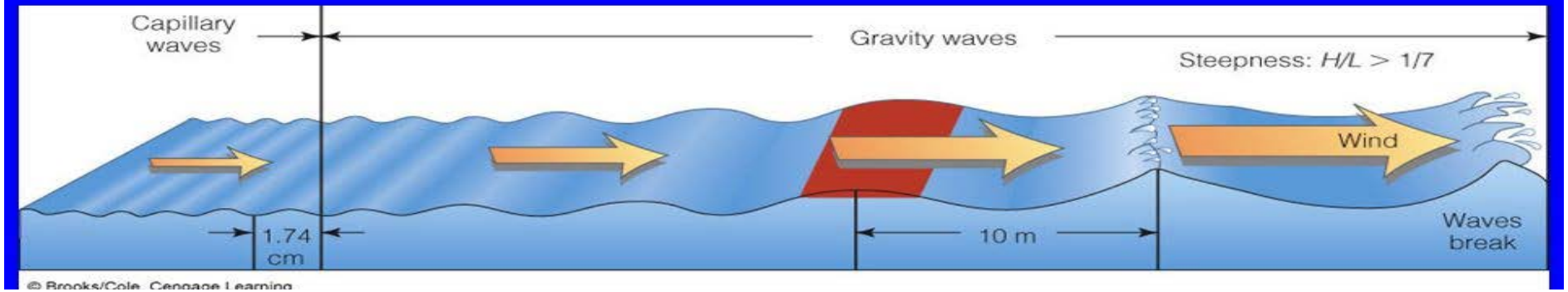

The sea surface is a complex superposition of waves with different wavelengths.
When the wind blows, it excites the **Capillary Waves** (with λ<1.7cm).
As the waves move farther, they get a longer wavelength and become **Gravity Waves** (with λ>1.7cm).
As the wind stops, capillary waves stop while gravity waves continue to propagate to larger distances for a longer time.
The backscattering coefficient from the sea is determined by roughness with wavelengths comparable with the radar wavelength, i.e., by capillary waves.
The roughness of the capillary waves is correlated with the wind speed

The dependence of the backscattering coefficient on wind velocity v and direction φ over ocean is described by:

$$\sigma^0 = a_0 + a_1 \cos\varphi + a_2 \cos 2\varphi$$

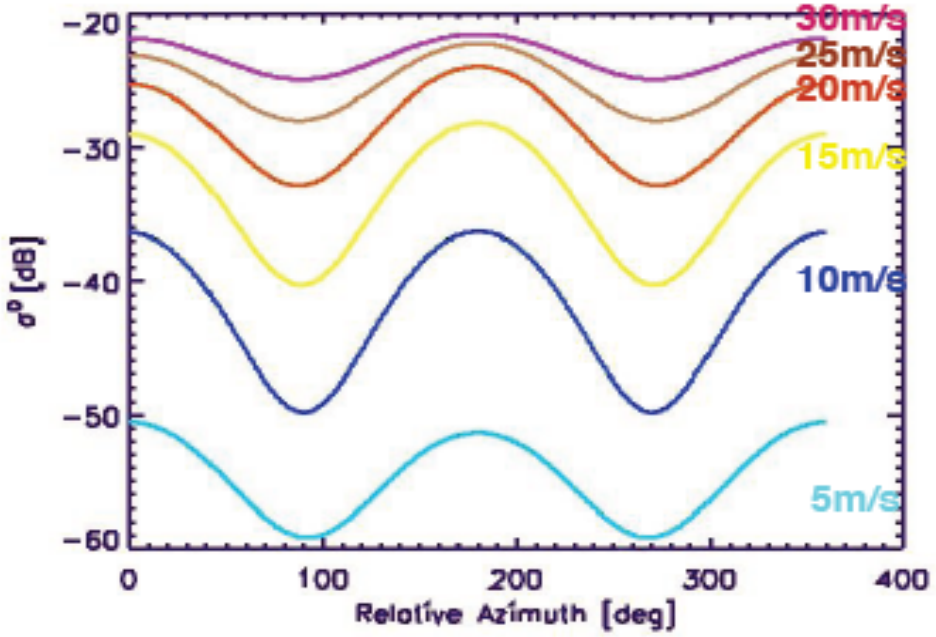

The coefficients a_i are functions of incidence angle ϑ and of wind velocity v

$$a_i = A_i(\vartheta) v^{\gamma}$$

A_i and γ have been determined empirically on the basis of a huge number of experimental data.
φ is the angle between wind direction and backscattering direction

Radar illumination

Top view

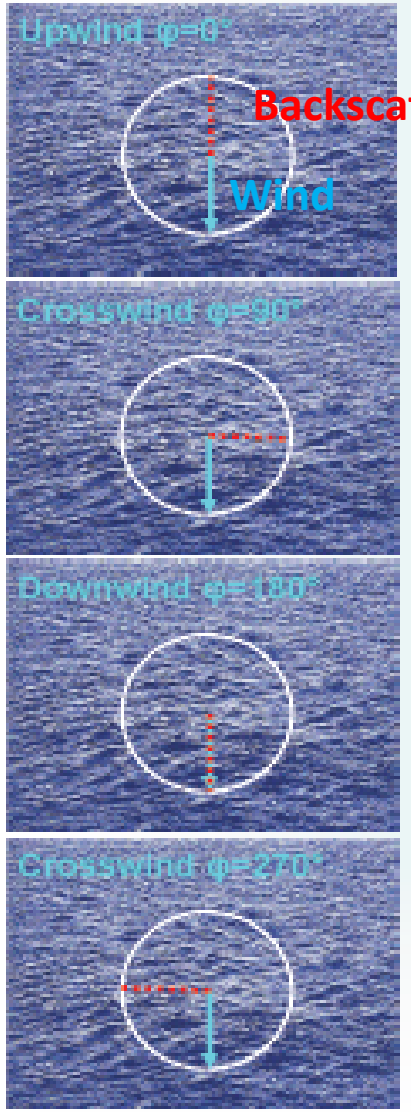

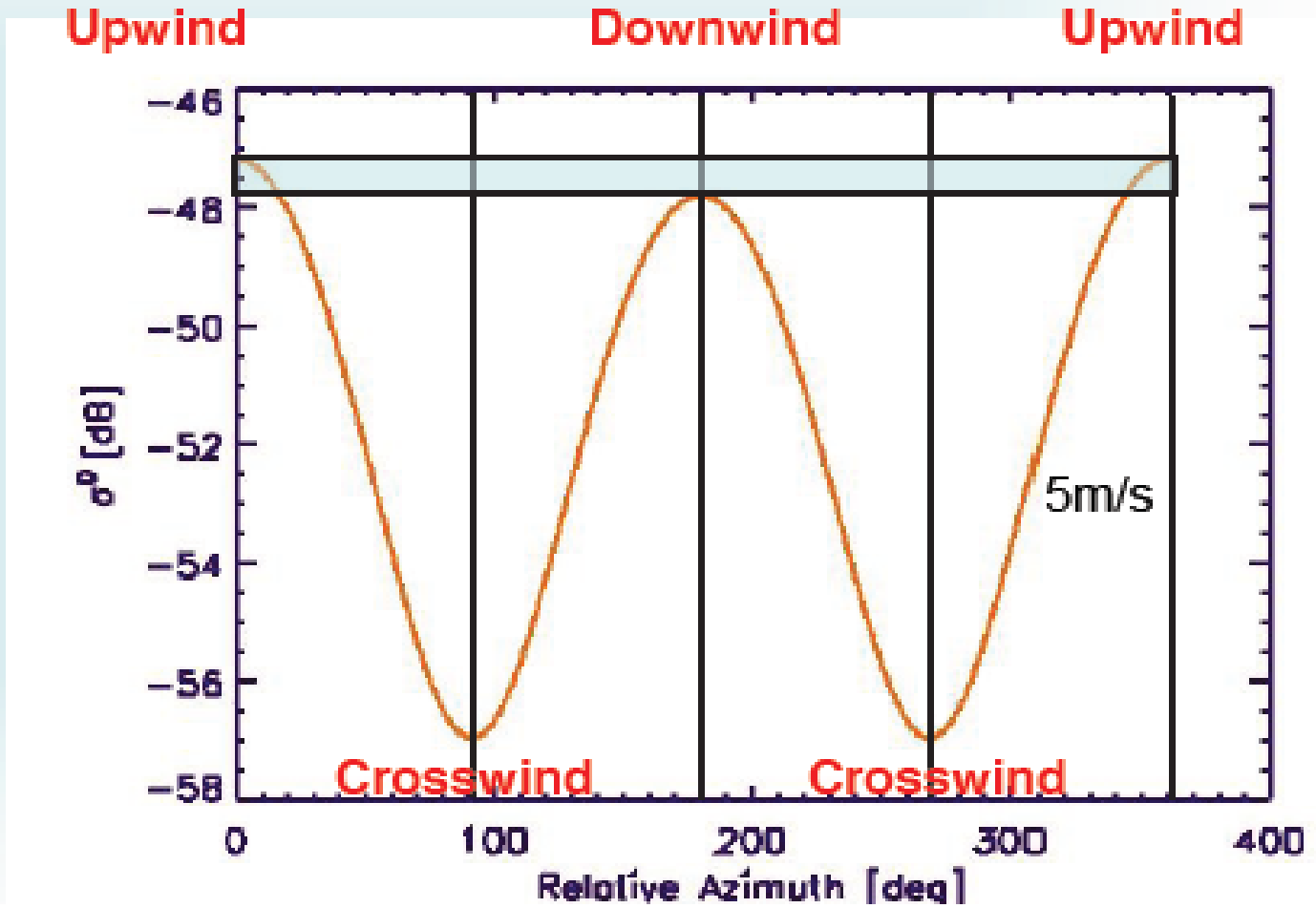

Easier to distinguish wind direction when winds blowing toward or away from satellite than blowing across track

Assume we have two measurements of the same sea surface performed with two different azimuth angles:

$$\sigma_1^0 = A_0 v^\gamma + A_1 v^\gamma \cos\varphi_1 + A_2 v^\gamma \cos 2\varphi_1$$

$$\sigma_2^0 = A_0 v^\gamma + A_1 v^\gamma \cos\varphi_2 + A_2 v^\gamma \cos 2\varphi_2$$

And that the measurements are performed with two antennas at 90° to each other:

$$\varphi_2 = \varphi_1 + 90$$

$$v = \left(\frac{\sigma_1^0}{A_0 + A_1 \cos\varphi_1 + A_2 \cos 2\varphi_1}\right)^{\frac{1}{\gamma}}$$

$$v = \left(\frac{\sigma_2^0}{A_0 + A_1 \cos(\varphi_1 + 90) + A_2 \cos 2(\varphi_1 + 90)}\right)^{\frac{1}{\gamma}}$$

Since we have 2 equations with two unknowns (v and φ), we can solve the problem.

Graphic solution:

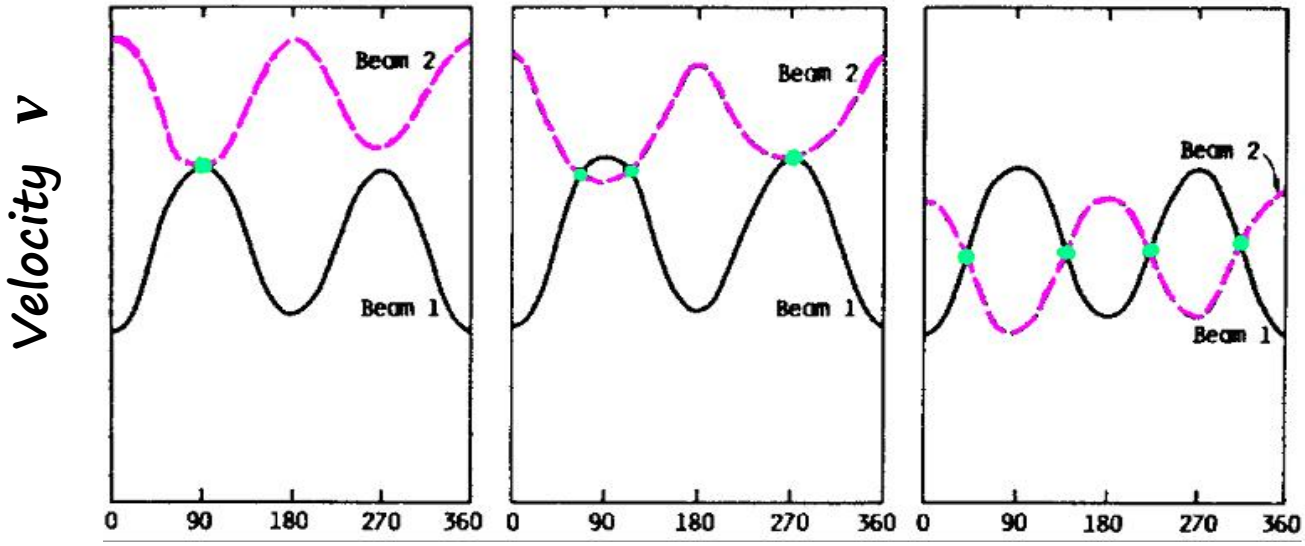

Azimuth angle φ

If only one measurement of σ^0 (continuous line) is available,
it is not possible to retrieve a univoque v and φ.

Even with two measurements, collected by two scatterometers oriented at 90° from each other,
it is not possible to solve the ambiguity.

With two measurements at 90° to each other, usually you get 2 couples of solutions. Each couple has the same direction but opposite sense:

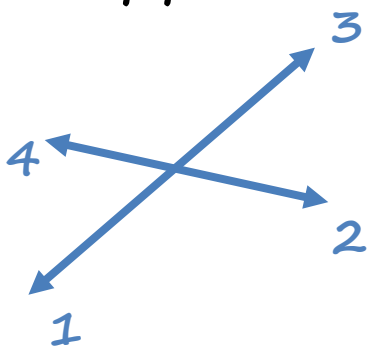

The ambiguity can be solved with ground processing using ancillary data, for example wind measurements along the coasts.

At least three measurements are necessary.

The wind-scatterometer is essentially a satellite RAR with three antennas at 45° to each other and with ground resolution of tens of kilometers.

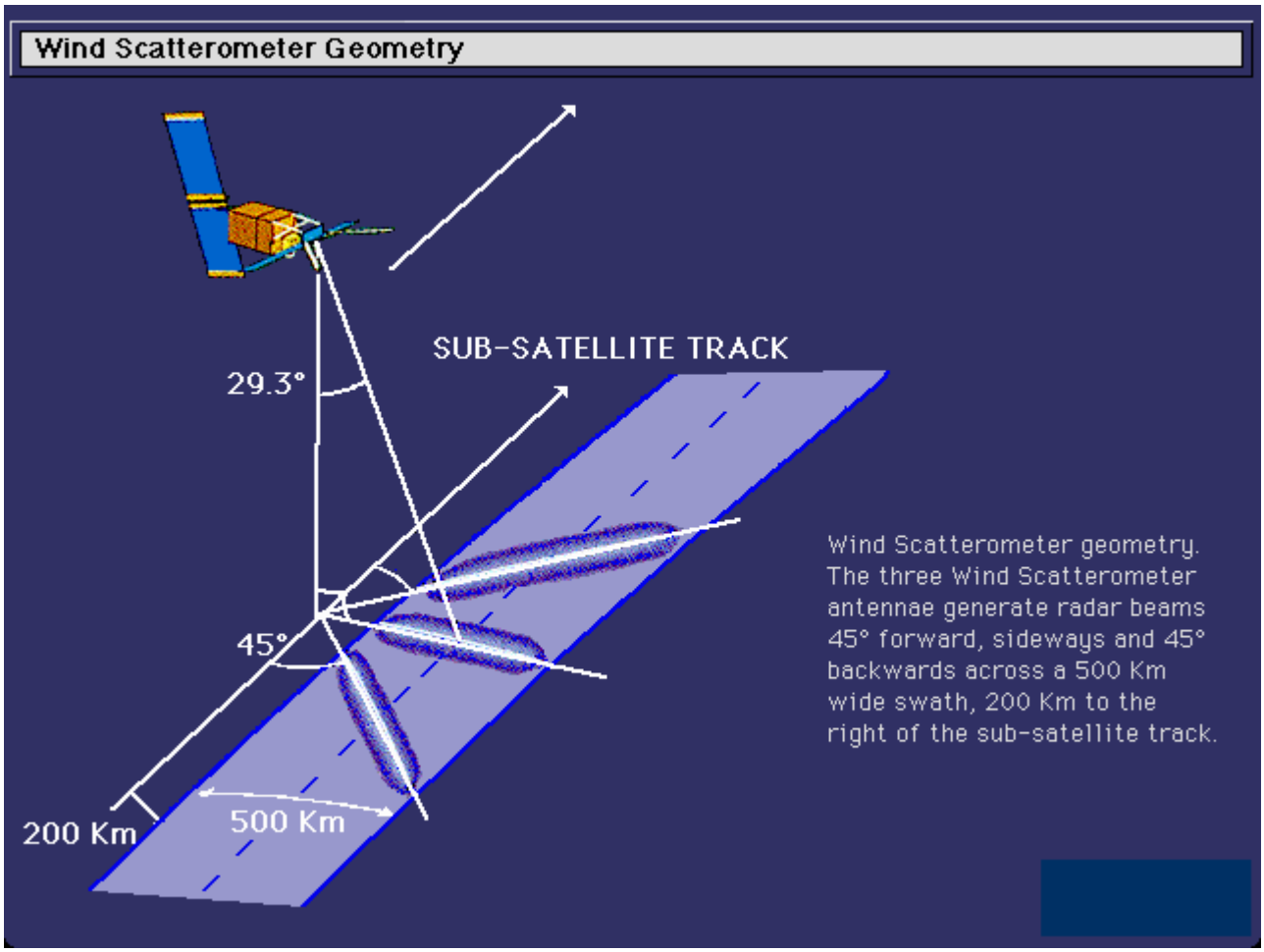

The purpose of the Wind Scatterometer is to obtain information on wind speed and direction at the sea surface for incorporation into models, global statistics and climatological datasets. It operates by recording the change in radar backscattering of the sea due to the perturbation of small ripples by the wind close to the surface. This is possible because the radar backscatter returned to the satellite is modified by wind-driven ripples on the ocean surface and, since the roughness in these ripples increases with wind velocity, backscatter increases with wind velocity.

The three antennae generate radar beams looking 45deg. forward, sideways, and 45deg. backwards with respect to the satellite's flight direction. These beams continuously illuminate a 500 km wide swath (see the figure) as the satellite moves along its orbit. Thus three backscatter measurements of each grid point are obtained at different viewing angles and separated by a short time delay. These "triplets" are fed to a mathematical model which calculates surface wind speed and direction.

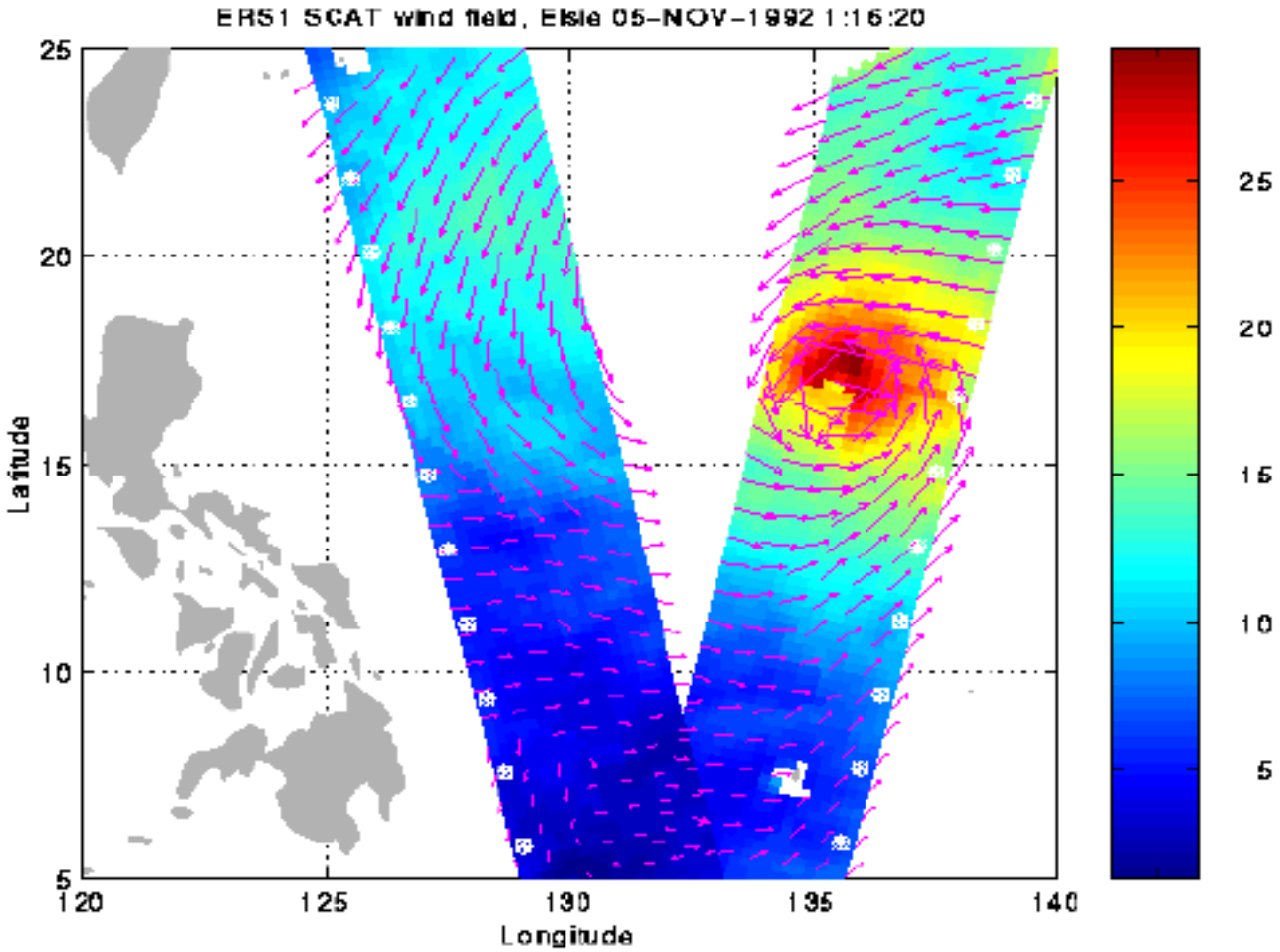
ERS1 SCAT wind field, Elsie 05-NOV-1992 1:16:20
25
20
15
10
5
Latitude
120
125
130
135
140
Longitude
25
20
15
10
5

$$B_\lambda = \frac{2hc^2}{\lambda^5}\left(e^{hc/\lambda KT} - 1\right)^{-1}$$

where h = Plank's constant = 6.6256×10^{-34} *Joule S*

and K = Boltzmann's constant = 1.3805×10^{-23} $J/_{\circ K}$

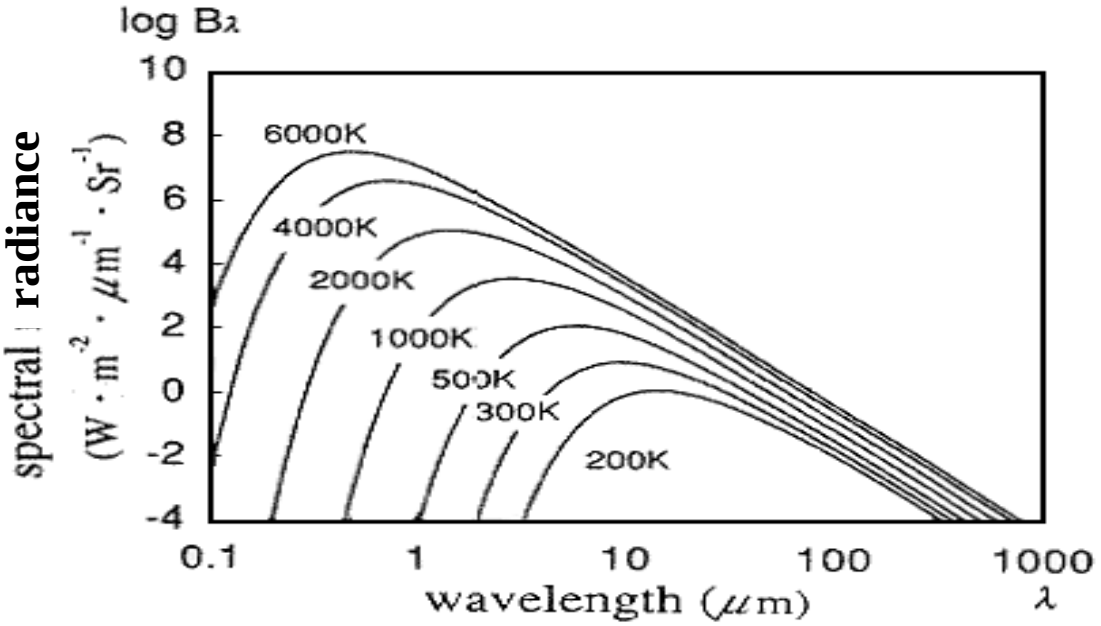

Any object at a physical temperature T_k owns a spectral radiance

$$L_\lambda = eB_\lambda(T_k)$$ (for a Lambertian surface)

e is the object emissivity ($0 \le e \le 1$).

Thermal IR sensors can measure the radiant temperature (or brightness temperature), that is the temperature of a blackbody with the same spectral radiance of the observed object

$$B_\lambda(T_{rad}) = L_\lambda = eB_\lambda(T_k)$$

Ocean currents (such as the Gulf Stream) bring excess heat absorbed in the Tropics towards the polar regions, thus maintaining the Earth's thermal equilibrium.

Then, ocean streams may be recognized because they have a higher (or lower) temperature with respect to near-by water.

For this reason, Sea Surface Temperature (SST) maps may be realized with thermal IR images.

The ocean temperature determines
- how much heat is transferred between atmosphere and ocean,
- and how much CO_2 can be absorbed from atmosphere (remember that carbon dioxide is one of the major greenhouse gases responsible of global warming).

The TIR signal is proportional to ocean temperature, however clouds may alter the measurement.

A thick cloud blocks all the radiation and we get no data.
But more confusing is a thin cloud that only blocks part of the radiation, making water appear cooler than it actually is.

One way of dealing this problem is to consider two images taken very close in time.
A third image is built using the warmer temperature of the two values at each pixel.

If the two images contain clouds at different spots, the third image will contain few clouds.

More than two images may be composited in the same fashion.

AVHRR sensors on board NOAA satellites, produce SST images almost in real time.

AVHRR Ch5: λ=11μ

June 1984

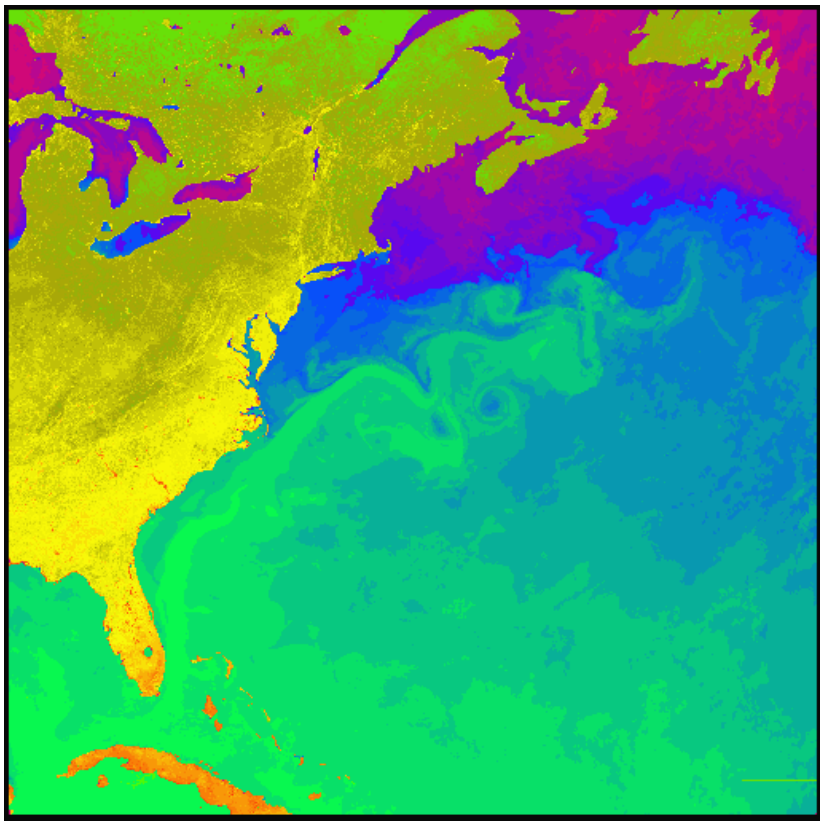

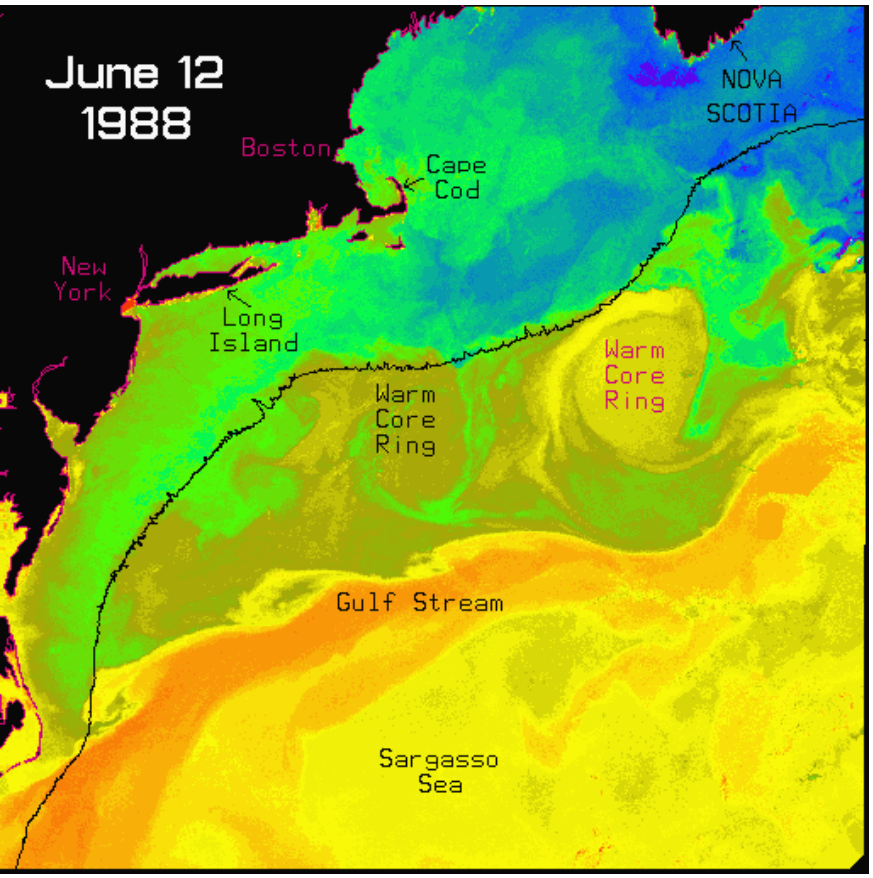

23°C

14°C

5°C

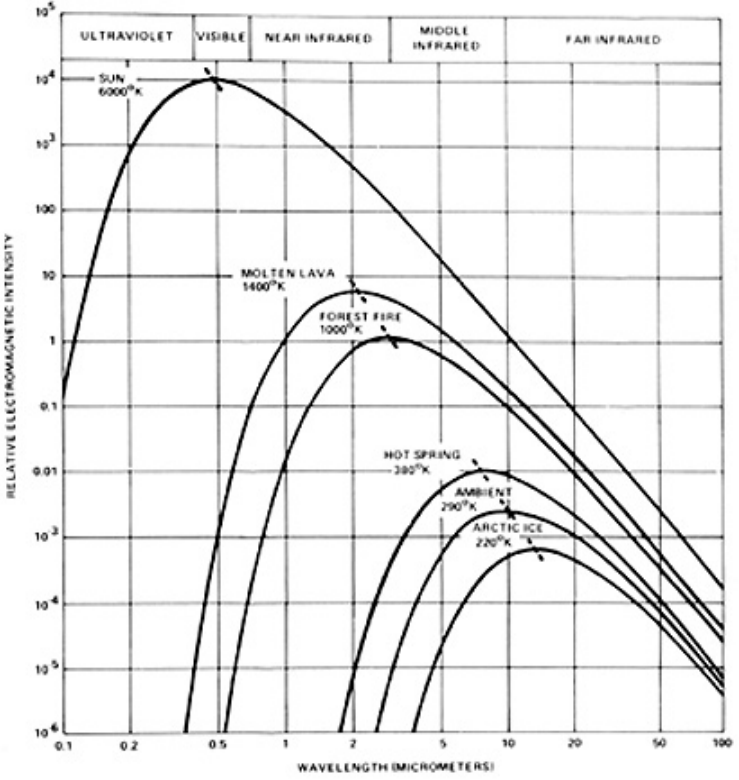

The Wien's law: $\lambda_M = \frac{2898}{T}$ [μm] with T in °K

As temperature increases, the maximum of radiated energy is displaced at lower wavelengths.

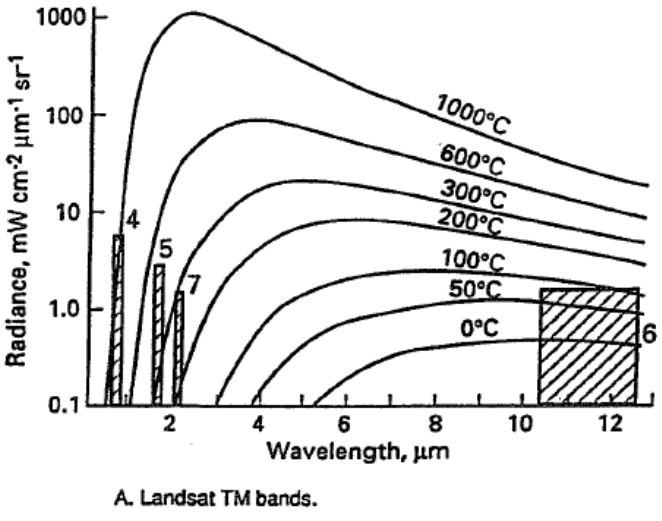

A. Landsat TM bands.

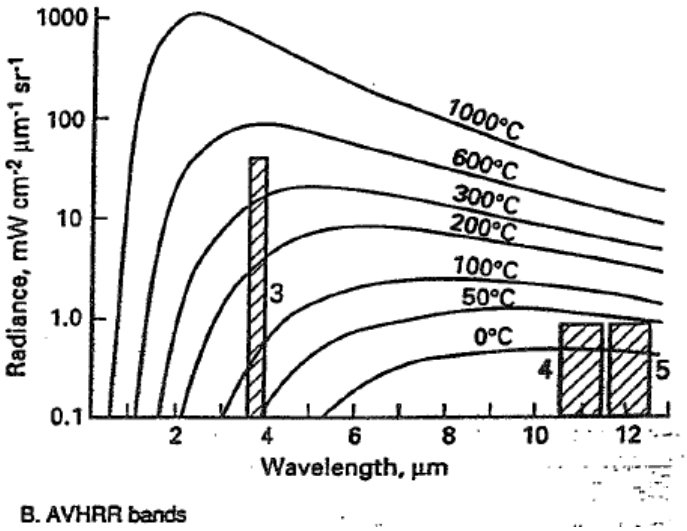

B. AVHRR bands

Also NIR channels of TM and AVHRR are used to study **hot surfaces**, like those covered by **lava or fires.**

Eruptive volcanic events have very short duration and may finish within a repeat cycle of LandSat.
For this reason, in order to monitor on going eruptions AVHRR images are mostly used.

In connection with the eruption of Krafla volcano in Iceland, in September 1984, the following images were selected:

- 3 pre-eruption images
- 5 images during the eruption
- 2 post-eruption images

Images in channels 4 and 5, prior to the eruption, did not show any early warning signal.

Krafla Volcano Eruption (Iceland)
AVHRR Channel 3B: 3.55-3.93μ

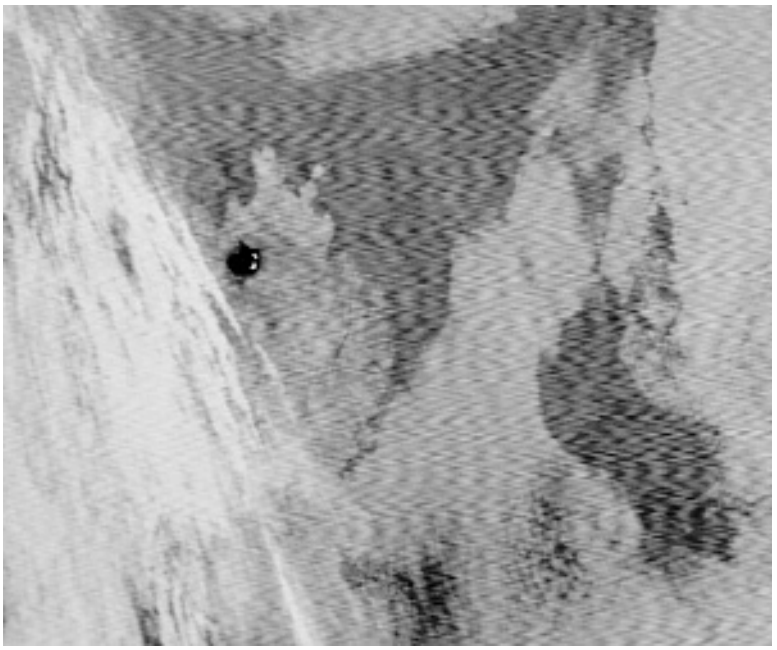

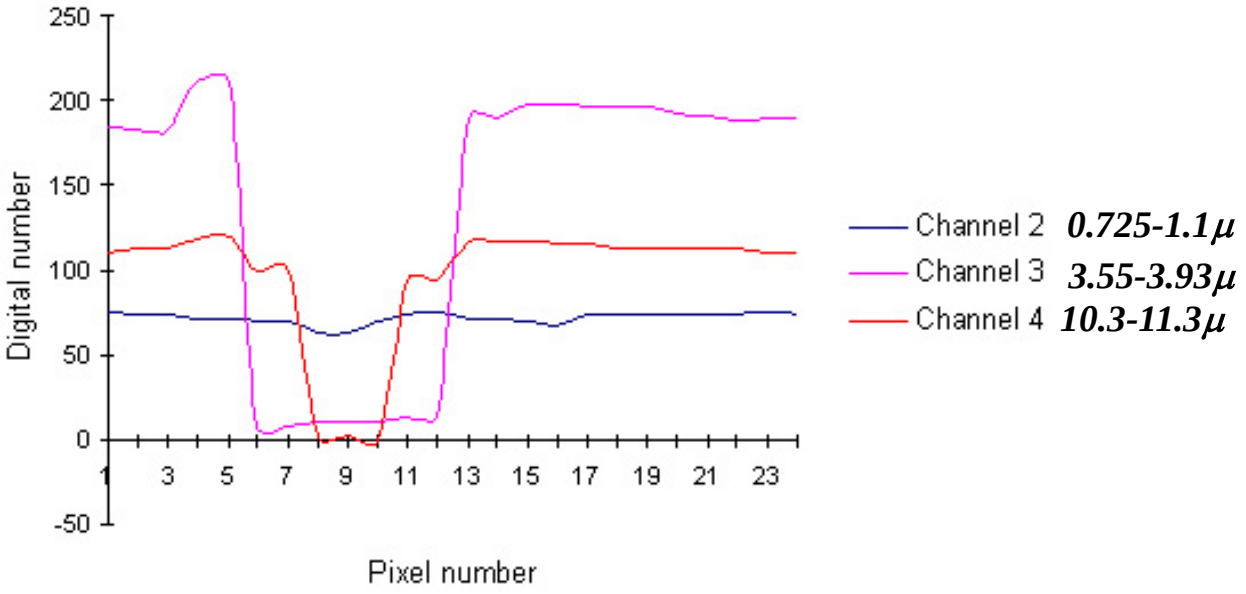

Channels 3 and 4 were used to classify images with the following procedure:

- pixels with **DN** < than a certain threshold are classified as lava
- pixels with **DN** > than a certain threshold are classified as soil

Identification of lava flow with AVHRR images is very efficient.
Estimation of its dimension and temperature is more problematic.

This problem is due to "mixed" pixels.

Since the AVHRR spatial resolution is low (1.1 km), inside one resolution cell it is possible to find both soil covered by lava and lava-free soil.
Because the radiance emitted by lava is very high, a small fraction of surface covered by lava in the resolution cell is enough to make its radiance very high, so that that pixel is classified as lava.
The inclusion, or exclusion, of mixed pixels gives rise to a overestimation, or underestimation, of the lava flow dimension.

In order to estimate the lava temperature of mixed pixels, the following equation is used:

$$L_i = pL_i(T_h) + (1-p)L_i(T_c)$$

- L_i is the radiance of channel i
- p is the pixel fraction covered by lava at temperature T_h (hot lava)
- $(1-p)$ is the pixel fraction covered by cool crust at temperature T_c

In order to find p, T_h and T_c, it is necessary to have available radiances measured at three channels.

Unfortunately, AVHRR channels 4 and 5 cannot be used simultaneously because they provide very similar radiances (since they are very close spectrally).
It is then possible to use only channels 3 and 4 (or 3 and 5), making some assumptions on one of the three parameters p, T_h and T_c.

Even though a fire is not very extended (with dimensions lower than the spatial resolution) its high temperature allows detection of the fire also with AVHRR channel 3 (3.8μ).

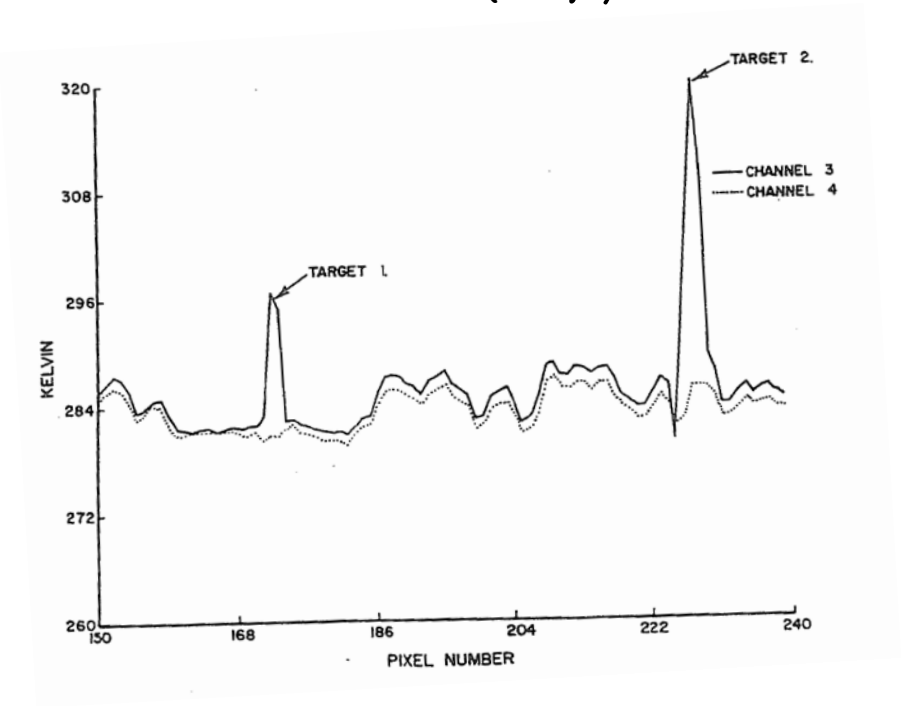

Target 1 = 160° C on 0.28 ha
Target 2 = 213° C on 1.7 ha

AVHRR resolution = 121 ha

In order to identify a fire,
algorithms such as the following are used:

$$T_{B3} > \text{threshold 1}$$
$$T_{B3} - T_{B4} > \text{threshold 2}$$

Multispectral images are often highly correlated. For example, this plot shows that band 1 and band 2 of an image have a high degree of correlation: if a pixel has a high reflectance in one band, it will have a high reflectance in the other band too.

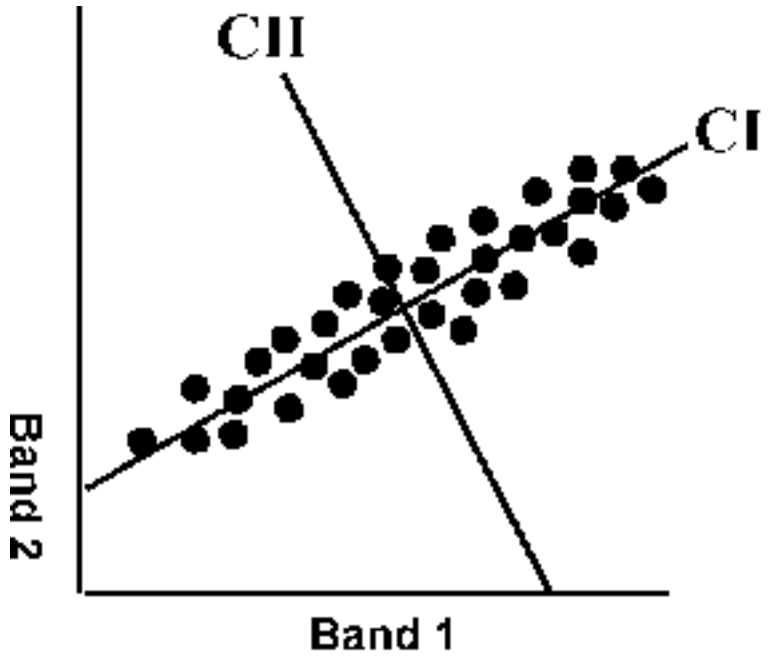

Figure 1 : The Principal Components Transform
[after Lillesand and Kiefer, 1994, 573]

As a consequence, the information contained in the two bands are not independent from each other.
The **Principal Components Transformation** allows removing the redundancy of information existing between two, or more, bands.

$\boldsymbol{X_p}$ is a vector containing the values of pixel $\boldsymbol{p}$ in $\boldsymbol{K}$ bands, i.e., it has $\boldsymbol{K}$ components.

If an image has $\boldsymbol{P}$ pixels, $\boldsymbol{P}$ vectors $\boldsymbol{X_p}$ exist ($\boldsymbol{p=1,P}$).

$\boldsymbol{\mu}$ is a vector containing the average of all pixels in one band. The $\boldsymbol{i}$ component of vector $\boldsymbol{\mu}$ is:

$$\mu_i = \frac{1}{P}\sum_{p=1}^{P} X_{pi}$$

with $\boldsymbol{i=1,K}$.
The variance tells how much the pixels of band $\boldsymbol{i}$ differ, on average, from the average $\boldsymbol{\mu_i}$:

$$\sigma_i^2 = \frac{1}{P-1}\sum_{p=1}^{P}(X_{pi}-\mu_i)(X_{pi}-\mu_i)$$

The covariance links the distance between one pixel and the average in one band with the distance of the same pixel from the average in another band:

$$C_{ij} = \frac{1}{P-1} \sum_{p=1}^{P} (X_{pi} - \mu_i)(X_{pj} - \mu_j)$$

This is a ***KxK*** matrix, whose elements on the main diagonal are the variances.
If the spectral bands are completely uncorrelated, the $\underline{\underline{C}}$ matrix is diagonal.

On the opposite, if they are very correlated, the elements outside the diagonal are high with respect to those on the diagonal.

The correlation matrix is defined as:

$$\rho_{ij} = \frac{C_{ij}}{\sqrt{C_{ii} C_{jj}}}$$

that expresses the percentage of correlation between bands ***i*** and ***j***.

$$\underline{\underline{C}} = \begin{matrix} 100.93 & 56.60 & 79.43 & 61.49 & 134.27 & 90.13 & 23.72 \\ 56.60 & 34.14 & 46.71 & 40.68 & 85.22 & 55.14 & 14.33 \\ 79.43 & 46.71 & 68.83 & 69.59 & 141.04 & 86.91 & 22.92 \\ 61.49 & 40.68 & 69.59 & 248.4 & 330.71 & 148.5 & 43.62 \\ 134.27 & 85.22 & 141.04 & 330.71 & 568.84 & 280.9 & 78.91 \\ 90.13 & 55.14 & 86.91 & 148.5 & 280.97 & 154.92 & 42.65 \\ 23.72 & 14.33 & 22.92 & 43.62 & 78.91 & 42.65 & 17.78 \end{matrix}$$

$$\underline{\underline{\rho}} = \begin{matrix} 1 & & & & & & \\ 0.96 & 1 & & & & & \\ 0.95 & 0.96 & 1 & & & & \\ 0.39 & 0.44 & 0.53 & 1 & & & \\ 0.56 & 0.61 & 0.71 & 0.88 & 1 & & \\ 0.72 & 0.76 & 0.84 & 0.76 & 0.95 & 1 & \\ 0.56 & 0.58 & 0.66 & 0.66 & 0.78 & 0.81 & 1 \end{matrix}$$

MULTIVARIATE DATA STATISTICS

idealized distributions with different correlations

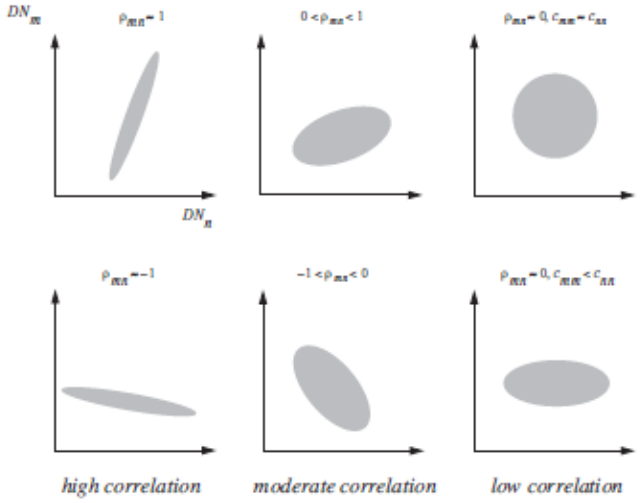

16-22

Correlation and covariance

Images here are of the covariance and correlation matrices for the ETM+ imagery of northern Tucson/southern Catalinas

- Covariance image on the left and correlation on right
- Note that the matrices are symmetric
- Bands close to each other spectrally tend to have higher correlation

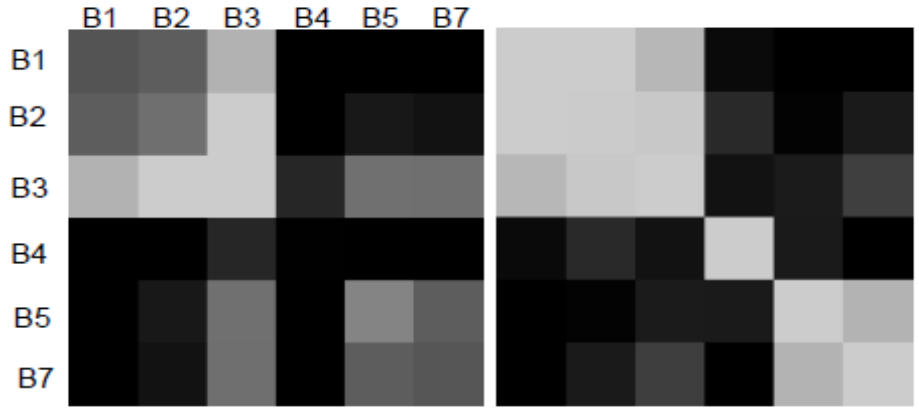

Band 1,2,3: strongly correlated mutually,
no correlation with band 4
Band 5,7: reasonably strong correlation
Band 4,7: varying correlation
Band 6: no or incidental weak correlation

The Principal Components transformation allows transformation of an image into a coordinate frame where the spectral bands are uncorrelated.
A coordinate transformation must be identified, that makes the covariance matrix diagonal.
This can be achieved looking for eigenvalues of the covariance matrix, i.e., solving the equation:

$$\left| \underline{\underline{C}} - \lambda \underline{\underline{I}} \right| = 0$$

$\boldsymbol{I}$ is the identity matrix
The eigenvalues λ_i represent the variances in the new coordinate frame. That is

$$\underline{\underline{C}}^{PC} = \begin{pmatrix} \lambda_1 & 0 & . & . & 0 \\ 0 & \lambda_2 & . & . & 0 \\ . & . & . & . & . \\ . & . & . & . & . \\ 0 & 0 & . & . & \lambda_K \end{pmatrix}$$

which is, by definition, a diagonal matrix.
The eigenvalues are ordered in such a way that

$$\lambda_1 > \lambda_2 > ..... > \lambda_K$$

Principal Components is a linear transformation that compresses the variance

$$\lambda_1 > \lambda_2 \ldots > \lambda_K$$

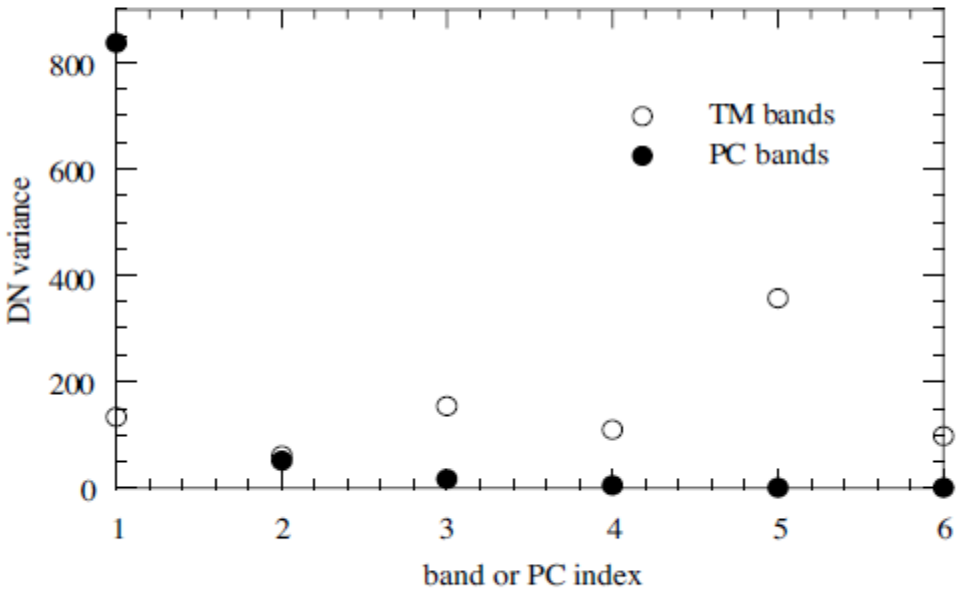

$$\underline{\underline{C}}^{PC} = \begin{matrix} 1010.92 & & & & & & \\ 0 & 131.2 & & & & & \\ 0 & 0 & 37.6 & & & & \\ 0 & 0 & 0 & 6.73 & & & \\ 0 & 0 & 0 & 0 & 3.95 & & \\ 0 & 0 & 0 & 0 & 0 & 2.17 & \\ 0 & 0 & 0 & 0 & 0 & 0 & 1.24 \end{matrix}$$

The eigenvectors $\mathbf{e_i}$, obtained from eigenvalues λ_i allow changing coordinate reference frame, and they represent the principal axes of the new reference frame.

$$\left(\underline{\underline{C}} - \lambda_i \underline{\underline{I}}\right) \cdot e_i = 0$$

The matrix that allows the transformation into the new reference frame is

$$\underline{\underline{W}} = \begin{pmatrix} e_{11} & e_{12} & . & . & e_{1K} \\ e_{21} & . & . & & \\ . & & & & \\ . & & & & \\ e_{K1} & . & . & . & e_{KK} \end{pmatrix}$$

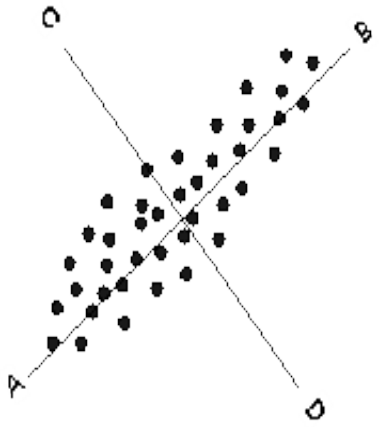

The direction of maximum variance in multi-spectral space (A-B) is calculated and the first principal component axis is rotated to align in this direction.

The second principal component axis is aligned in the directionof the second largest variance (C-D) and orthogonal to the first principal component axis.

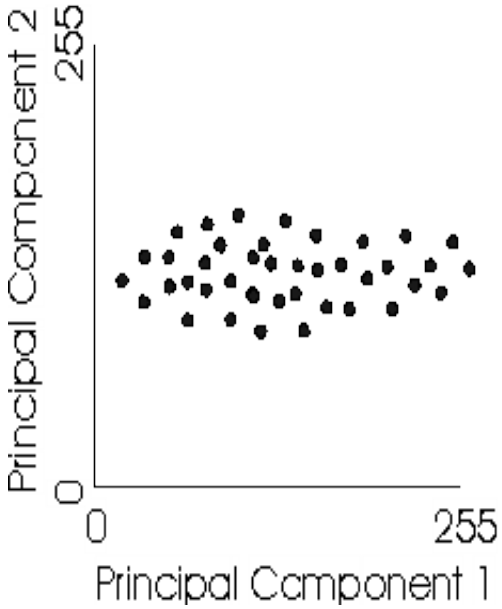

A new principal component image is written. The new PC bands are expressed as a linear combination of the original image bands.

There is no longer any correlation between channels in the image.

All pixels in the image must be transformed into the new reference frame

$$X_p^{PC} = \underline{\underline{W}} X_p$$

The pixel values in the Principal Components frame is obtained as a linear combination of the pixel values in the original $\boldsymbol{K}$ spectral bands

$$X_1^{PC1} = e_{11}X_{11} + e_{12}X_{12} + \cdots + e_{1K}X_{1K}$$
$$X_1^{PC2} = e_{21}X_{11} + e_{22}X_{12} + \cdots + e_{2K}X_{1K}$$
$$\vdots$$
$$X_1^{PCK} = e_{K1}X_{11} + e_{K2}X_{12} + \cdots + e_{KK}X_{1K}$$

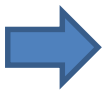

It is possible to determine the weight of each one of the $\boldsymbol{K}$ original band in the construction of the $\boldsymbol{K}$ Principal Components, through the Load matrix:

$$L_{ij} = e_{ji}\sqrt{\frac{\lambda_j}{C_i}}$$

that tells us what is the weight of the original band $\boldsymbol{i}$ in the evaluation of the Principal Component $\boldsymbol{j}$

SPECTRAL DATA PROCESSING

Example

- ***Original data in DN-space***

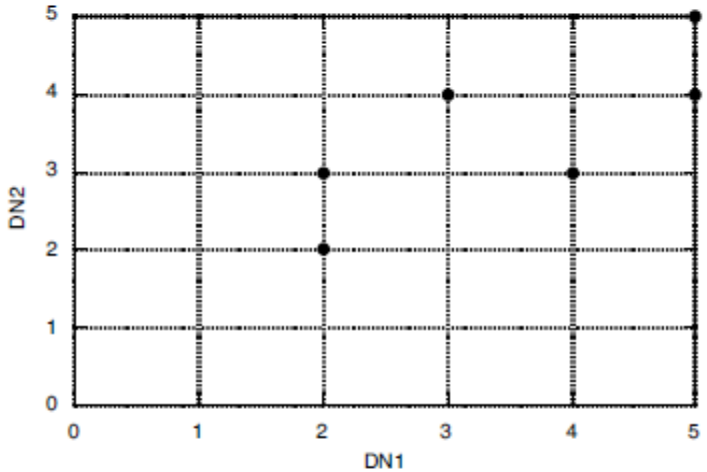

pixel	DN1	DN2
1	2	2
2	2	3
3	3	4
4	4	3
5	5	4
6	5	5

$$\mu = \begin{bmatrix} 3.50 \\ 3.50 \end{bmatrix}$$

$$C = \begin{bmatrix} 1.9 & 1.1 \\ 1.1 & 1.1 \end{bmatrix}$$

$$R = \begin{bmatrix} 1 & 0.761 \\ 0.761 & 1 \end{bmatrix}$$

- ***1. Find eigenvalues***

Characteristic Equation

$$|C - \lambda I| = 0$$

$$\begin{vmatrix} 1.9 - \lambda & 1.1 \\ 1.1 & 1.1 - \lambda \end{vmatrix} = 0$$

$$\lambda^2 - 3\lambda + 0.88 = 0$$

which has solutions

$\lambda = 2.67$ ***and*** $\lambda = 0.33$

SPECTRAL DATA PROCESSING

Therefore $C_{PC} = \begin{bmatrix} 2.67 & 0 \\ 0 & 0.33 \end{bmatrix}$

Note that PC1 accounts for 2.67/3 = 0.89 of total variance in data

- *2. Find eigenvectors*

$(C - \lambda_k I)e_k = 0$

For eigenvector 1, $\begin{aligned} -0.77e_{11} + 1.10e_{21} &= 0 \\ 1.10e_{11} - 1.57e_{21} &= 0 \end{aligned}$

which are not independent. From either equation $e_{11} = 1.43e_{21}$

Orthonormality of the eigenvectors implies $e_{11}^2 + e_{21}^2 = 1$

Solving simultaneously with the above equation gives $e_1 = \begin{bmatrix} 0.82 \\ 0.57 \end{bmatrix}$

SPECTRAL DATA PROCESSING

Similarly, for eigenvector 2, $e_2 = \begin{bmatrix} -0.57 \\ 0.82 \end{bmatrix}$

and the PCT matrix is $W_{PC} = \begin{bmatrix} 0.82 & 0.57 \\ -0.57 & 0.82 \end{bmatrix}$

- ***Transformed data in PC-space***

pixel	PC1	PC2
1	2.78	0.50
2	3.35	1.32
3	4.74	1.57
4	4.99	0.18
5	6.38	0.43
6	6.95	1.25

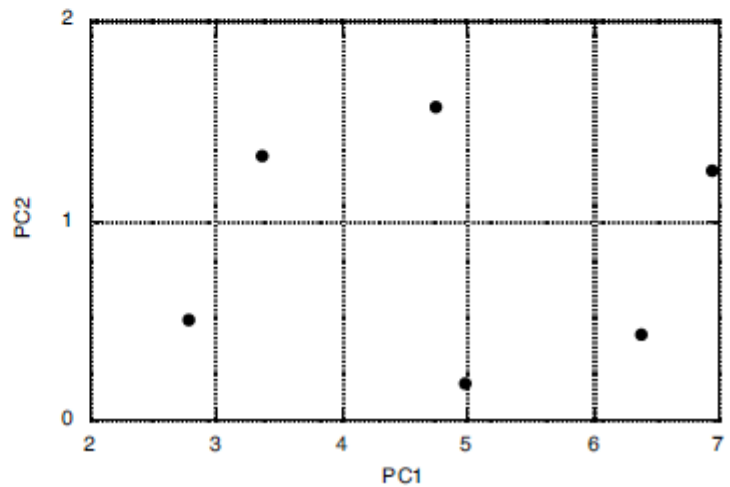

2-D Scatterplots

Create 3-D scatter-plots looking at 3-band combinations or examine multiple 2-D plots for multiple band combinations

- Graphs here show reflective bands of ETM+
- All plots are versus the band 3 DN

B1 vs. B3

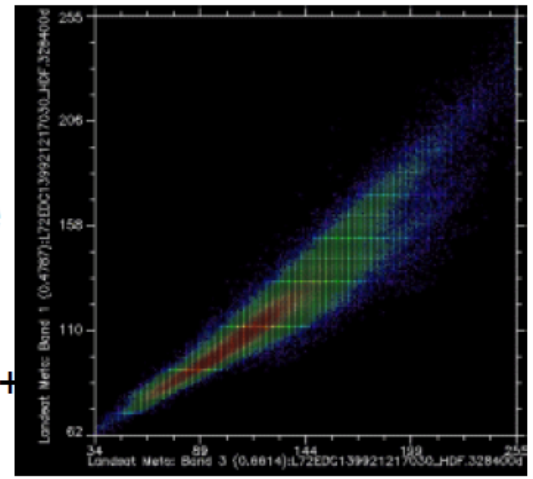

B2 vs. B3

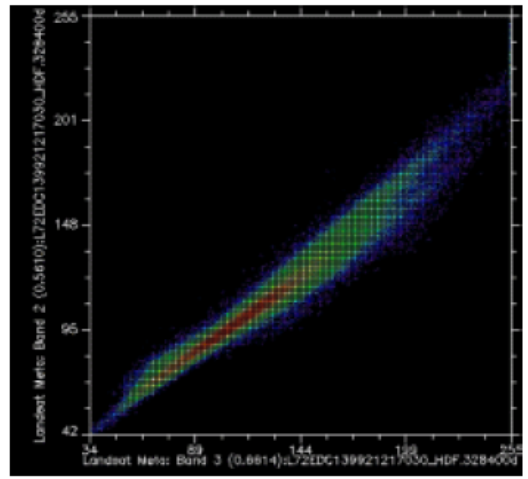

B4 vs. B3

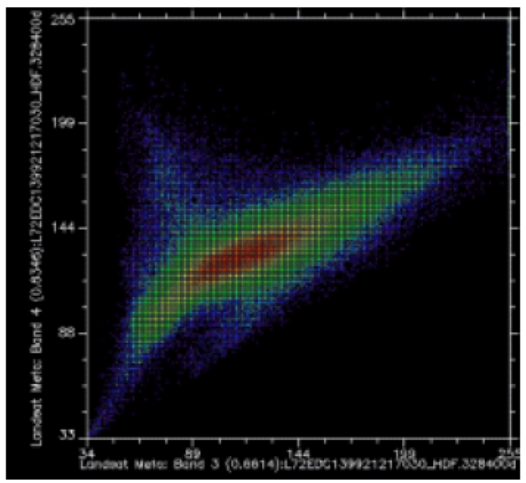

B5 vs. B3

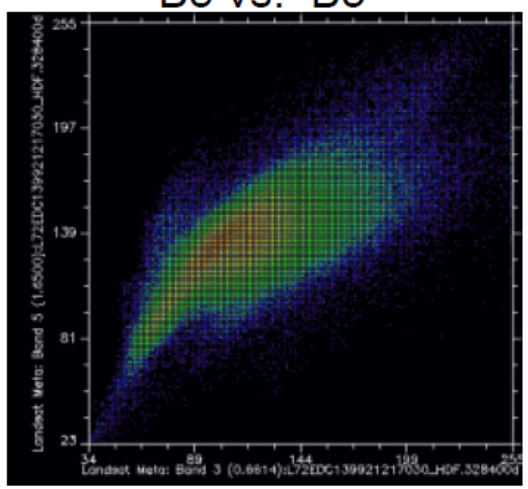

B7 vs. B3

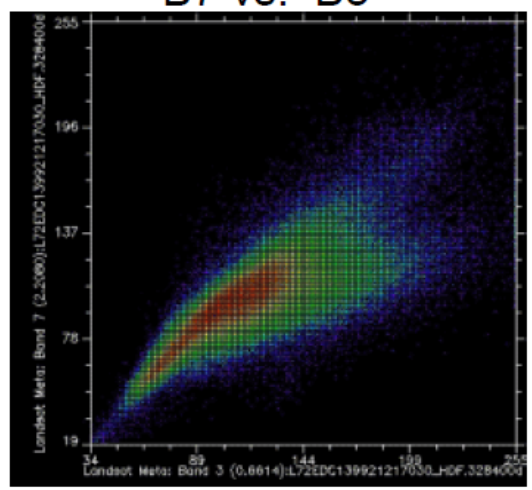

PCA scatterplots

The purpose of the PCA is to attempt to de-correlate the data between bands

- The scatterplots shown here for the previous case illustrate this
- Note the circular shape of the scatterplots

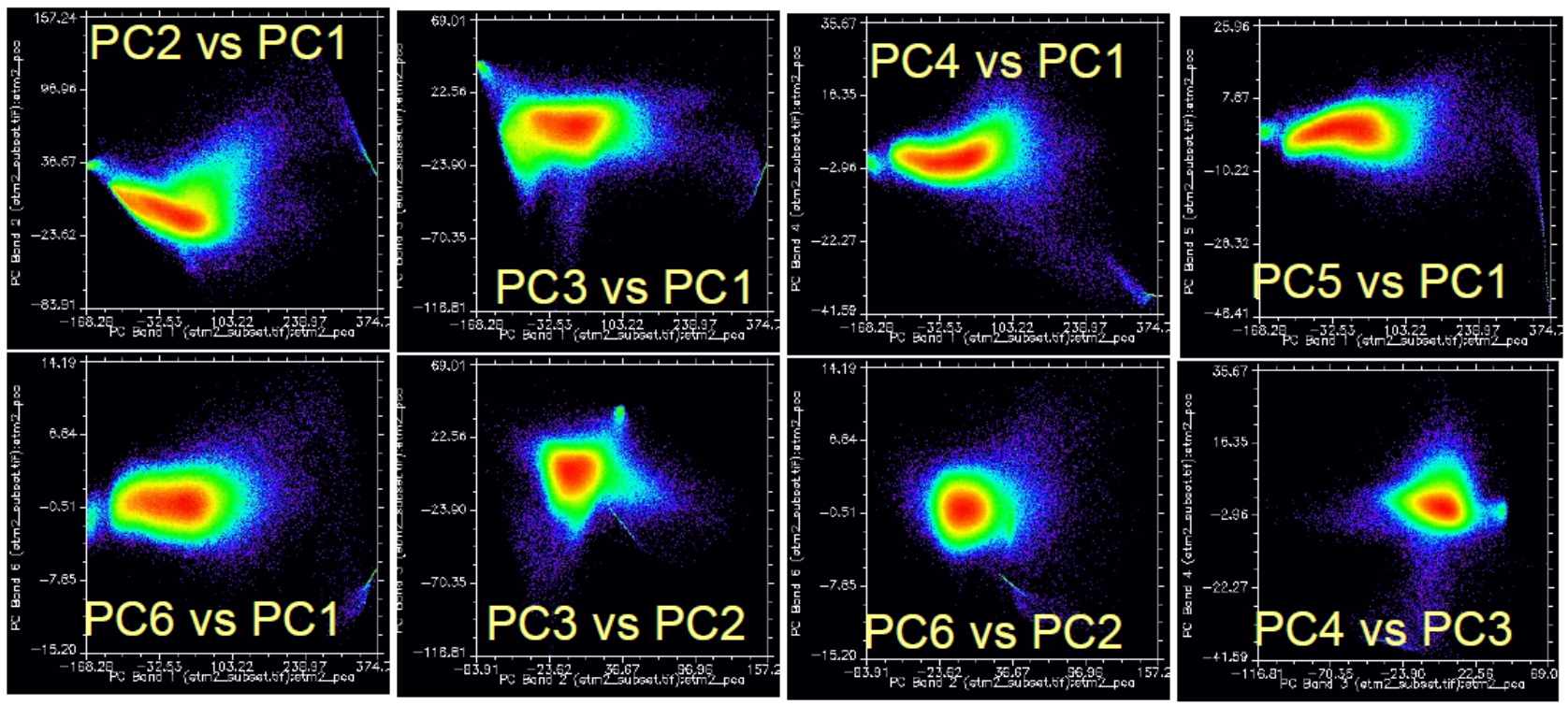

$$\underline{\underline{L}} = \begin{matrix} 0.36 & .72 & .53 & -.09 & -.21 & -.04 & 0 \\ .59 & .63 & .36 & -.08 & .16 & -.03 & -.23 \\ .39 & .8 & .37 & -.09 & .17 & -.03 & .1 \\ .97 & -.23 & .04 & .002 & .001 & .004 & .0012 \\ .93 & .33 & -.11 & -.001 & -.005 & -.02 & 0 \\ .22 & .68 & .33 & .63 & .01 & -.03 & 0 \\ .73 & .64 & .01 & 0 & -.006 & .2 & 0 \end{matrix}$$

Principal component 1.

Principal component 2.

Principal component 3.

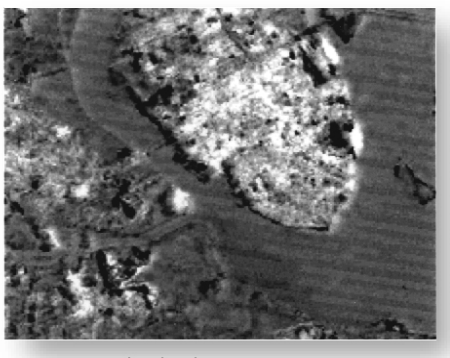

Principal component 4.

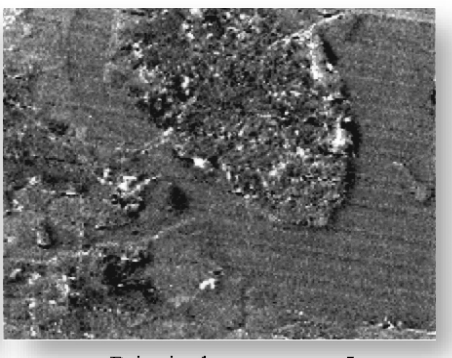

Principal component 5.

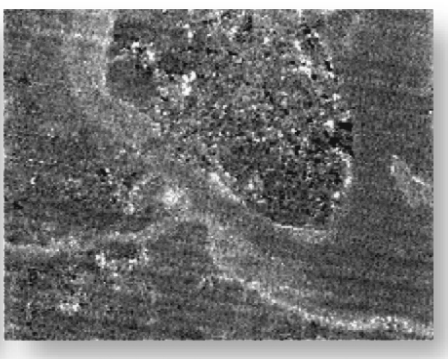

Principal component 6.

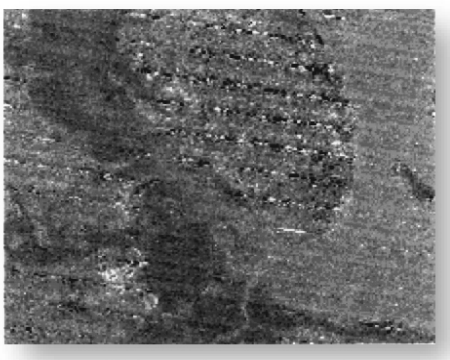

Principal component 7.

The Principal Components images are more difficult to interpret, since there is no longer a direct correspondence between ***DN*** and the datum acquired in the single band, since the single pixel in the Principal Components has been calculated through a linear combination of different bands.

The Principal Components images are uncorrelated, and they are ordered according to decreasing variance.
The maximum dispersion is found within the first Principal Component, therefore the corresponding image will show the highest contrast, i.e., it owns the maximum information content.
Viceversa, the last Principal Component contains little information.
The parameter

$$\%V = \frac{\lambda_i}{\sum_{i=1}^{K} \lambda_i}$$

tells what is the percentage of total variance contained in the $\mathbf{i}$-th Principal Component.
Discarding the Principal Components with the lowest information content, the quantity of data to be taken into account is decreased.

$$\underline{\underline{\rho}} = \begin{matrix} 1 \\ 0.85 & 1 \\ 0.89 & 0.9 & 1 \\ 0.21 & 0.44 & 0.21 & 1 \\ 0.52 & 0.73 & 0.59 & 0.82 & 1 \\ 0.66 & 0.62 & 0.69 & 0.07 & 0.4 & 1 \\ 0.72 & 0.85 & 0.81 & 0.56 & 0.89 & 0.6 & 1 \end{matrix}$$

$$\underline{\underline{C}}^{PC} = \begin{matrix} 890.14 \\ 0 & 114.83 \\ 0 & 0 & 15.53 \\ 0 & 0 & 0 & 3.85 \\ 0 & 0 & 0 & 0 & 1.79 \\ 0 & 0 & 0 & 0 & 0 & 1.78 \\ 0 & 0 & 0 & 0 & 0 & 0 & 0.76 \end{matrix}$$

$$\%V = (86.53, 11.16, 1.51, 0.37, 0.17, 0.17, 0.07)$$

- **Examples**
  - **nonvegetated scene** *Fig. 5-13*

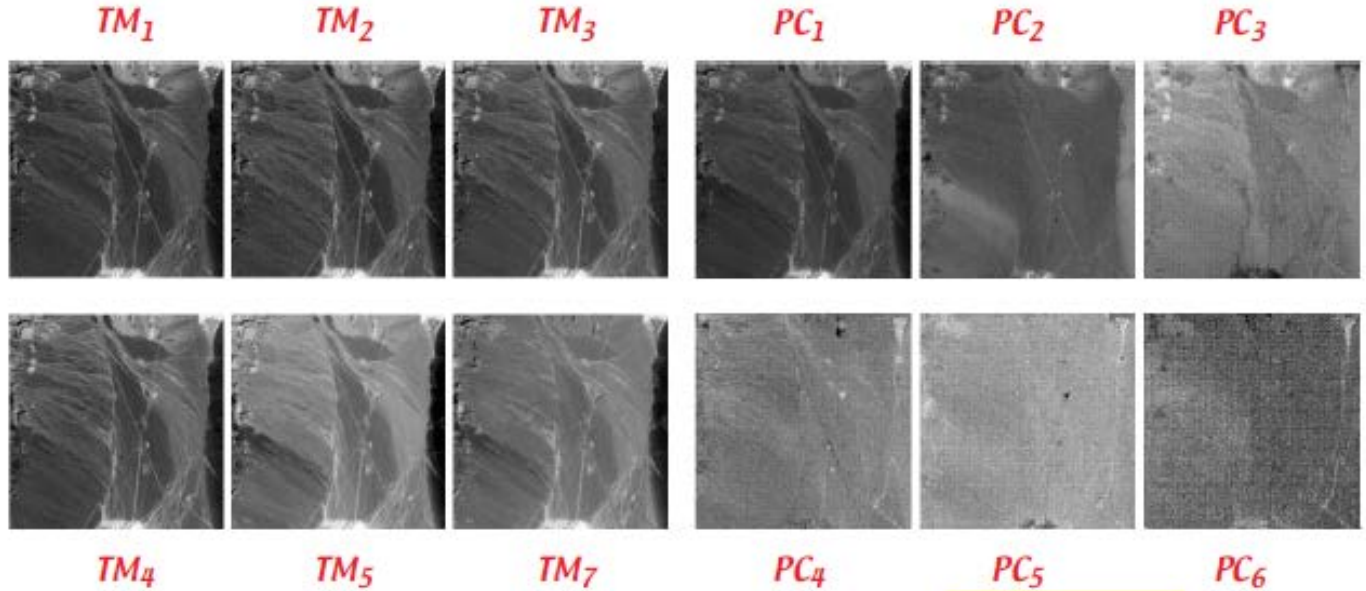

high spectral correlation removed by PCT

- *noise detection by spectral correlation* *Fig. 7-9*

spectrally-uncorrelated noise is isolated by PCT

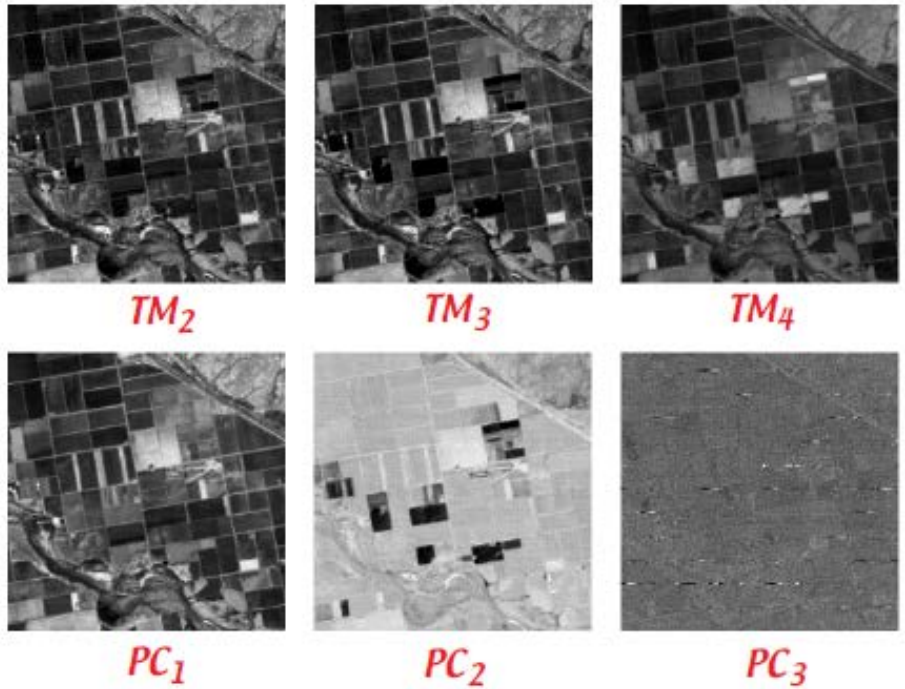

Tasseled Cap is a linear transformation used with the goal of maximizing the information related to agricultural applications.

It is employed to enhance the development stage of agricultural plants, or to distinguish agricultural vegetation from other kind of vegetation.

It is based on the observation that, during the development cycle, the reflectance of agricultural plants follow a specific trend in the spectral frame Red/NIR

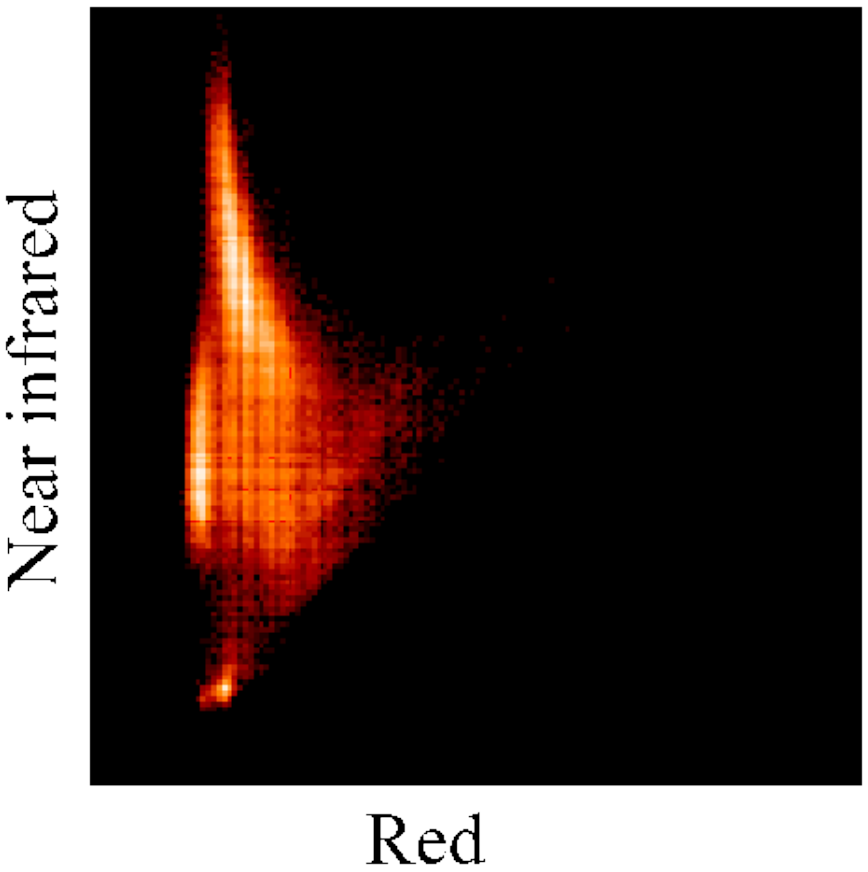

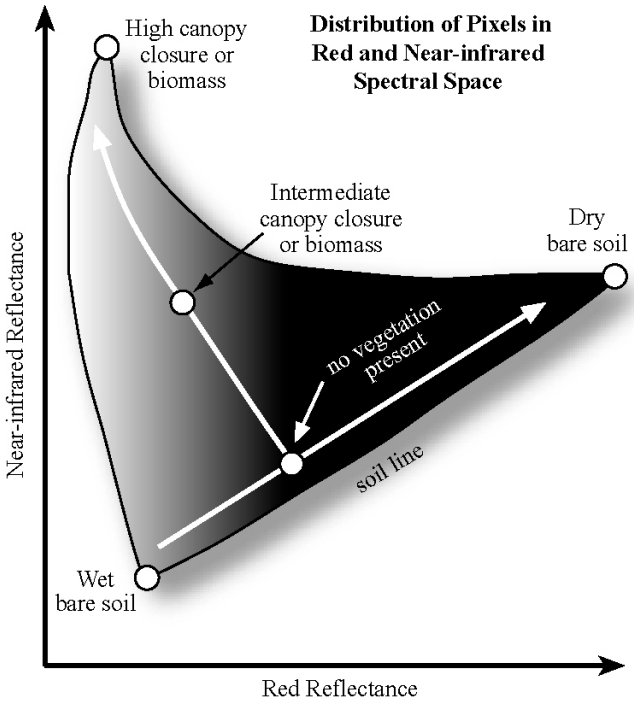

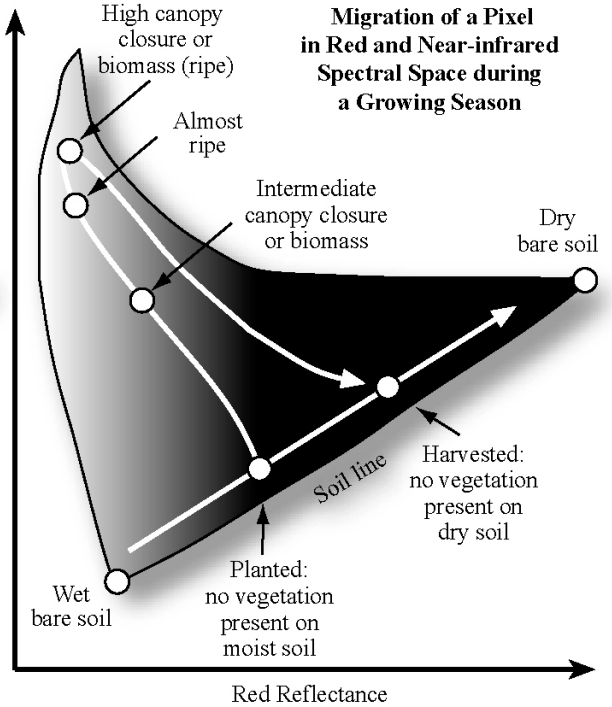

- The soil line corresponds to spectral responses of different kind of soils where plants can grow.
- During vegetation growth, the spectral response of plants will differ depending on soil type.
- The maturity point (canopy closure) represents the spectral response of the sole vegetation (soil reflectance is no longer visible).
- After yellowing, the spectral responses will separate in the frame Red/Green

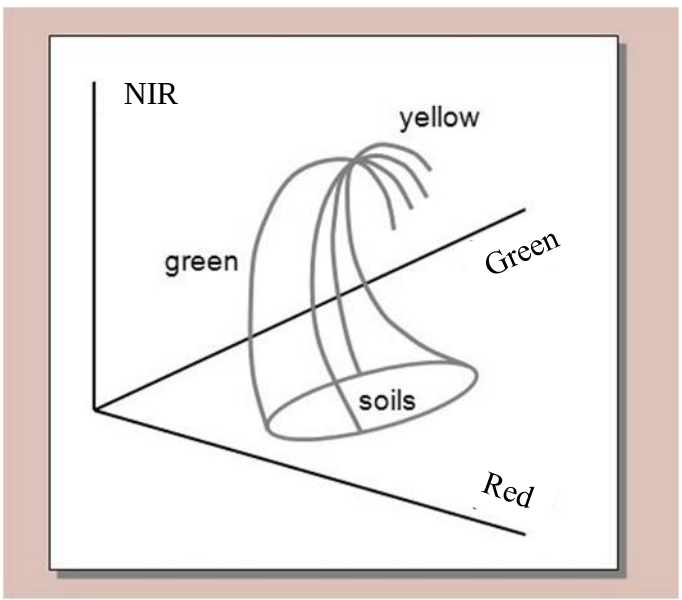

In the Red /NIR space, vegetation depicts a "tasseled cap".
The first Tasseled Cap frame has been proposed for MSS data, and it was composed by the following axis:

- Soil Brightness axes: parallel to the diagonal of the soil plane
- Greeness axes: orthogonale to SB, along which the maximum vegetation development takes place
- Yellow-Stuff axes: orthogonal to SB and G
- Non-Such axes

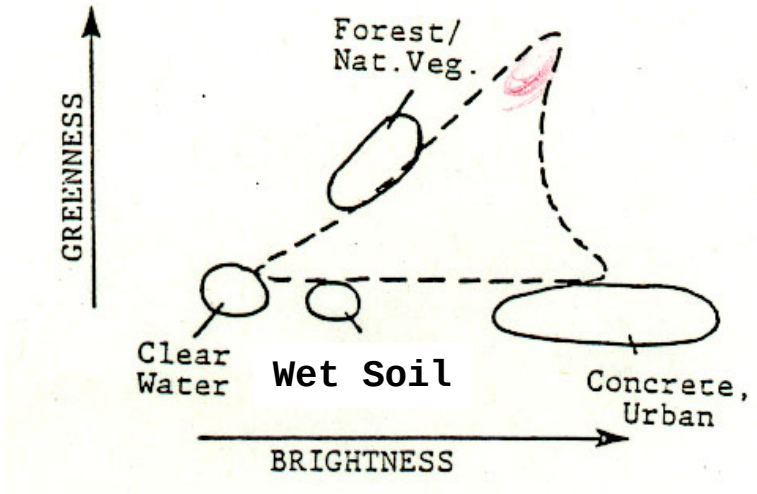

SB accounts for all possible soil types. More than 95% of variances of bare soils is distributed along the SB axes.
The Greeness value is an indicator of vegetation amount (biomass).
Yellow is an indicator of vegetation yellowing.
Non-Such accounts for variations not associated with soil differences, plant development or yellowing.

The TC transformation is linear, like the PC one:

$$X_p^{TC} = \underline{\underline{W}}^{TC} X_p$$

The $\underline{\underline{W}}^{TC}$ matrix depends on the sensor channels and spectral resolution, and it is found on the basis of available multispectral data.
For MSS:

$$\underline{\underline{W}}^{TC} = \begin{matrix} .433 & .632 & .586 & .264 \\ -.29 & -.562 & .6 & .49 \\ .83 & .522 & -.04 & .194 \\ .223 & .12 & -.543 & .81 \end{matrix}$$

For TM:

$$\underline{\underline{W}}^{TC} = \begin{matrix} & & & & & & \\ SB & .303 & .279 & .474 & .558 & .508 & .186 \\ Greeness & -.285 & -.243 & -.543 & .724 & .084 & -.18 \\ Wetness & .151 & .197 & .328 & .34 & -.711 & -.457 \\ Haze & -.824 & .85 & .44 & .058 & .201 & -.276 \\ TC5 & -.328 & .055 & .107 & .185 & -.435 & .808 \\ TC6 & .108 & -.902 & .412 & .057 & -.025 & .024 \end{matrix}$$

Usually, a $\underline{\underline{W}}^{TC}$ is created ad hoc for the crop area under study, applying a Gram-Schmidt orthogonalization.

- *Why use the TCT?*
  - *It is a fixed reference, related to geophysical properties of the scene*
    - *First component is "soil brightness"*
    - *Second component is "greeness"*

  Fig. 5-17

- *Why not use the TCT?*
  - *Nonoptimal compression of data*
  - *requires multitemporal data for each sensor to derive W_{TC}*

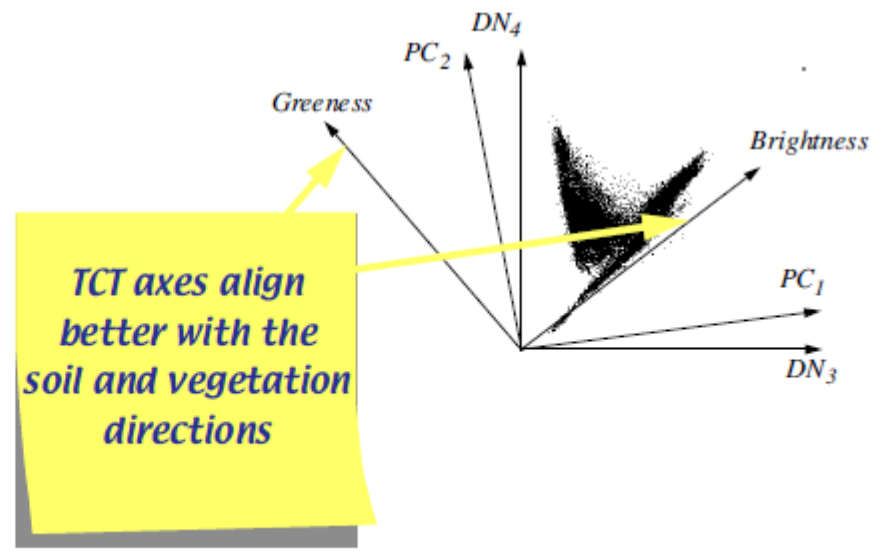

Comparison of PC and TC component images (Fig. 5-18)

- The PC axis are determined on the basis of purely statistic criteria.
- TheTC axis have a physical interpretation.

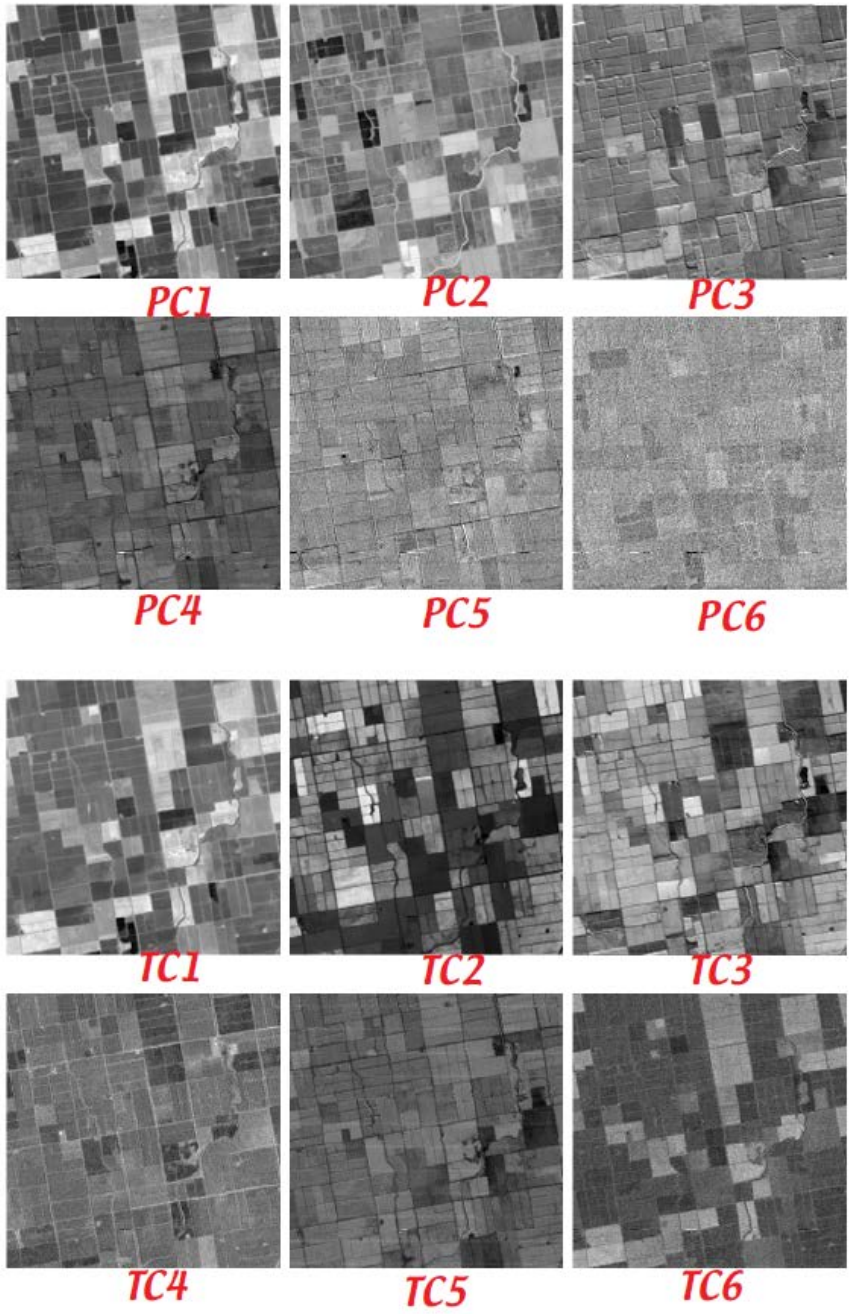

- *All VIs defined in terms of reflectance, not DN*
  - *require calibrated data*
- *Ratio Vegetation Index (RVI)*

$$RVI = \frac{\rho_{NIR}}{\rho_{red}} \quad \text{(Eq. 5-9)}$$

- *Normalized Difference Vegetation Index (NDVI)*

$$NDVI = \frac{\rho_{NIR} - \rho_{red}}{\rho_{NIR} + \rho_{red}} = \frac{RVI - 1}{RVI + 1} \quad \text{(Eq. 5-10)}$$

  - *VIs and the NIR/red scattergram*

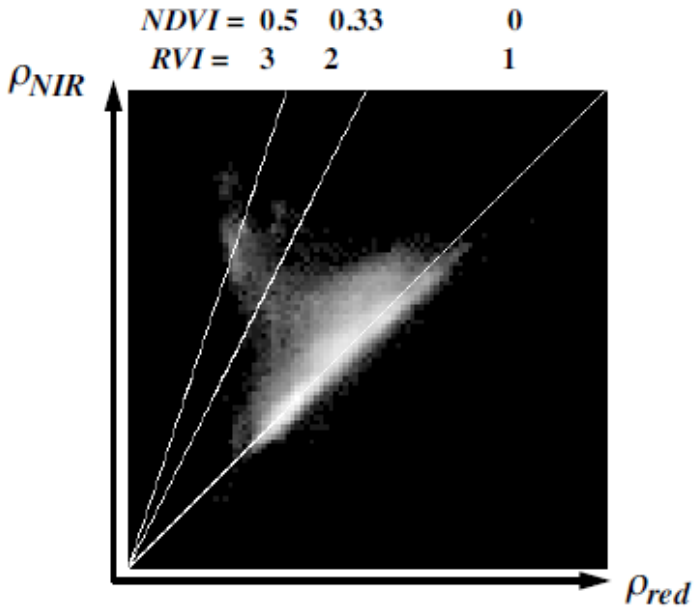

- ***Interpretation of VI images***

CIR composite (Landsat TM)

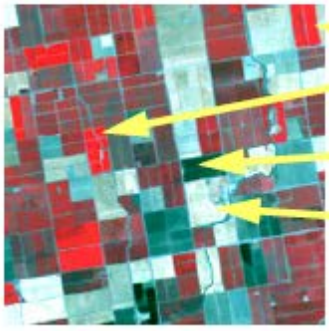

RVI

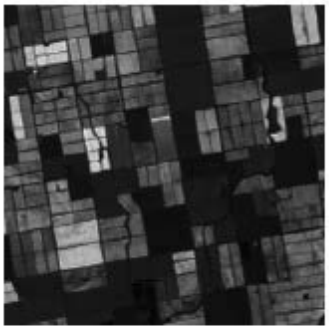

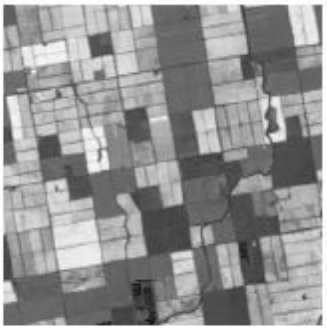

NDVI

The vegetation indexes RVI and NDVI are influenced also by reflectance properties of the soil underlying vegetation.

The ideal vegetation index is the one sensitive to vegetation contribution only

$$\textit{Leaf Area Index} = LAI = \frac{\textit{Leaf Total Area}}{\textit{Ground Surface Area}}$$

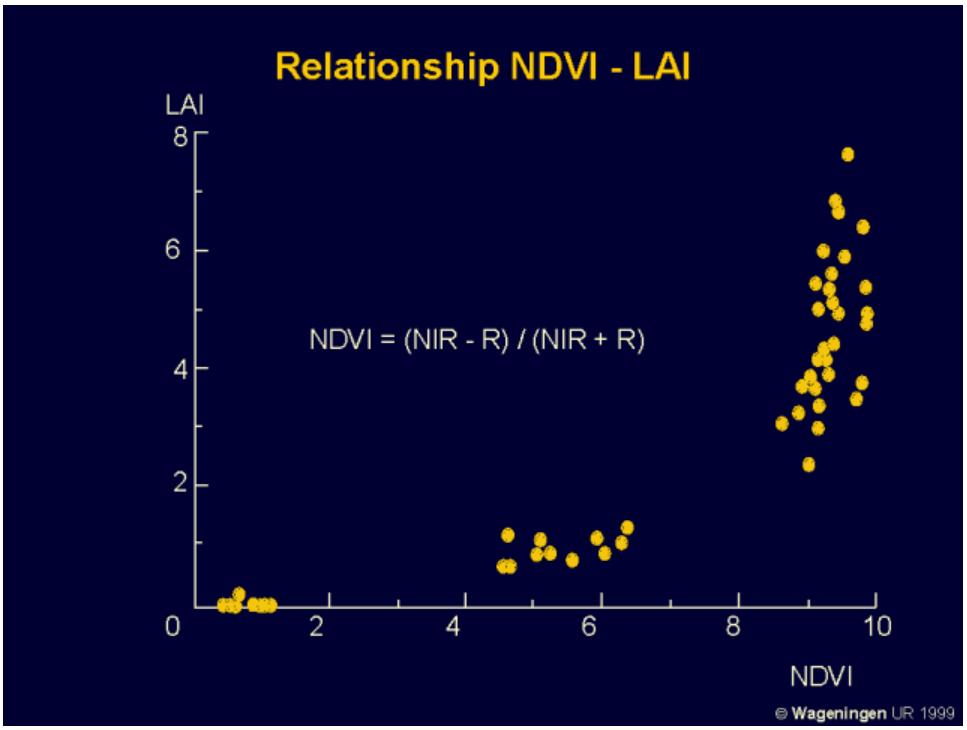

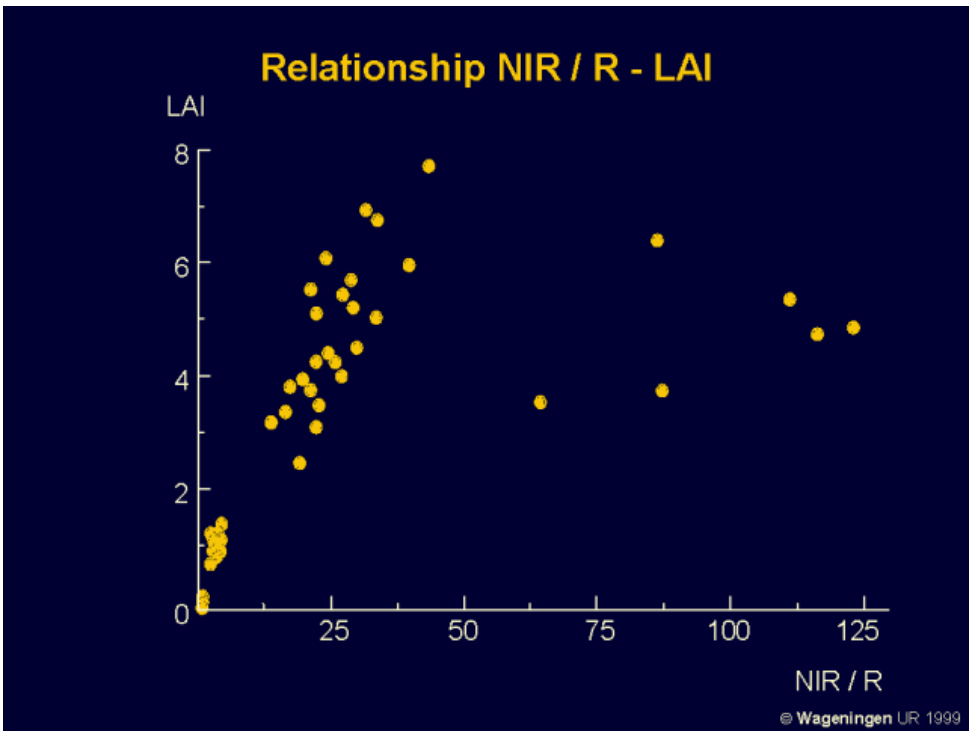

As a vegetation index, one could use the Greeness component of the TC transformation. This parameter is scarcely influenced by the soil type, but it depends on the sensor and on the observed scene.

Another indicator of the plant development is the

Perpendicular Vegetation Index

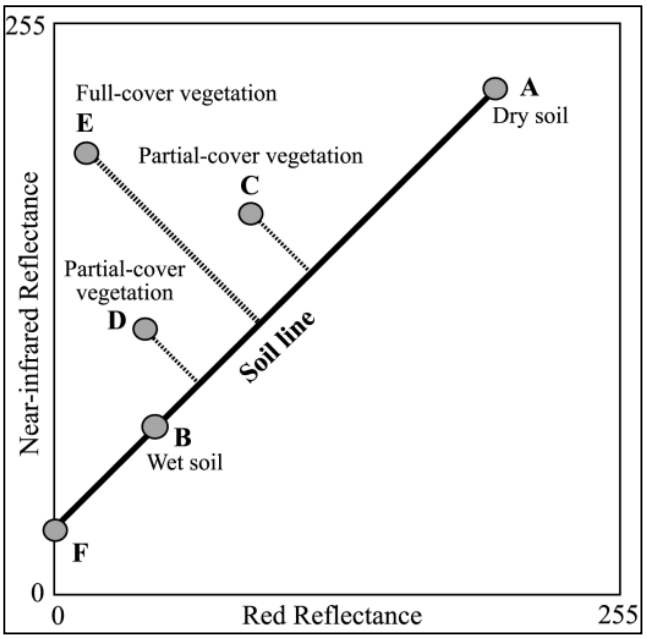

PVI=0 corresponds to bare soil

The farther the pixel lies on the left of the bare soil line, the more developed the vegetation is, and the PVI value increases.

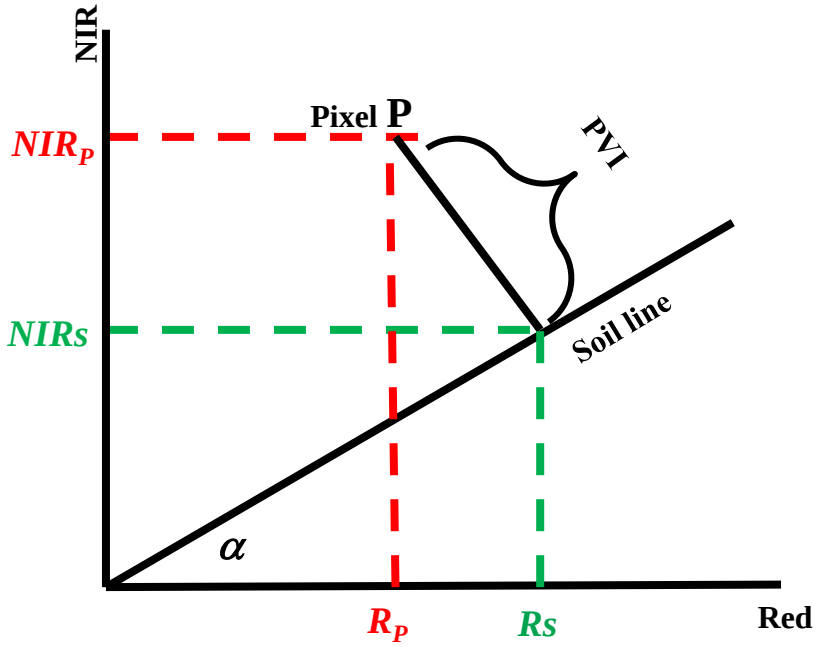

$$PVI = \sqrt{(R_s - R_P)^2 + (NIR_s - NIR_P)^2}$$

is the PVI of pixel **P**.
However, to apply this formula, you should know the coordinates of the bare soil ($\boldsymbol{R_s}$, $\boldsymbol{NIR_s}$) below the vegetation cover in pixel ***P***.
An alternative formulation is:

$$PVI = \frac{NIR_P - R_P \cdot tg\alpha}{\sqrt{1 + tg^2\alpha}}$$

where the equation $\boldsymbol{NIR = R \cdot tg\alpha}$ of the soil line is used.

NDVI and ***PVI*** represent vegetation in two different ways:

NDVI represents pixels with the same ***LAI*** (i.e., the same vegetation cover), but with different soils, by means of lines passing through origin.

PVI represents pixels with the same ***LAI***, but with different soils, by means of lines with the same slope (i.e., parallel to the soil line).

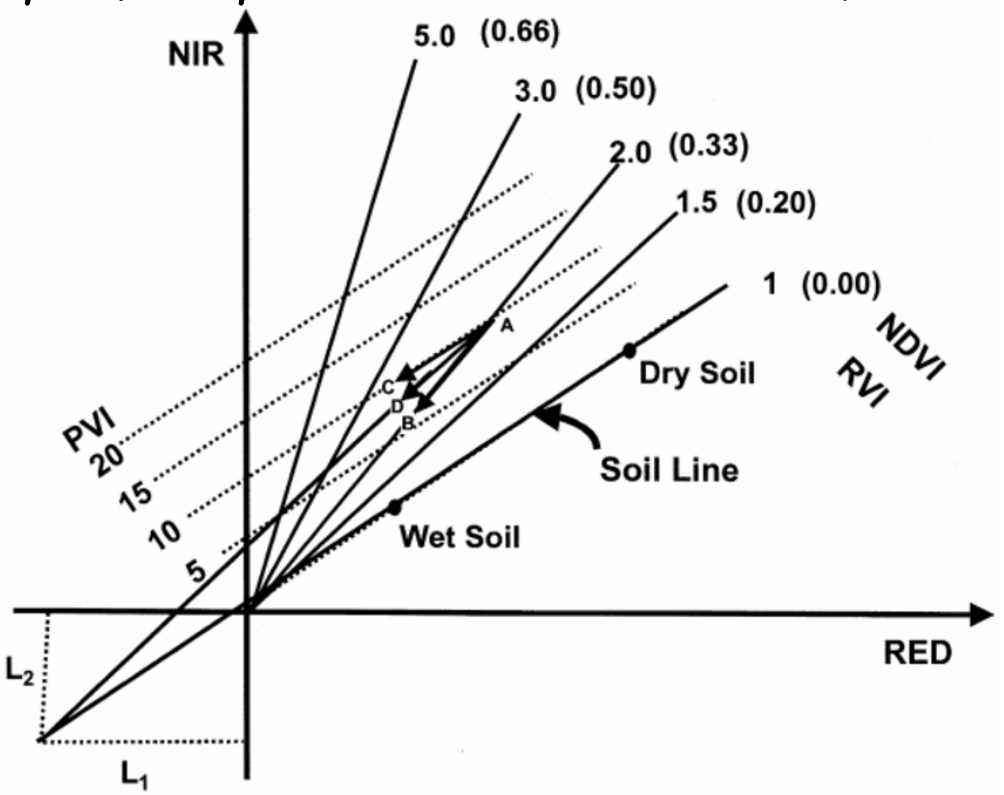

Let's assume we have a pixel representing a given ***LAI*** correponding to

NDVI=0.33 and ***PVI=10***.

If the soil gets wetter, the pixel would change its spectral response (its ***NIR*** and ***RED*** reflectances). Would the pixel move along the line with ***NDVI***=costant, or along the line with ***PVI***=costant?

- ***Soil-Adjusted Vegetation Index (SAVI)***

$$SAVI = \left(\frac{\rho_{NIR} - \rho_{red}}{\rho_{NIR} + \rho_{red} + L}\right)(1 + L) \quad \text{(Eq. 5-11)}$$

  - ***L is an empirical constant, typically about 0.5***
  - ***reduces to NDVI for L = 0***
  - ***superior to NDVI for low vegetation cover and to PVI for large vegetation cover***

It is an NDVI with the origin translated

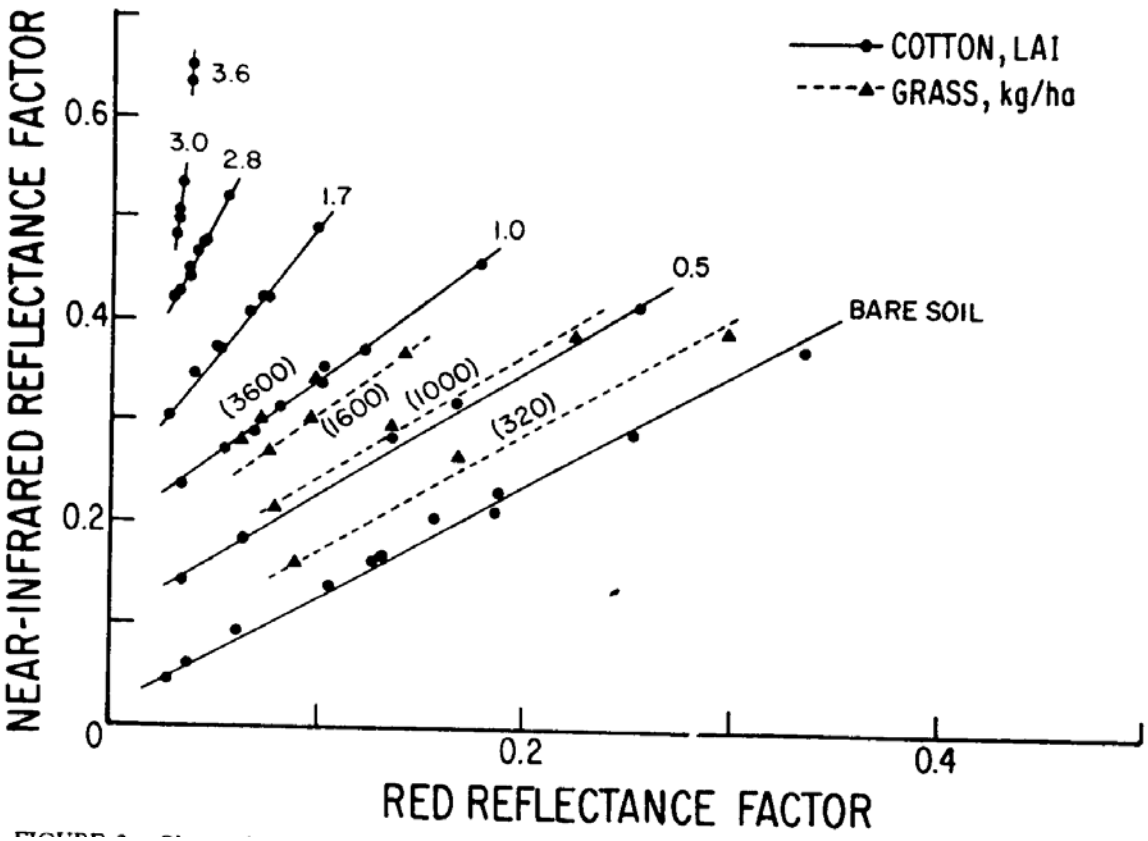

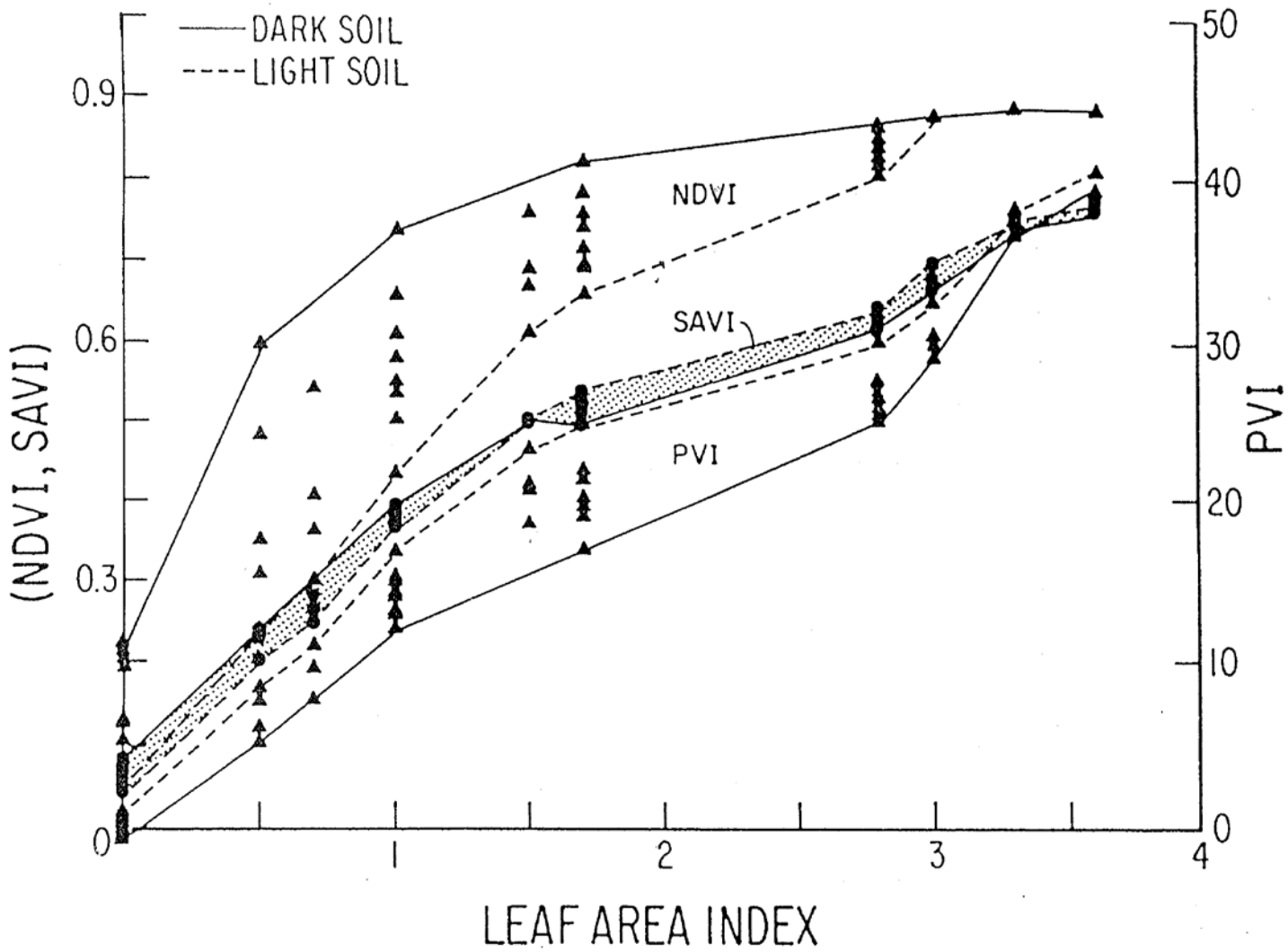
DARK SOIL
LIGHT SOIL
NDVI
SAVI
PVI
(NDVI, SAVI)
PVI
LEAF AREA INDEX
0
0.3
0.6
0.9
1
2
3
4
0
10
20
30
40
50

Classification of an image consists in attributing a label to every pixel, thus identifying a type of surface that it is being observed (for example, bare soil, water, vegetation...).

Remote Sensing offers the opportunity to classify the Land on the basis of spectral information, or polarimetric, or temporal information, contained in images.

Many classification methods exist, and the choice depends on applications or on available data. Visual interpretation or density slicing are classification techniques also.

Classification is based on the fact that each land cover has a typical signature (spectral or polarimetric, etc.), and it consists in grouping pixels with similar properties into the same class.

The feature space is a graphical representation of image **DN**'s, and it is K-dimensional.
A histogram is a 1-dimensional feature space.

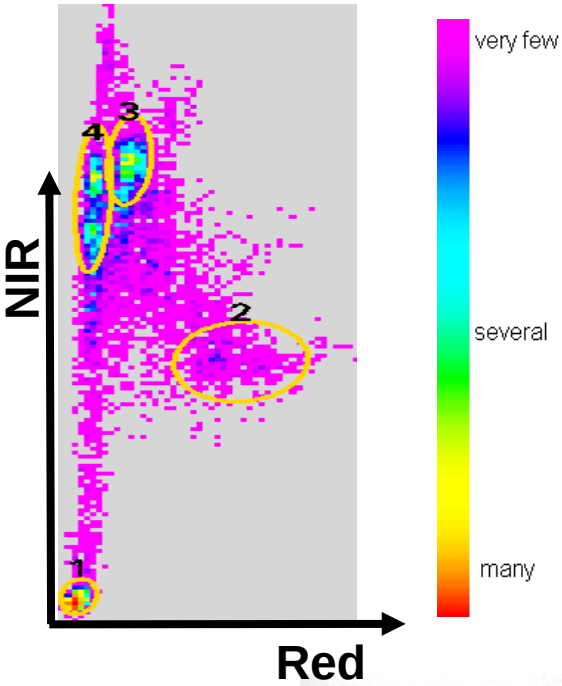

2-D Feature Space

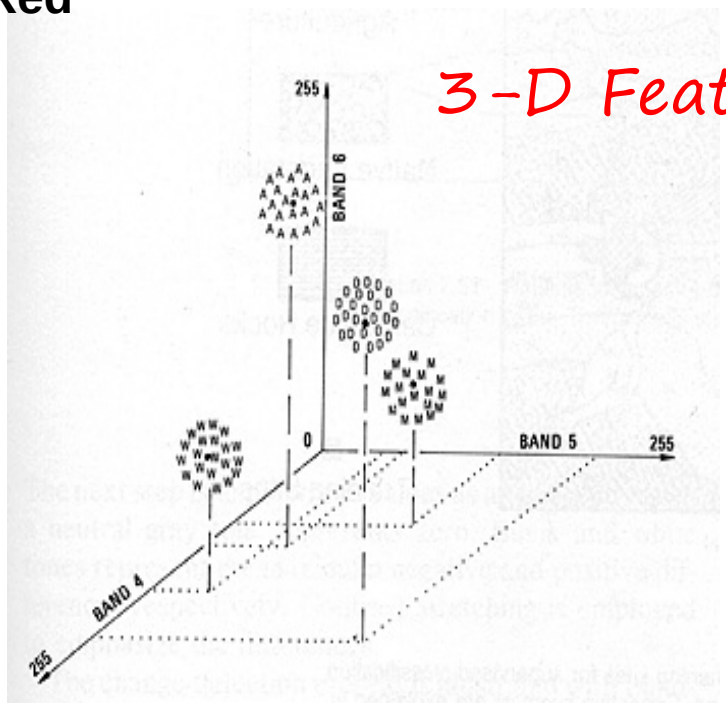

3-D Feature Space

Feature Extraction

- Can use in a classification:
  - original multispectral bands
  - subset of bands
  - derived features
    - principal components
    - vegetation indexes
    - spatial properties
- Good features

  provide high separability of classes

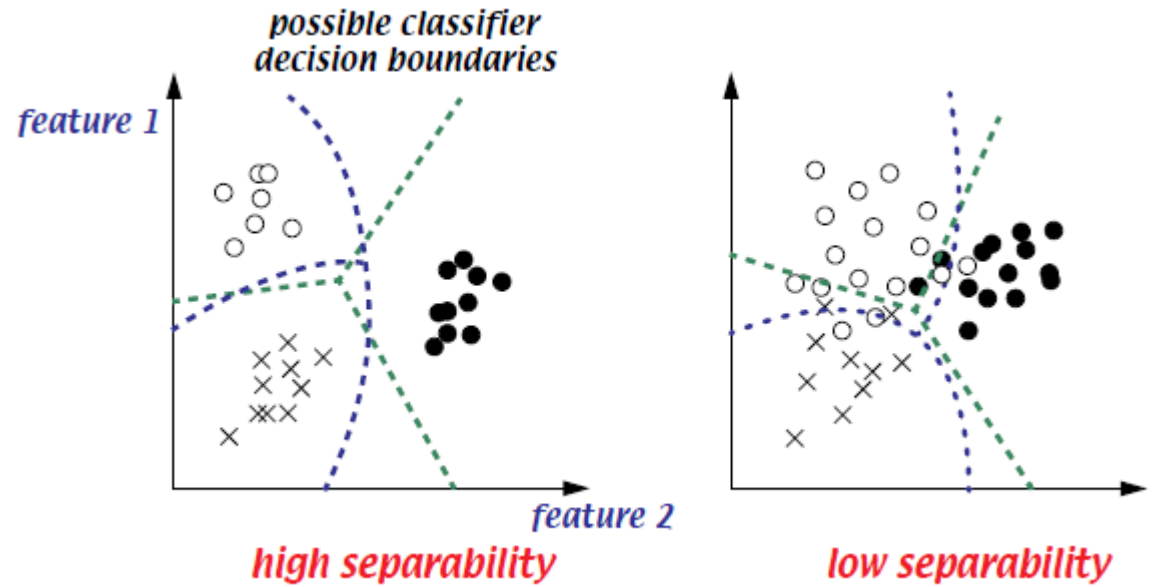

DR. ROBERT A. SCHOWENGERDT schowengerdt@ece.arizona.edu 520/621-2706 (voice), 520/621-8076 (fax)

The groups that are found into a feature space are called clusters. The classification consists in the identification of the cluster positions and in their association to a specific land cover (class).

The classification techniques may be subdivided into

Supervised and Unsupervised

that differ because of the information that are a-priori known about clusters.

In the Supervised classification, some representative pixels of each class are known (training pixel). The statistical parameters of these pixels are then used to recognize the class of all other pixels in the image.

In Unsupervised classification, training pixels are not available. An algorithm is then used to group pixels on the basis of their closeness in the feature space. Clusters obtained in this way are then "manually" associated to a class.

Supervised Training

- Training samples are labeled
  - Ground truth
  - Interpretation of higher resolution imagery (e.g. aerial photography)
  - Existing maps
- Identifying training sites (pixel samples) for each class can be laborious
  - Desire class-homogeneous sites, without mixture among classes
  - Also desire representation of full within-class variability
  - Therefore, often need more than one site/class
  - The number of training pixels must be large enough:
    >10·K for each class

DR. ROBERT A. SCHOWENGERDT schowengerdt@ece.arizona.edu 520/621-2706 (voice), 520/621-8076 (fax)

☞ Plate 9-1: Color IR composite

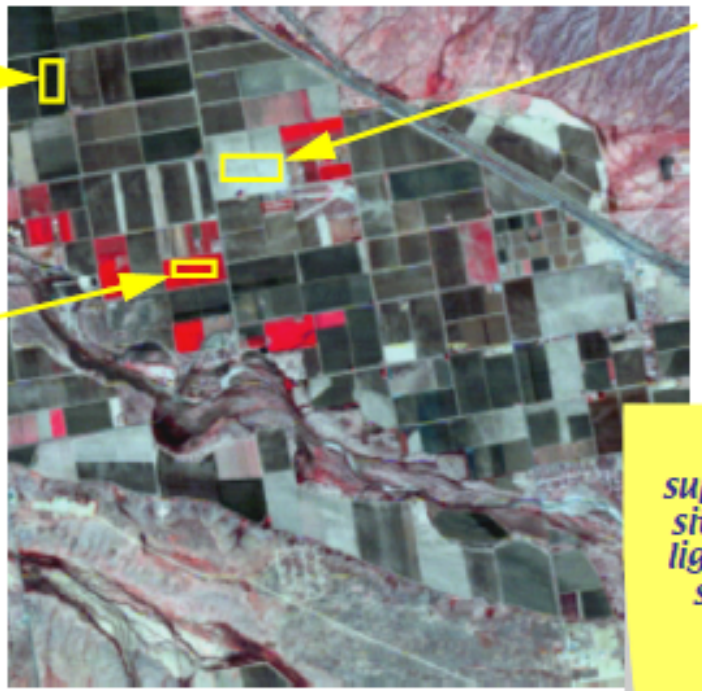

supervised training sites for dark soil, light soil, and crop shown in yellow

DR. ROBERT A. SCHOWENGERDT schowengerdt@ece.arizona.edu 520/621-2706 (voice), 520/621-8076 (fax)

Let's suppose we have m classes ω_c (with $c=1, m$).
For each class, it is possible to create a vector μ_c that contains the average of pixel DN's in the training sites, for each feature f_k (f_k are the feature space axis).

$$\mu_c = (\mu_{cf1} \quad \mu_{cf2} \quad \cdots \quad \mu_{cfk})$$

And also a covariance matrix C_c that contains the covariance between each feature for the class ω_c.

$$C_c = \begin{matrix} C_{cf1f1} & C_{cf1f2} & \cdots & C_{cf1fk} \\ C_{cf2f1} & \ddots & & \vdots \\ \cdots & & \ddots & \vdots \\ C_{cfkf1} & C_{cfkf2} & \cdots & C_{cfkfk} \end{matrix}$$

Correlations Landsat-TM Spectral Bands

	1	2	3	4	5	7	6
1	1						
2	0.83 0.90 0.92 0.89	1			a b c d		
3	0.81 0.84 0.88 0.91	0.83 0.92 0.90 0.91	1				
4	-0.34 0.16 0.12 -0.01	-0.01 0.31 0.26 0.15	-0.39 0.51 -0.38 -0.07	1			
5	0.41 0.27 0.54 0.54	0.57 0.41 0.62 0.62	0.59 0.61 0.56 0.66	0.14 0.88 0.43 0.27	1		
7	0.44 0.40 0.75 0.68	0.43 0.52 0.79 0.69	0.76 0.71 0.85 0.79	-0.61 0.81 0.04 -0.08	0.61 0.96 0.78 0.84	1	
6	-0.20 0.07 . -0.15	-0.18 -0.10 . -0.17	0.24 -0.21 . -0.15	-0.72 -0.49 . 0.02	0.16 -0.39 . 0.03	0.64 -0.34 . 0.07	1

Four classes

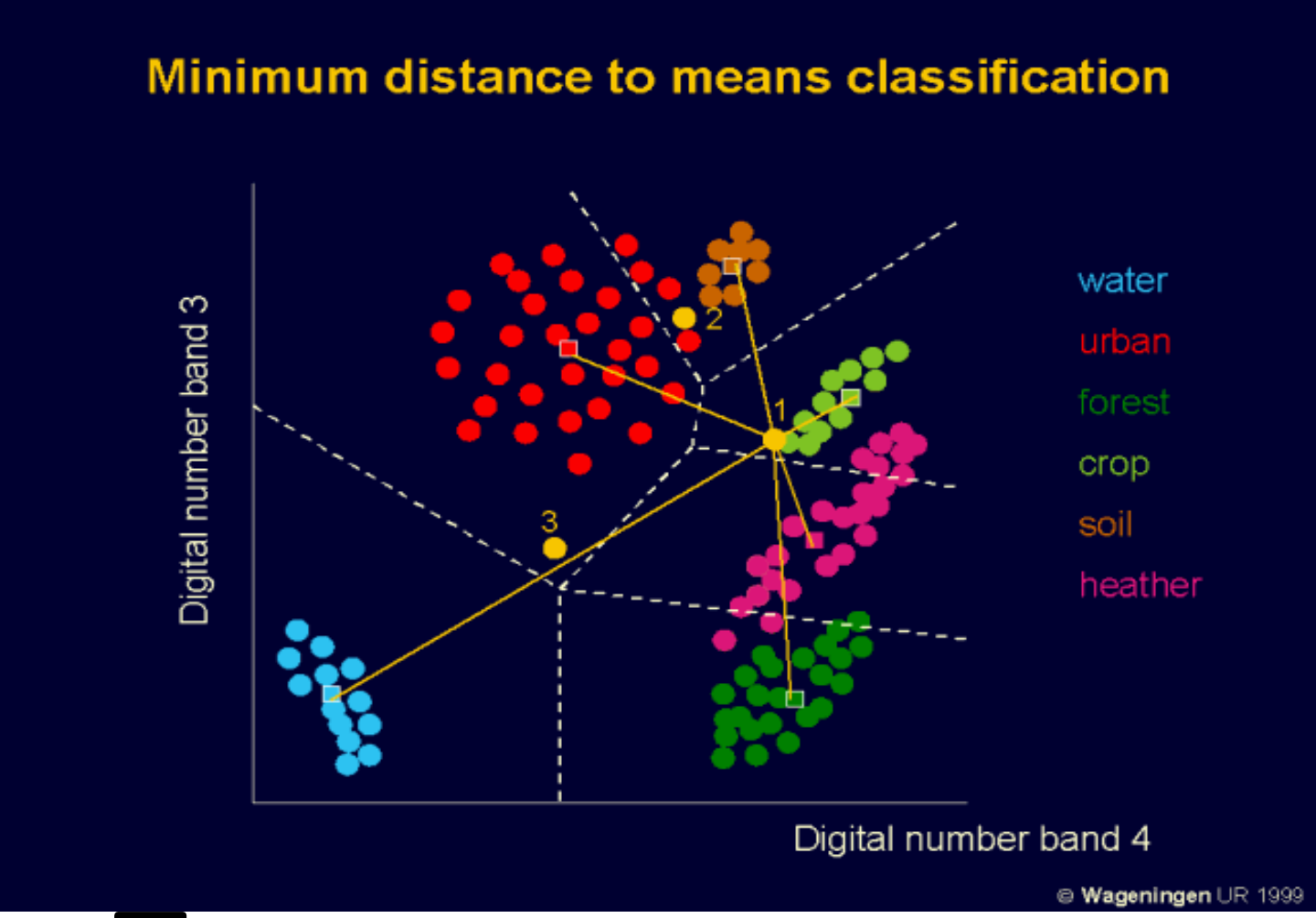

□ represents the mean μ_c of each class

X_{ij} is the pixel to be classified (i,j= row and column image indices)

$$\Delta_{ijc} = \sqrt{(X_{ijf1} - \mu_{cf1})^2 + (X_{ijf2} - \mu_{cf2})^2}$$

(In this case, f_1 = Band 4 and f_2= Band 3)

The pixel X_{ij} is assigned to the class the yields the minimum Δ_{ijc}

This method does not take into account the class variances: as a consequence, pixel 2 is classified as soil and not as urban

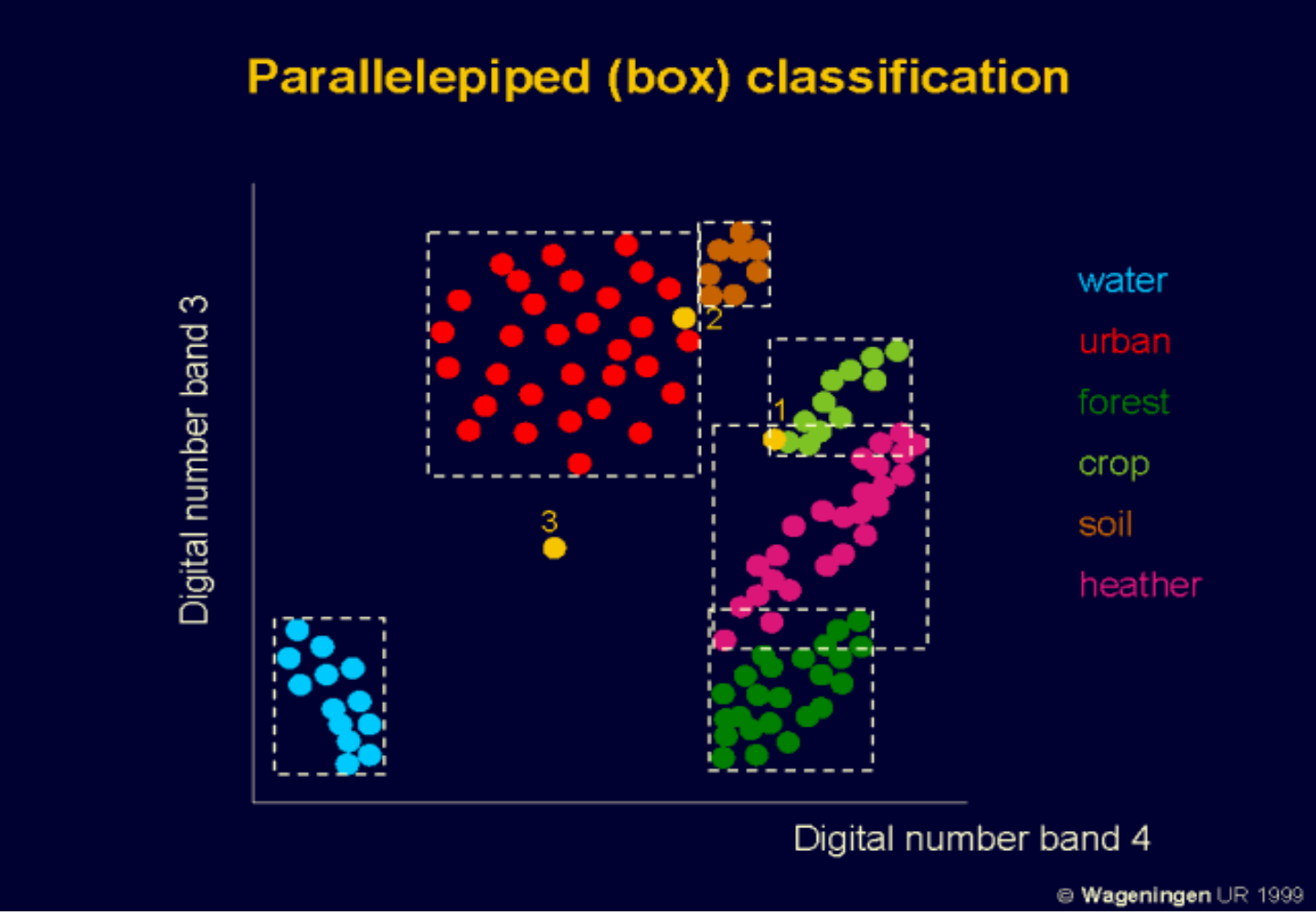

The pixel X_{ij} is assigned to class ω_c if

$$\mu_c - D\sigma_c < X_{ij} < \mu_c + D\sigma_c$$

D is a threshold chosen arbitrarily

The class borders may overlap: pixel 1 could be classified both as crop and as heather

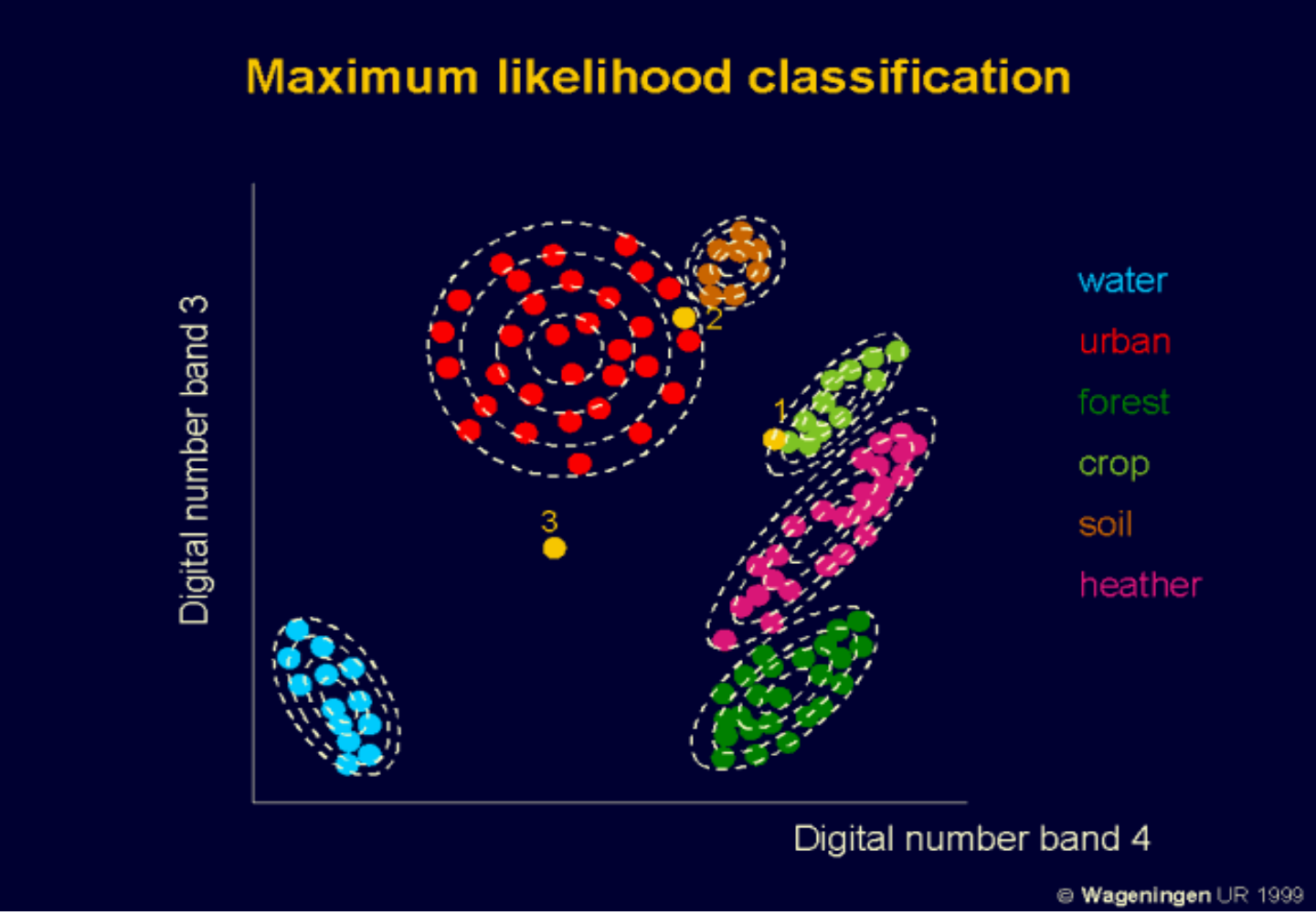

The dashed curves join points with equal $P(X_{ij} \mid \omega_c)$ that is the probability that the pixel $\boldsymbol{X_{ij}}$ belongs to class $\boldsymbol{\omega_c}$.

This method attributes pixel $\boldsymbol{X_{ij}}$ to class $\boldsymbol{\omega_c}$ if the probability $P(X_{ij} \mid \omega_c)$ is the largest.

It is usually assumed that probability $P(X_{ij} \mid \omega_c)$ follows a normal distribution with mean $\boldsymbol{\mu_c}$ and covariance matrix $\boldsymbol{C_c}$.

Maximum Likelihood Classification (MLHD)

N-dimensional Gaussian (normal) distribution = idealized distribution

$$P(\underline{X} \mid \omega_i) = \frac{1}{(2\pi)^{N/2} \, |C_i|^{1/2}} \cdot e^{-\frac{1}{2} d_i^2(\underline{X})}$$

$|C_i|$ = determinant of C_i

with $d_i^2(\underline{X}) = (\underline{X} - \underline{M}_i)^T \, C_i^{-1} \, (\underline{X} - \underline{M}_i)$

(1x1 = 1xN · NxN · Nx1)

This is the square of the standardized distance of $\underline{X}$ with respect to class ω_i.

Mahalanobis distance

Rejection Class

When the distances from a pixel to each class centre become too large (larger than a threshold D), in other words: a and b both very small, then one often wants the pixel to be called "unclassified" → **rejection class**.

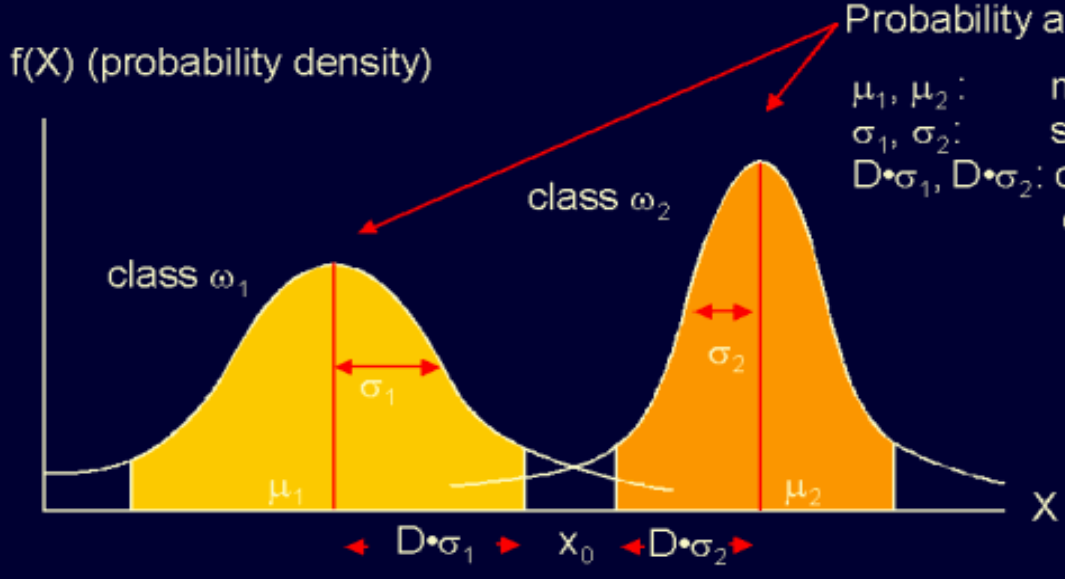

☞ *Fig. 9-25, p433: nearest-mean classification in image and feature space*

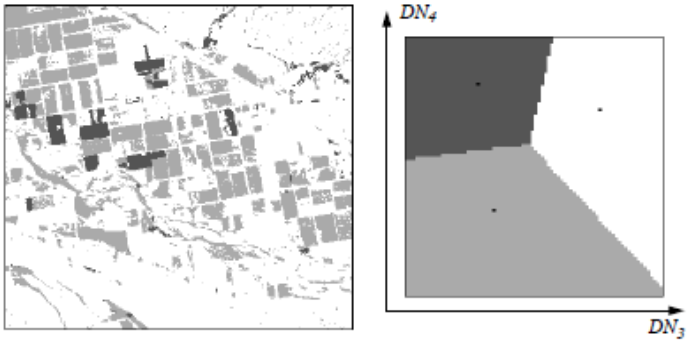

☞ *Fig. 9-17, p420: example level-slice classification*

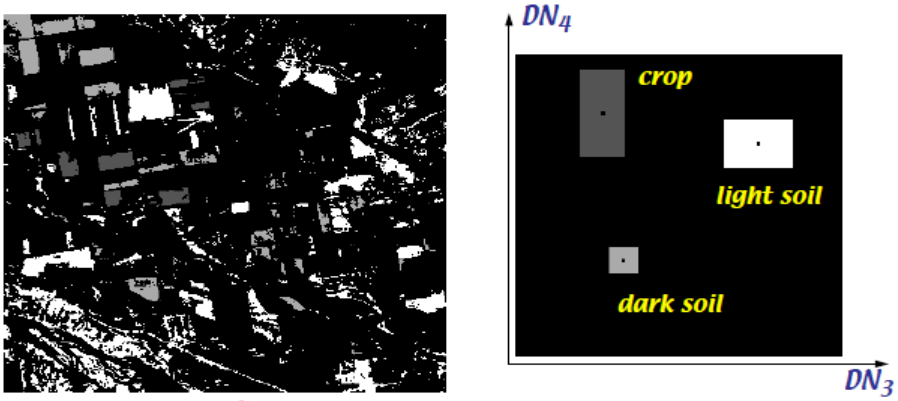

☞ *Fig. 9-26, p434: maximum-likelihood classification in image and feature space, without and with probability threshold*

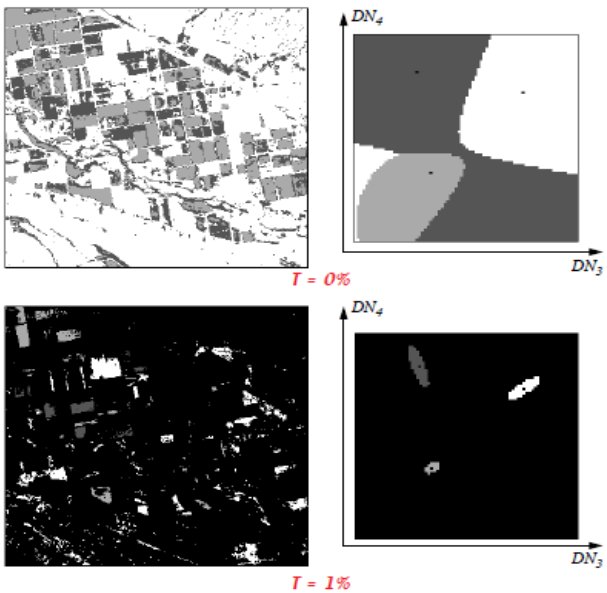

One Unsupervised technique

K-Means Clustering

- Specify K initial cluster mean estimates ("seeds")

  Note: K is not the number of features) but the number of clusters you wish to identify
- Partition feature space according to nearest-mean rule
- Calculate revised cluster mean estimates from partitioned data
- Repeat 2 and 3 until convergence criterion is met

Specify K initial cluster mean estimates ("seeds") and partition feature space

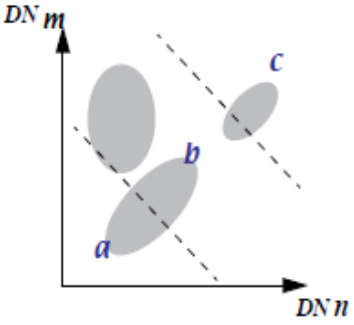

Calculate revised cluster mean estimates from partitioned data

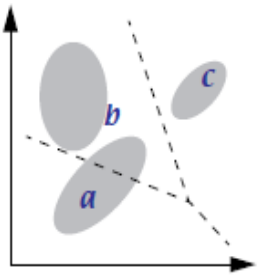

after iteration 2

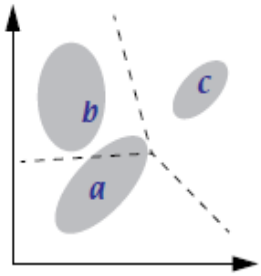

after iteration 3

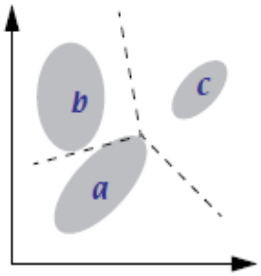

mean vector migration

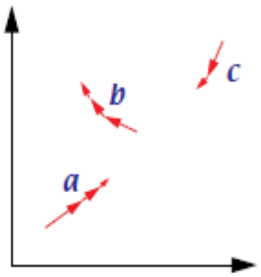

☞ Fig. 9-9, p408: feature space cluster mean locations corresponding to Fig. 9-8

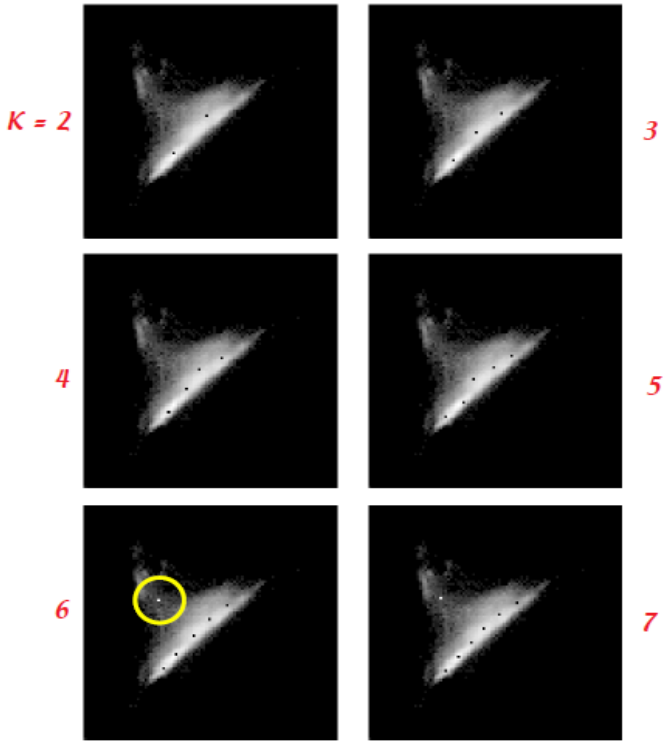

at least 6 clusters needed to "capture" crop class

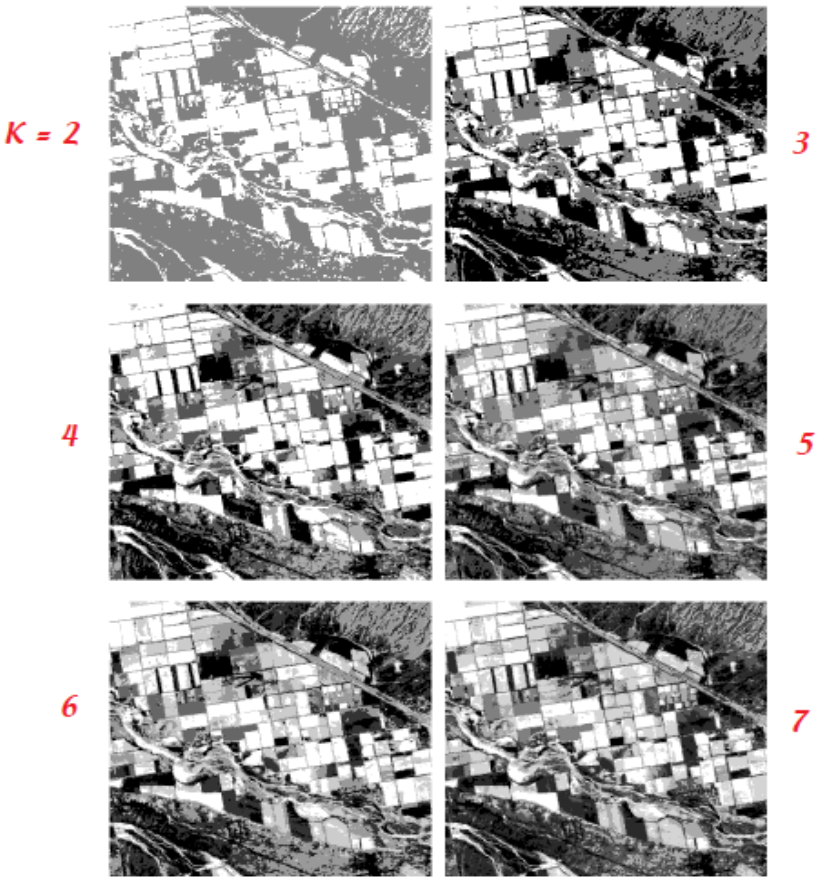

☞ Fig. 9-8, p407: unsupervised cluster maps for various values of K

Usually, **K~20** and, in the *labeling* phase, some clusters are fused.

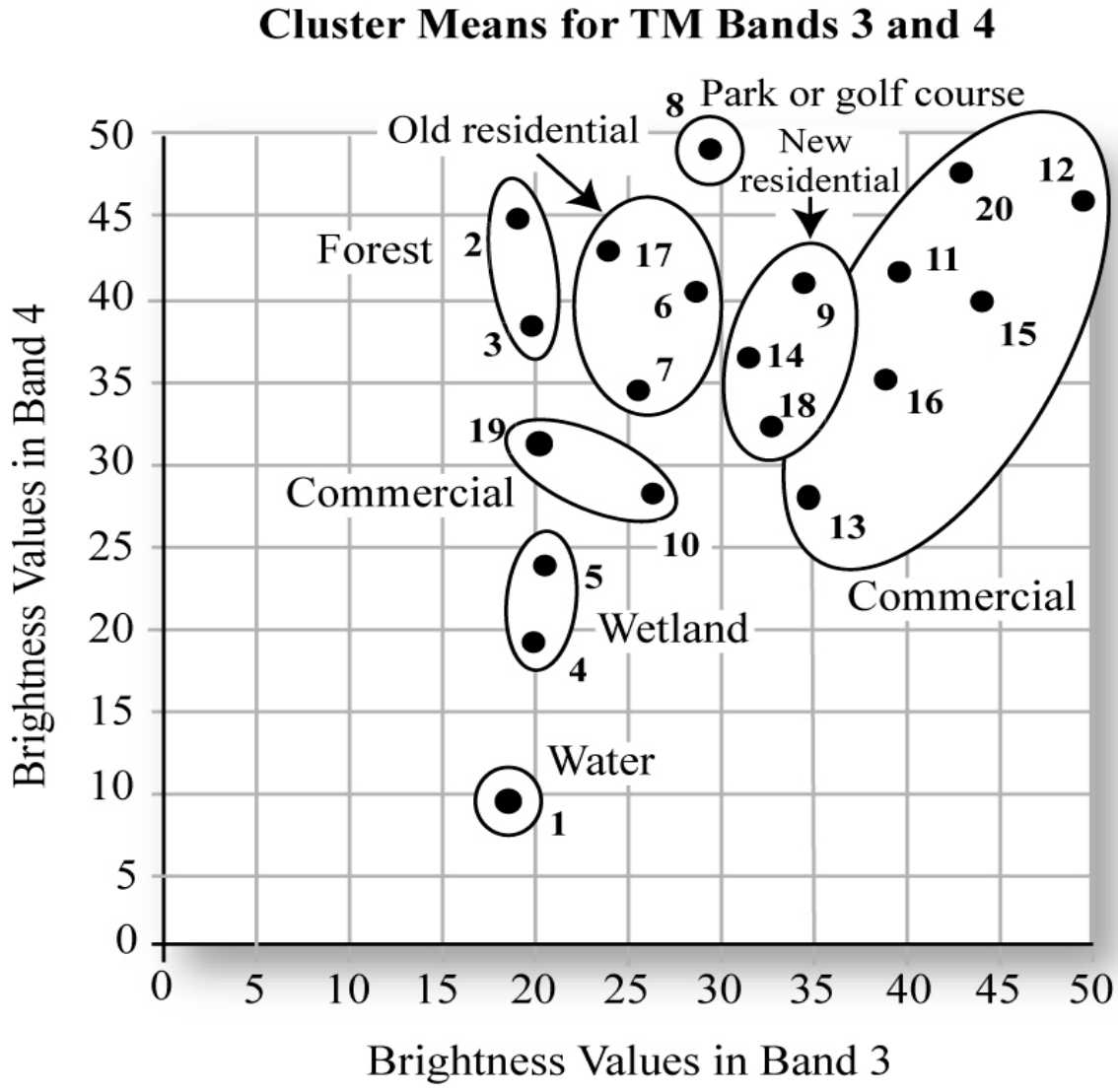

Classification Accuracy

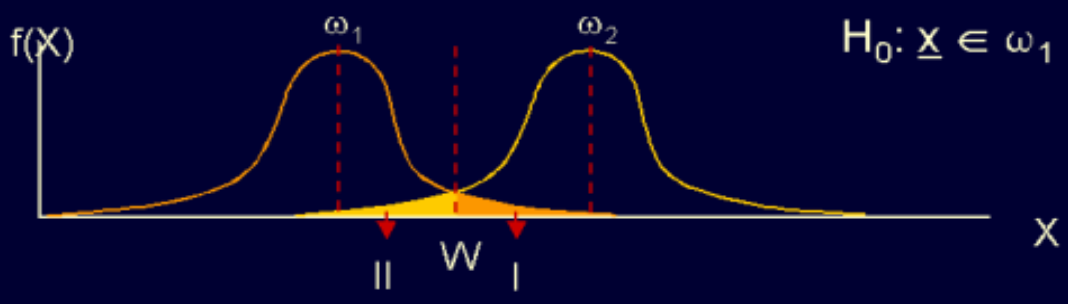

Assume we are concerned with class ω_1.

I = probability called size of a type I error,
meaning that the null hypothesis is rejected when it is true.

II = probability called size of a type II error,
meaning that the null hypothesis is accepted when it is false.

I =	error of omission	II =	error of commission
1-I =	accuracy	1-II =	reliability

The classification procedure is examining pixel $\underline{X}$ in order to decide if it must be labelled as class ω_1.

Two kinds of error may arise:

I: pixel $\underline{X}$ is not attributed to ω_1, whereas it belongs to that class (exclusion error)

II: pixel $\underline{X}$ is attributed to ω_1, whereas it does not belong to that class (inclusion error)

Accuracy is the probability to classify a pixel correctly.

Reliability is the probability that a pixel classified in a certain class belongs really to that class.

The classification accuracy is described by means of the Confusion Matrix (or error matrix).
It is necessary to know the real cover of some reference pixel (ground truth), that must be different from training pixel.

The element E_{tc} of the confusion matrix represents the number of pixels classified in class ω_c and belonging to ground truth t

The values on the main diagonal are pixels classified correctly

Confusion Matrix

unknown ← Classification result "LABELLING"

Ground truth "TRUE"	ω_0	ω_1	ω_2	ω_3	ω_4	ω_5	ω_6	Total
ω_1	117	**897**	308	75	65	17	33	1512
ω_2	72	65	**347**	141	105	0	26	756
ω_3	56	0	7	**110**	131	3	71	378
ω_4	36	0	0	18	**117**	32	49	252
ω_5	105	2	0	101	127	**294**	127	756
ω_6	38	0	0	3	12	0	**325**	378
Total	424	964	662	448	557	346	631	4032

"TRUE"	Accuracy (%)	Omission (%)	Commission (%)
ω_1	59.3	40.7	7.0
ω_2	45.9	54.1	47.6
ω_3	29.1	70.9	75.4
ω_4	46.4	53.6	79.0
ω_5	38.9	61.1	15.0
ω_6	86.0	14.0	48.5

Accuracy ω_1 = 897/1512 * 100% = 59.3%

Error of omission = 1 - accuracy: ω_1 --> 40.7%

Error of commission ω_1 = 67/964 * 100% = 7.0%

Total classification accuracy: 100% * (897+347+110+117+294+325)/4032 = **51.8%**